Review of Domestic Radiometric and Spectrometric Systems Applicable for MC&A purposes

Contents

List of abbreviations and acronyms

ADC – analog-to-digital converter;

DU – detection unit;

GS - gamma spectrometer;

GEM –Gas Electron Multiplier;

LS – liquid scintillators;

MDS – metal-dielectric semiconductor;

HPGe – high pure germanium;

PC – personal computer;

PM – organic and plastic scintillators;

SCD – semiconductor detectors;

FWHM – energy resolution of spectrometer calculated from the detected peak full width at half maximum;

RM - radiation monitor;

SSAC– state system of accounting and control;

MC&A – NM accounting and control;

PD – photodiode;

PEM – photo electronic multiplier;

NM – nuclear material;

T – scintillation duration corresponding to maximum of scintillator luminescence spectrum;

τ – time characteristic of scintillation luminescence;

λ_{max} – maximal wave length of scintillator luminescence spectrum.

Introduction

At present some domestic radiometric and spectrometric systems used in state system of accounting for and control of nuclear materials are morally and physically outdated and should be replaced with new ones in order to meet the requirements of nuclear material accounting and control and modern metrological requirements. The experience has shown that there are some problems with implementation of foreign instrumentation for MC&A purposes, including its high cost and impossibility to install such instrumentation within the areas of enhanced security. This leads to requirement of priority equipping the Rosatom facilities with Russian instrumentation meeting the MC&A requirements, also to provide the long-term functioning and vitality of MC&A systems at Rosatom facilities.

The key elements of radiometric and spectrometric systems used for MC&A are the radiation detectors, data acquisition systems, and data analysis algorithms. Recently the new detector types enter the market, what can be used in modern devices for measuring NM characteristics. Equipping the existing Russian devices with modern Russian detectors will improve their characteristics and significantly raise their applicability for replacement of foreign measuring systems with Russian ones.

Radiation monitors (RM) and gamma spectrometers (GS) are one of the basic means of nuclear materials accounting and control. Last years the gamma spectrometers being conventional devices of analytical control aim at assimilation with radiation monitors. Development of portal technologies leads to implementation of possibility of nuclear material (NM) or radioactive source real-time identification during control with radiation monitor.

Radiation monitor is the device for unauthorized movement control of nuclear and other radioactive materials and is intended for detection of accidental, short duration, weak exceeding of signal controlled over the background level. Efficiency of detectors detecting the radioactive material radiation and power of used algorithms of statistical data processing make the most significant contribution to implementation of maximal sensitivity of radiation detectors.

Development and production of first foreign RMs is dated by early 70-th. Since then the different designers have used the different algorithms of statistical data processing for their RM versions, but mainly the narrow range of detectors limited by *NaI(Tl)* crystals, plastic scintillators and ^{3}He neutron counters. Since the moment of first Russian radiation monitors entered the market in the end of 80-th of past century there appears a set of new algorithms of data processing and detection instruments including patented ones.

Principle of amplitude-to-time conversion created in 1950 gave an opportunity to design one of the complex devices for measuring the ionizing radiations – multichannel analyzer. At the end of the fifties in the USSR there was developed the industrial multichannel analyzer АИ-100. Prerequisites for enhancing the analyzer have arisen with creation of solid-state (semiconductor) units – diodes, transistors, stabilitrons. First domestic industrial gamma spectrometers - devices for study of gamma radiation energy distribution was produced in 1956 – 1958. At the present, the gamma spectrometers are complex devices based on programmable logical integrated circuits that concentrate the experience gained in area of

microelectronics and computer engineering and contain the fast-response spectrometric detectors. It should be noted that at the initial stage of gamma spectrometers development they were created by individual specialists, but now their development requires collaboration of many expert groups, namely, physicists, electronics engineers, designers, programmers, metrological and production engineers.

Appearance of new materials and qualitative improvement of existing ones for last two decades made it possible to considerably enlarge the range of gamma and neutron detectors that are already used in gamma spectrometers and can be used in radiation monitors after some research of such possibility. They are high pure germanium, *CdTe, HgI_2, BGO, BaF_2, $LaBr_3$, LiGdBO, CWO*, microfibers organic scintillators ant others.

Summary of new materials advantages let's say that they cover all basic technical characteristics of detector – energy resolution, detection efficiency, possibility and convenience of data processing, availability and cost. Some of the new possibilities have been implemented in the serial production. However, many of them are known only from several publications. At this, the information on comparative characteristics of different detectors is very limited.

Lately, the photodiodes used as the recorders of scintillations became the competitive recorders in comparison with photoelectronic multipliers (PMs). Competitive ability as against vacuum PMs is provided with high quantum yield, lower operating voltage, higher stability, mechanical strength. The possibility of using the scintillator-photodiode system has already been implemented in the gamma spectrometers, but not in the radiation monitors.

The subject of given work is the review and analysis of new detectors, scintillator-photodiod recorders, data processing algorithms, as well as commercially available detection units, gamma spectrometers and radiation monitors. This report doesn't include such well-known scintillators as *LiI(Tl), LiI(Eu)*, anthracene, naphthalene, toluylene, *ZnS(Ag)*.

1 Scintillation and solid-state detectors of X-rays and gamma radiation

1.1 Inorganic scintillators

Scintillation detectors on the base of inorganic monocrystals are the classic detectors used for detecting X-ray and gamma radiation. Early period of developing the theory and practice of scintillator use has presented in Birks's monographic [1]. The main application of these crystals is low energy gamma spectrometry in the range of less than 3 MeV and applied radiometric measurements.

In 70-s the inorganic scintillators became replaced with more precise semiconductor detectors in the low energy spectrometry area. However, the inorganic scintillators are beyond comparison when detecting the low particle flows not requiring the high resolution, in spectrometric detectors of large volume and 4π multichannel spectrometric systems.

And now the monocrystals of *NaI(Tl)* and *CsI(Tl)* are basic detectors of X-ray and gamma radiation used for applications on the base of nuclear-physical methods of analysis and control in spite of appearance of new prospective scintillation materials. Their characteristics are well-known and presented in [2,3].

1.1.1 *NaI(Tl)* monocrystal

Thallium-activated sodium iodide monocrystal was discovered by R. Hofshtadter more than fifty years ago. This scintillator is notable for high light yield – about 25 eV are required for single photon formation. Luminescence spectrum well matches the spectral sensitivity of standard PM photocathodes. Monocrystal has high transparency to intrinsic radiation and is easy-to production. The great disadvantage of the crystal is its high hygroscopic property.

The light yield of *NaI(Tl)* is maximal in the room environment. The light yield significantly reduces below 0 °C and above 60 °C. Lowering of temperature leads to deterioration of monocrystal self-resolution caused by inhomogeneity of light yield. It was noted [4] that to the greater extent this phenomena becomes apparent when increasing the activator concentration, i.e. the lower temperature, the lesser thallium concentration should be. Scintillator luminescence time also depends on the temperature. When increasing the temperature, it first decreases sharply up to 150 ns about 60°C and then smoothly to 100 ns [4].

Temperature coefficient is 0.22 -0.5 %/°C and depends on the sample. When temperature is sharply changed, the crystal can be destroyed.

The energy resolution for small crystal is determined mainly by photoelectrons statistics. Measurement the energy resolution for 662 keV photons from ^{137}Cs radioactive source is standard. The resolution obtained for crystal of D = 25 mm diameter and $H = D$ height was 5.6 % [5]. Usually the resolution is 6.5—7.5 % for crystals of up to $D = H =$ 8 cm and 7.5—10 % — for larger volume crystals.

1.1.2 Cesium iodides *CsI(Tl)* and *CsI(Na)*

The need for sealed package of *NaI(Tl)* crystals introduce the corresponding limitation to their simultaneous use as gamma detectors and detectors of low energy charged particles. In such a case the monocrystal of *CsI(Tl)*, whish is almost nonhygroscopic, is more preferable. Small leakages won't lead to monocrystal destruction as it is in case of *NaI(Tl).* However, in during long-term using *CsI(Tl)* should be isolated into dry environment.

Plastic nature of cesium iodide provides ease of its mechanical treatment as opposite to sodium iodide that splits or cracks under mechanical or thermal shock. Cesium iodide use allows for manufacturing the variety of detectors of different shapes and dimensions.

CsI(Tl) emission spectrum has maximum at $\lambda = 550$ nm and poor matches the characteristic of standard photocathode S-11. For this photocathode the *CsI(Tl)* signal amplitude is usually 45 % of signal amplitude obtained from *NaI(Tl)*. Photocathode of S-20 type is more suitable for *CsI(Tl)*. Under condition

of larger cathode sensitivity in the green area and signal shaping time constant of about 5 μs its amplitude increases to 85 %. The signal of such duration is required due to the increased luminescence time (~1μs), that, of course, is the disadvantage of given scintillator.

Scintillation efficiency of *CsI(Tl)* is even higher than that of *NaI(Tl)*. According to [6], when energy loss is 1 MeV, $4 \cdot 10^4$ photons are generated in *NaI(Tl)*, and $4.5 \cdot 10^4$ photons - in *CsI(Tl)*. Free radiation length for *CsI(Tl)* is X_0 =1.85 cm, that is lesser than for *NaI(Tl)*.

Thallium-activated crystal is much more agreed with spectral characteristic of S-11 photocathode than sodium-activated one. At this the luminescence time also decreases to 630 ns. Signal amplitude from *CsI(Na)* is 85 % of signal amplitude from *NaI(Tl)* [7]. Moreover, according to [8] the scintillation efficiency of both crystal is almost equal but *CsI(Na)* is lesser hygroscopic than *NaI(Tl)*. Disadvantage of *CsI(Na)* and *CsI(Tl)* as well as of *NaI(Tl)* is well high afterglow — up to 5 % after 3—6 ms, that significantly limits the counting rate.

Energy resolution of *CsI(Tl)* is absolutely on 3-5 % poorer than that of *NaI(Tl)* under similar measuring conditions.

Cesium iodide has extremely low level of inherent radioactivity.

Production technology of cesium iodides is simple, especially of *CsI(Tl)*. *CsI(Tl)* is relatively no big coast, including the large size crystals.

1.1.3 Bismuth orthogermanate *BGO*

Chemical formula of this scintillator [9,10] named usually as *BGO* is $Bi_4Ge_3O_{12}$**.** Luminescence centers of the monocrystal are bismuth ions and they don't require the activators. Main *BGO* advantage is its short free radiation length X_0 — 1.13 cm. With the same volume the crystal of *BGO* allows to have greater efficiency of photon detection than the crystals described above.

Luminescence spectrum of the crystal is shifted slightly to the right (λ_{max} = 480 nm) against the sensitivity spectrum of S-11 photocathode. Crystal's refraction factor n = 2,13 is much greater than that of photomultiplier glass. Both these factors lead to decrease of photoelectrons number.

One more technical problem is a formation of air bubbles inside the crystal volume during the crystal production process. Bubbles disperse the light and so lead to light losses. Number of *BGO* photoelectrons can be from 8 % to 16 % of that from *Nal(Tl)* depending on the quality and size of the crystal. Even 20 % data were obtained [11]**.**

BGO luminescence time at room temperature is 300 ns, that is negligibly poor than that of *Nal(Tl)*. However, in contrast to the latter the BGO's afterglow in millisecond region is very small — 0,005%. So, in whole, *BGO* is faster than *NaI(Tl)*. Duration of *BGO* light flash strongly depends on the temperature. It is 400 ns at 0°C, and 200 ns at 40 °C. Light yield also strongly depends on the temperature. Temperature factor is 1.55 % /°C for room environment [12]**.** Temperature decrease below 100 ^{o}K increases the light yield by a factor of 2 [13]

Resulting light yield of *BGO* significantly lesser than that of *NaI(Tl)* is accompanied with corresponding deterioration of energy resolution. The best results include the resolution of 9.3% for gamma radiation of ^{137}Cs obtained with Harshaw company's crystal of Ø 25x25 mm size made of twice recrystallized raw material [14]**.** The energy resolution strongly depends on crystal size because of insufficient transparency of *BGO* crystals to self-radiation. Thus, if the resolution for crystal size of Ø 25x25 mm was 10.5%, the resolution for crystal of Ø 25x100 mm made of the same raw material is 13.3 % [15]**.** Resolution of 13 % has been obtained for Ø50x200 mm crystal [16].

BGO advantages are its stress-strain properties under mechanical treatment and hygroscopic property.

It was shown [17], that 4-17 MeV photon detection efficiency of the detector on the base of relatively small Ø75x25 mm^2 *BGO* crystal is comparable with that of Ø150x100 mm^2 *NaI(Tl)* scintillator.

Reference [18] presents one of possible applications of *BGO* scintillator together with *NaI(Tl)* and *CsI(Tl)* when searching the radioactive sources and determining the direction of gamma radiation source location.

For NM accounting and control purposes *BGO* is used in design of fast neutron coincidence counter [19]. Several studies [20, 21] have shown the possibility of *BGO* scintillator use for simultaneous detection of gamma and neutron radiations. At this the boron-activated plastic scintillator *BC454* and thin *BGO* plates are used. Figure 1.1.1 presents the gamma spectrum obtained with such detector. At this, the line of 478 keV corresponds to radiation of excited ^{7}Li nucleus from $^{10}B(n,\alpha)^{7}Li$ detected with *BGO*. Line of 93 keV corresponds to α-particle and lithium nucleus absorption within plastic *BC454*.

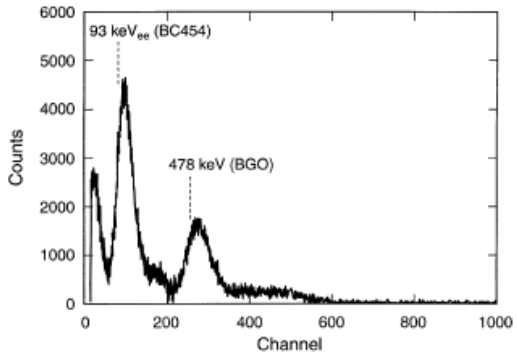

Figure 1.1.1 – Gamma radiation spectrum

Coincidence of these two peaks allows to make a decision about neutron radiation presence during in several microseconds, that is significantly lesser time than that allowing for neutron detection with ^{3}He tubes. Such saving of time is very important in the well neutron coincidence counters and allows for reducing the uranium mass measurement error from 26 to 7 % and counter dead time from 52 to 3.7 μs.

1.1.4 Fluorides (*BaF_2, CaF_2-Eu*)

Barium fluoride *BaF_2*

Plastic scintillators having the short luminescence time are usually used for precision time measurements. However, their radiation length is large (42 cm) that limits their application for high energy gamma radiation.

BaF_2 crystal has the fast component 0.6 and 0.76 ns, that gives a stimulus for new stage of high energy scintillation gamma spectrometry development [22].

Main portion of scintillation light in *BaF_2* falls at the component with λ_{max} = 320 nm having τ = 620 ns. Fast luminescence occurs in the wavelength range of ~ 200 nm. Photomultiplier with quartz glass is required for detection of ultraviolet light. Refraction factors of *BaF_2* and the glass are close to each other enough. According to [23] *BaF_2* has n = 1.495 at 320 nm; for λ = 200 nm n = 1.63, and quartz's n = 1.53 [24].

Data on the crystal light yield presented in [25, 26, 27] are very ambivalent. This is 8-30 % of the *NaI(Tl)* light yield. In addition to the crystal quality the technical problems of estimating the light yield for different spectral luminescence regions can affect the measurement results. Light yield of *BaF_2* comparative to *NaI(Tl)* can be taken as 5 % for fast component and 16% - for slow component.

Crystal has a weak hygroscopic property. To stabilize the light yield the crystal should be hermetically sealed. In reference [28] the crystal sides were polished and covered, except for light-collecting side, with white powder of *$A1_20_3$*. *MgO* is also used for covering, but the most popular is winding the several layers of teflon tape (up to ~0.3 mm) [29]. The Teflon refraction factor in ultraviolet region is 0.95 [24].

The main advantage of *BaF_2* is the possibility to obtain with this relatively heavy crystal the same time resolution as with plastic scintillator. Thus, with small crystal of Ø2x1 cm there was obtained 80 ps time resolution for gamma radiation of *^{60}Co* radioactive source [28]. Energy resolution of Ø40x20 mm monocrystal at 662 keV is 18 % [30].

Calcium fluoride *CaF_2-Eu*

CaF_2-Eu crystals are the prospective scintillation materials for X-ray detection and beta spectrometry in presence the gamma and neutron background [31]

Optimal impurity concentration ensuring the maximal scintillation yield is 0.5-0.7 weight %. Absolute energy yield is 50 % relatively to *NaI(Tl)*. Basic luminescence spectrum matches the spectral photocathode sensitivity of many photoelectric multipliers.

Temperature influence on the luminescence spectrum is negligible in the range of -100 to 100 ^oC. Crystals have low afterglow level.

Gamma spectrum of *^{137}Cs* measured with *CaF_2-Eu* crystal has the sharp Compton increase above the photo peak. The lesser error of photo peak parameters determination is required the greater

measurement statistics should be obtained at longer exposition times of 20-30 min. At this, the energy resolution is 9.5-10 %.

Thermal luminescence suppression and, respectively, the decrease of scintillation light yield start from 20 ^{o}C. Temperature coefficient of light yield is 0.4-0.5 %/ ^{o}C [31].

CaF_2-Eu scintillator together with liquid scintillator was successfully used in two-component forswitch-detector [32] applied for detection of neutrons and charged particles.

1.1.5 Yttrium-aluminum oxides (*YAP)*

Yttrium-aluminum oxides – crystals of $Y_2A1_5O_{12}$ (garnet) and $YAlO_3$ (perofskite, *YAP*) are well known from laser technology [33]. Cerium activation (0.1 —1.0 weight %) allows to made scintillators of them. Their characteristics are close to that of *CsI(Tl)*, but the response speed is much faster.

$Y_2A1_5O_{12}(Ce)$ has the light yield about 4 % of that of *NaI(T1)*, T = 70 ns and λ_{max} = 550 nm [34]. Light yield of $YA1O_3(Ce)$ at CeO_2 concentration of 0.2 weight % is 40 %, T= 28 ns, n =1.93 and λ_{max} = 350-390 nm [35,36]. Luminescence time can be twice reduced by additional co-activation by *Yb* ions (l weight %), but the light yield drops at this to 6 %. $Y_3A1_5O_{12}$ crystallophor luminescence is suppressed by ions of Pb^{2+} [37].

There were obtained the monocrystals of high optical quality of 8x10x1.5 cm size [38]. The crystals are no hygroscopic, chemically stable and have the good mechanical properties.

Detectors on the *YAP:Ce* base ensure the high resolution in the soft X-ray and gamma radiation region. Energy resolution for α-particles from ^{226}Ra of 7687 keV energy is 2.5% and almost constant within the wide energy range [38].

YAP:Ce scintillators can be used for developing the alpha spectrometers with good energy resolution, low background, and acceptable cost. Also it is possible to manufacture the optical microtubes on the base of this scintillator.

1.1.6 Beryllium oxide *BeO*

Beryllium oxide is widely used due to the good combination of thermal, mechanical, electrical, and optical properties [39]. In radiation tecnique *BeO* is more often used for alpha and beta spectrometry.

Estimation of *BeO* light yield is 40-75 % relatively to that of *CsI(Tl)*. Curve of sctintillation decay consists of three components: 20 ns, 115 ns, and 1.85 μs [40].

Beryllium oxide monocrystals are activated with lithium and sodium in form of tangstates. *Li* content is $(4\text{-}6)\cdot10^{-2}$ mass %, *Na* content is $2\cdot10^{-2}$ mass %.

Scintillation efficiency of *BeO(Li)* and *BeO(Na)* are slightly differ for alpha and beta radiations. Lithium activation gives the odds when detecting the alpha particles, *BeO(Na)* has a small advantage when detecting the beta radiation.

Monocrystal samples strikingly show the thermostimulated spontaneous luminiscence, that cause their use as the termoluminiscent detectors of ionizing radiations.

1.1.7 Lanthanum halogenides *$LaBr_3(Ce)$, $LaCl_3(Ce)$*

In 2001 Saint-Gobain Corporation (France) patented (international patents WO 01/60944, WO 01/60945) the new group of scintillation crystals – cerium-doped lanthanum halogenides (halides) *$LaBr_3(Ce)$* and *$LaCl_3(Ce)$*. Possibility of commercial production of large sized *$LaBr_3(Ce)$* и *$LaBr_3(Ce)$* crystals is the most significant achievement of modern technologies in the area of scintillation methods of ionizing radiation detection. Combination of perfect spectrometric properties and good counting properties of these scintillators allows specialists to put a question: whether the conventional *NaI(Tl)* crystal become obsolete? [41].

$LaBr_3$ is really not only doesn't inferior to *NaI(Tl)*, but does surpass in some parameters. Crystals are grown of relatively large size [42] using the syntethis technology developed by Czochralsky and Bridgman. Ref. [42] studies the crystals of *$LaBr_3(Ce)$* grown by Bridgman's method using the nanomaterials *$LaBr_3$* and *$CeBr_3$* with purification efficiency of 99.99 %. Temperature of crystal fusion was 783 °C, crystal density was 5.3 g/cm^3. Maximum of *LaBr* scintillator emission spectrum falls at 350 nm.

In ref. [43] the energy resolution for photon energy of 140 keV was obtained as 7.5 % for crystals of 5x5 mm size and 4 and 5 mm height, and 12 % for crystal of 10 mm height.

In later studies the crystals with different cerium content of 0.2-10 % have better energy resolution in the range of 2.9 to3.9 % [44].

The best resolution of 2.8 % for photon energy of 662 keV was obtained in the study in ref. [45].

The energy resolution of industrial spectrometers on the base of *$LaBr_3(Ce)$* for gamma radiation energy more than 350 keV is approximately half of the energy resolution of detectors on the base of conventional *NaI(Tl)* crystals of the same size. Detection efficiency is 10 - 70 % higher than that of the detectors on the base of conventional *NaI(Tl)* crystals of the same size [46].

Reference [47] demonstrates the advantages of lanthanum bromide above the *BaF_2* and *NaI*. Figure 1.1.2 presents the comparative spectra obtained with these scintillators.

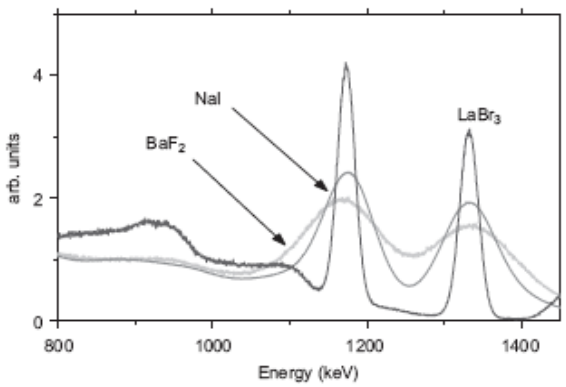

Figure 1.1.2 – ^{60}Co energy spectra measured with 1"x1" *$LaBr_3(Ce)$*,

2”x3” BaF_2 and 3”x3” *NaI*

Study on reference [48] uses the unique characteristics of $LaBr_3(Ce)$ scintillator for detecting the 14,1 MeV neutrons and beta radiation with energy below 2 MeV.

$LaCl_3$ – as well as $LaBr_3$ is a new crystal, what characteristics are not worse than that of *NaI(Tl)* crystals. This crystal as well as $LaBr_3$ can be synthesized by technologies developed by Bridgman and Czochralsky [49]. Crystal density is 3.64 g/cm^3. Scintillator spectra emission of *LaCl* is in the region of 350 nm and 420 nm. According to [49], this crystal has the following characteristics:

- light yield - 50 photoelectrons/keV (70 % for τ = 20 ns, 30 % for τ = 213 ns);
- radiation length X_0 is 2.8 cm;
- luminescence time <30 ns.

Reference [50] studied the characteristics of 1 cm^3 crystal with cerium concentration of 0.1 to 20 %. It was noted that the crystal response has became faster with increasing the cerium concentration within the range mentioned above, but the total light yield of the crystal reduced. The cerium concentration of 10 % was selected as the optimal.

For such crystal the energy resolution of 3.2 % (FWHM) was obtained for photon energy of 662 keV. The energy resolution of the larger crystal (Ø25x25 mm) was 4.2 %, while the resolution of the same size *Nal(Tl)* was 6.7 % [51].

Both scintillators $LaBr_3(Ce)$ and $LaCl_3(Ce)$ have the intrinsic activity caused by presence of instable isotope ^{138}La and ^{227}Ac impurity, see Table 1.1 [47].

Intrinsic activity and strong anisotropy of temperature coefficient of linear expansion are considerable shortcoming of this scintillator.

Table 1.1 – Intrinsic β-activity of $LaBr_3(Ce)$ crystal

Isotope	Decay	$E_{\beta-}$, keV	I_e, %	E_γ, keV	I_γ, %
^{138}La	β- EC	252±12	34 66	789 1436	34 66
^{211}Pb	β-	1378±8	100		
^{207}Tl	β-	1423±5	100		

1.1.8 Zinc oxide *ZnO*

Scintillation property of *ZnO* powder is well known for a long time [52]. Recently this substance was manufactured in the crystalline state by using the high temperature heating (1900°C) causing the powder melting and the high pressure [53]. Crystal size was Ø8x5 mm. Indium-activated crystal emitted the light radiation at λ_{max} = 395 nm with intensity of 10^4 photons/MeV, that is about equal the intensity of fast plastic scintillator. Light flash rise time was less than 100 ps, and fall time was < 1 ns. FWHM for fast

photoelectric multiplier (Hamamatsu R1564U-06) combined with plastic scintillator was ~ 1 ns, and with *ZnO* crystal was ~ 0.65 ns, that is record value. Ref. [54] cites the value of λ_{max} = 380 nm and luminescence time of τ = 440 ps with decay to 3.8 ns. According to [54] when *ZnO* is activated by *Ga* and *In* these parameters are decreased: luminescence time of 100 ns with decay to 1 ns. Decreasing the temperature leads to reduce of τ, that is 290 ps at 85 K, that is not typical for scintillation crystals. Usually the crystal cooling leads to increase of luminescence time.

ZnO is the more dense material than the plastic scintillator, non hygroscopic, stable within the wide temperature range, mechanically and radiation resistant, cheap. *ZnO* crystals are considered as the prospective scintillators for precise time measurements within the wide temperature range. Spectrometric properties of *ZnO* are a little better than that of plastic scintillators [55]. Figure 1.1.3 shows their comparative spectra.

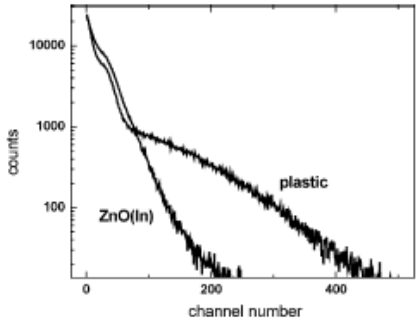

Figure 1.1.3 – Spectra obtained with plastic and *ZnO(In)* scintillators

Addition of ^{6}Li allows to obtain the neutron detector for fast counting rate applications [56]. *ZnO:Zn* ceramics also has good thermoluminescence properties [55]. Luminescence spectrum is presented on figure 1.1.4 referencing the *BGO*.

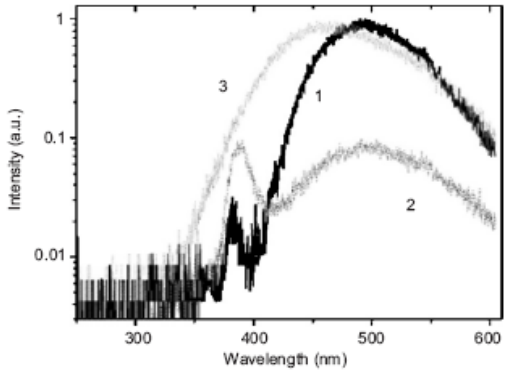

Figure 1.1.4 – Luminescence spectra of *ZnO:Zn* ceramics (1), *ZnO* polycrystal (2), and *BGO* (3)

1.1.9 Lutetium silicate $Lu_2SiO_5:Ce$

$Lu_2SiO_5:Ce$ or *LSO* belongs to the group of rare earths orthosilicates.

Detection efficiency depends to a great extent on the scintillator physical properties. Since the *LSO* crystal has monoclinic symmetry, the scintillator is not isotropic and has the dedicated optical axes. Coefficient of light gathering from different sides can differ.

LSO has:

- high light yield;
- good energy resolution;
- resistance to aggressive mediums;
- chemical and radiation stability;
- short luminescence time;
- high density.

There are some questions about peculiarities of *LSO* crystal structure and, correspondingly, its operating characteristics:

- monoclinity of crystal;
- biaxiality and presence of two independent luminescence centers;
- strong non-linear light yield dependence on the energy;
- thermoluminescence presence;
- crystal activation with following afterglow;
- contamination with own radioactive isotopes.

LSO crystals was studied [57] for detecting the light yield. Table 1.2 and Figure 1.1.5 present the study results.

Table 1.2 – Gamma energy dependence of absolute light yield

E_γ, keV	6.0	16.0	30.0	60.0	662.0
Light yield, photoelectrons/keV	13.3	16.3	23.2	23.9	27.6

Since the *LSO* refraction factor is rather large, the thin layer of substance with refraction factor of ~ 1.5 added between the scintillator and photocathode to provide the good optical contact. Different mineral and silicone oils were used for this purpose [58]. Sometimes the scintillator has been glued to photomultiplier photocathode with special optical adhesive. Light yield increase for crystal with oiling was 1.87 of the light yield for crystal without oiling.

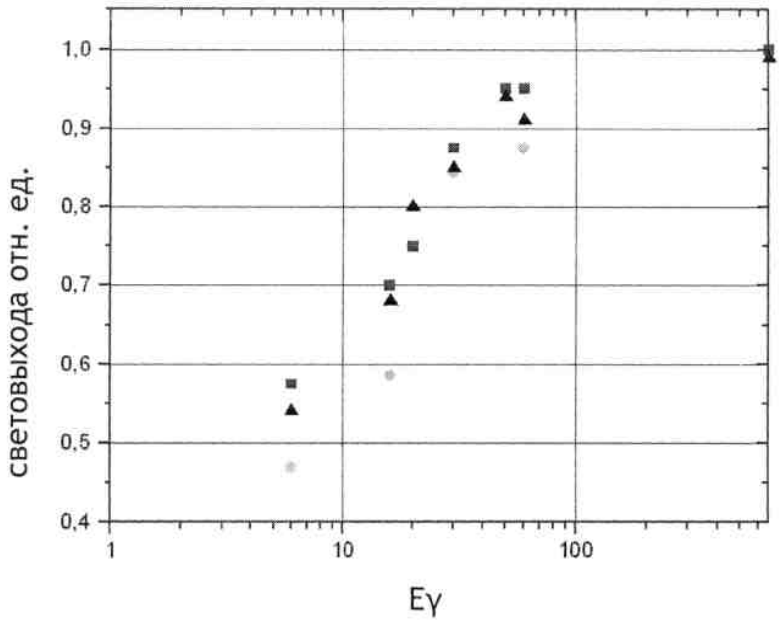

Figure 1.1.5 – Gamma energy dependence of the light yield

During the work the different types of investigated crystal packages have been studying. The most value of scintillation flash light yield was achieved for crystal packed in Mylar truncated cone with thin side surface as shown at Figure 1.1.6. The ratio of light yield for crystal with “cone”-type package to the light yield for unpacked crystal is 2.16.

The crystals investigated were grown by Czochralsky method at Research Institute «Polus» [58]. The samples was cut out of different forms from thin long “matches” to cubes of different dimensions. The least thickness of the crystals investigated was 0.7 mm.

The rare earth lutetium metal is used for crystal production, what has the radioisotopes. The raw charge includes both stable and radioactive isotopes of ^{176}Lu, what decay is accompanied with gamma ray emission with energy of 201.8 and 306.8 keV [57].

The afterglow of $Lu_2Si0_5(Ce)$ crystals of 1x1x1 mm with different *Ce* concentration [57,58] was studied under sun light irradiation for 10 minutes, see Figure 1.1.7. It was determined that the afterglow

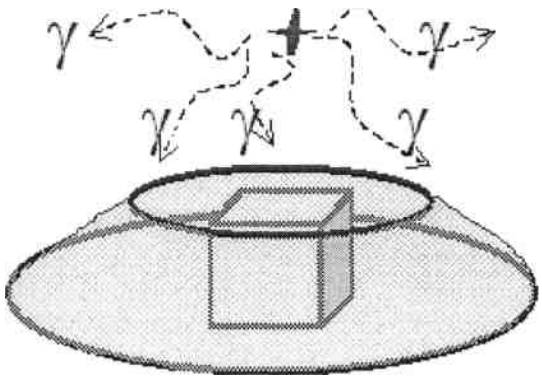

Figure 1.1.6 – Scheme of light-reflecting cone

consists of several components, what duration changes from a few minutes to a few hours. At this the afterglow intensity and duration depend on *Ce* concentration in crystal and radiation doze [59]. Crystal lattice defects in form of vacant sites (vacancies) and dislocations, point defects and cracks, impurities of foreign atoms promote the intensity and duration of afterglow.

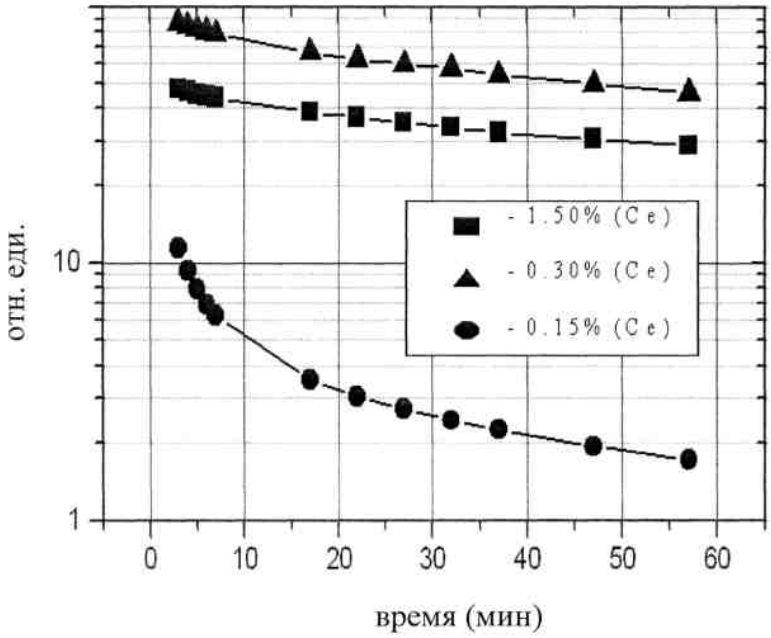

Figure 1.1.7 – Afterglow of $Lu_2Si0_5(Ce)$ crystals

Spectrum of gamma quantum of 511 eV is easy resolved from the noise spectrum of scintillator. Energy resolution results are well correlated with results obtained in Reference [60].

1.1.10 Cadmium tungstate $CdWO_4$

Monocrystals of cadmium tungstate $CdWO_4$ or *CWO* are relatively new scintillation material obtained in 90-s. High quality crystals are grown by Czochralsky method up to Ø60x150 mm [61].

Emission spectrum is basically located in “blue-gray” region of 500-600 nm, although spectra of some crystals are in the “red” region of 650-700 nm. Light yield is 19.5 photoelectrons/keV.

This crystal energy resolution for 662 keV energy is 7.5 % [62], that corresponds to *NaI(Tl)* resolution. So, the spectrometric characteriistics of *CWO* are not unique.

Presented below (chapter 2) is the *CWO* implementation for neutron detection.

CWO is most widely used in tomography and X-ray scanning installations both individually and in combination with *ZnSe(Te)* and *CsI(Tl)* [63].

1.2 Organic scintillators

Usually the organic scintillators are two-, three-component mixtures. Primary fluorescence centers are excited by colliding particles’ energy loss. When these excited states are decaying, the light is emitted

within the ultraviolet wavelength range. However, the absorption path for this ultraviolet is very short: the fluorescence centers are non-transparent for intrinsic emission light. Light is brought out by addition of the second component to scintillator that absorbs the primary emitted light and reemits it in isotropy with long wave length (so called spectra dislocator or shifter).

Two active components in organic scintillators are either dissolved in organic liquid or mixed with organic material in such a way to form the polymer structure. Such technology allows for production of liquid or plastic scintillator of any geometry.

Luminescence times of organic scintillators is much lesser (by order of a few to tens nanoseconds) than that of inorganic ones, but the light yield is less that that of inorganic ones.

Organic scintillators are widely used for detection and spectrometry of gamma radiation, since the back scattering form such scintillator surface is much lesser than that from detector with high atomic number. For this purpose the plastic scintillators with geometry providing the reduction of back scattering effect are used more often.

Organic scintillators (PM) are mostly presented by polymorphous state of styrene, vinyltoluene, vinylxylene, methyl methacrylate, chemically pure solar and others with different luminescent dopes – paratherphenyl, diphenyline oxazol, benzol, oxazol, POPOP, and others [3].

Polymerized structure converts to solid plastic scintillator, see Figure 1.2.1.

Different manufacturers and different countries use their own designations of PM scintillators. In Russian Federation PM scintillators are designated as ПСХХХ. Three figures determine the detector components. Number of hundreds determines the basic detector bode, number of tens determines the luminescent dope, number of ones determines the presence of shifters.

In many cases the plastics have advantages over inorganic scintillators due to their properties. First of all, it is their fast performance, transparency, and possibility to provide the high efficiency due to the large volume and almost any configuration at relatively low cost and high thermal stability of light yield, and easy of treatment.

Main disadvantage of PM scintillators is poorer energy resolution in comparison with inorganic scintillators.

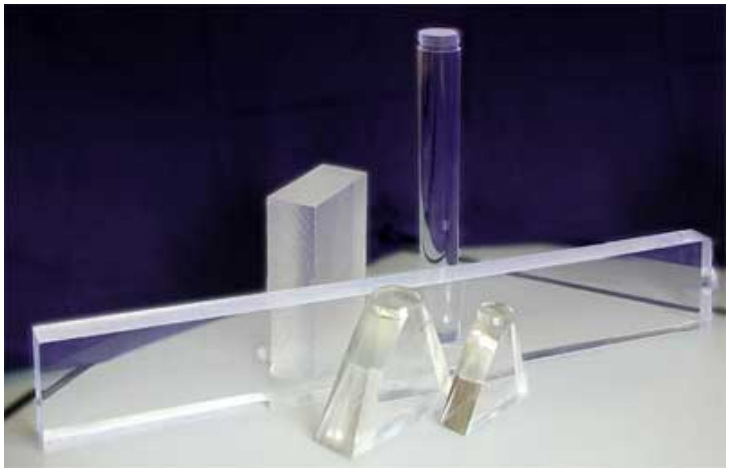

Figure 1.2.1 – Plastic scintillators

Traditional method of PM detector production is a mechanical treatment of scintillation composition pills obtained by polymerizing the luminescent dope solution in monomer. In addition to this method starting at the end of 80-s the PM scintillators are obtained from the melt without subsequent mechanical treatment [64]. This method allows for improving the thermostability of PM detectors.

Time resolution of PM-based detectors is up to 80 ps. Maximal size of PM scintilators is limited by intrinsic radiation attenuation length that can achieve 5 m. At this, the full energy pseudopeak arrises only at large PM volumes. Figure 1.2.2 demonstrates the intrinsic PM resolution [65].

PMs are usually used as guard detectors or in coincidence circuits, during control of radioactive containment or detection of separate reactions under condition of multiple events of ionizing particles interactions with material. At this, the intrinsic radiation background of PM considerably affects the detector sensitivity.

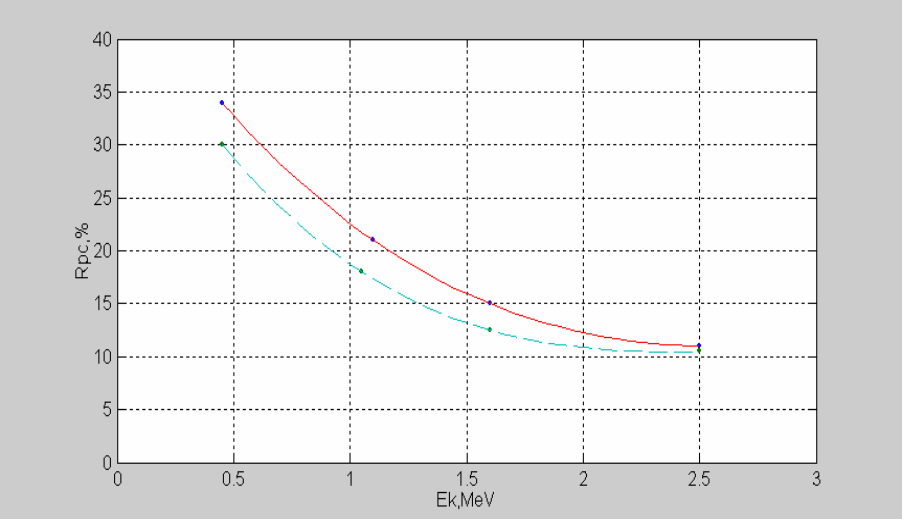

Figure 1.2.2 – Intrinsic resolution of the same volume PM detector of cylindrical (-) and squared (---) shape

Table 1.3 demonstrates the specific background activity of PM detectors [66].

Table 1.3 – Specific background pulse-repetition rate per 1 kg of scintillator for 1 s

Detector		Energy range (MeV)				
Body	Size (mm)	0.1-0.8	0.8-1.2	1.2-1.8	1.8-3.5	0.1-3.5
Polystyrene	80x80x40	9.390	0.026	0.026	0.016	9.441
Polystyrene	150x150	0.314	0.032	0.011	0.004	0.361
NaI(Tl)	63x63	0.156	0.022	0.018	0.007	0.203

The source of intrinsic radiation background are radionuclides of uranium-thorium family. The main contribution to gamma energy region below 0.5 MeV is from alpha-active members of that family. Uranium content in PM may be $(2\text{-}40)\cdot10^{-9}$ g/g, that is the low detection limit for PM.

1.3 Liquid scintillators

Liquid scintillators (LS) are mainly the organic compounds (base), into what the scintillating dope is added. The wide set of hydrocarbons is used as the base, namely, methylmethacrylate, methylnaphthalene, toluene, phenylethylamine, and others. Scintillating dopes are quate different, there are paratherphenyl, oxazol, phenyloxazol, xenyl. For neutron detection such dopes as *Li, B, Cd, Gd* are introduced in solution.

As well as for PM scintillators the different manufacturers and different countries mostly use their own designations. In Russian federation LS are designated as ЖС-XX. Two-figure number defines the detector material, dopes and their concentration [3].

LS are not spectrometric ones. Their basic advantage is the possibility to made scintillator of arbitrary large volume. In this connection LS are often used in fundamental studies of high-energy physics. In some cases LS are used for radiation monitoring. However this application has not been developed further because the monitor with LS has the characteristics similar to that of monitor with PM scintillators, but is much heavier, has the more complex design, and requires the delicate handling.

LS has the high *n*-γ separation capability, i.e. can separate the neutron and gamma components of radiation by pulse shape [67]. Table 1.4 presents the separation capability of different scintillators, what is determined by coefficient ξ

$$\xi = \sigma_n/\sigma_\gamma \ , \qquad (1.1)$$

where σ_n and σ_γ - ratio of number of pulses detected in slow component to number of pulses detected in fast component for neutron and gamma excitations, respectively.

Possibility of *n*-γ pulses separation can reduce the false alarm probability of portal monitors installed in places with neutron background.

Table 1.4 –*n*-γ separation capability coefficients (t_n and t_γ – durations of neutron and gamma pulses, respectively)

Scintillator	t_n, ns	t_γ, ns	ξ, rel.units
NE-213	350	950	6.3
ЖС-13	1130	2900	7.4
ЖС-65	500	1400	6.1
ЖС-76	530	1450	2.4
ЖС-77	470	1450	4.5

Toluylene	65	160	8.0

1.4 Nanocrystal scintillators

Institute of Solid-State Physics of Russian Academy of Science (RAS ISSP) has mastered several methods of nanocrystal scintillator synthesis [68] from water solutions or solutions in low-melting substances melt like ammonium nitrate. Oxides or nitrates of source components (for example, lutetium oxide Lu_2O_3) are first dissolved in these melts, and then are subject to low-temperature pyrolysis. At this, unreacted solvent is evaporated, leaving so called precursor in form of amorphous mixture of composition being synthesized (for example, lutetium borate $LuBO_3$) and residues of source nitrates and oxides. Subsequent low-temperature annealing the precursor leads to final nitrate decomposition with evolving the gaseous nitric oxide. At this, the gas escaping by microexplosions has separated and fined the grains of crystallized lutetium borate up to nanoparticles.

Peculiarities of structural and light-emitting characteristics of oxide and fluoride nanoscintillators allows for their wide application. Described below are possible directions of nanoscintillator applications:

1. Radiation detectors with enhanced energy sensitivity, energy, spatial, and angular resolutions (transmission inspection installations of antiterrorist, guard and custom designation, medical diagnostic devices, environment radiation monitoring systems).
2. Radiation detectors with essentially increased radiation resistance (on-line automated control of active atomic reactors and radioactive substance storages directly within the hot radiation zones), that can independently measure the radiation flows of gamma, beta and alpha radiations, protons and neutrons.
3. Super-high-performance radiation detectors for time-of-flight detection of three-dimensional, high-resolution images of human body internals, reveal of dangerous substances and items hided in closed spaces.
4. High resolution express *in vivo* diagnostics inside the living organisms of viruses, bacteriums, carcinogenic and other pathogenic bio-organelles. On-line destruction of pathogenic bio-organelles detected immediately during diagnostic séance.

Possibility and effectiveness of construction the regular structures like photon crystals from the nanocrystals require the additional discussion. Fist of all, there is the problem with delivery of the light emitted by nanoscintillators to photodetector irrespective of whether photon crystal contains the nanoscintillators or not. This problem is caused by high light dispersion at the nanoparticle edges. In that connection, as it is shown by practical experience, the photodiodes can gather the scintillation light at the thickness of nanoparticles layers below 0.5 mm, the more thick layers lead to great light losses due to the multiple reflections. As a result, the real nanoscintillation detectors are arranged by setting the sufficiently thin layers of nanoparticles (no more that mentioned above 0.5 mm) on the carriers transparent to the light

emitted by them that are used for light delivery to the photodetectors. These carriers can be made in form of the plates, light-guide rods or capillaries, what internal cavities contain the nanoparticles and transparent walls are light-guides delivering the light to the photodetectors.

1.5 Xenon gamma chambers

Development of cylindrical xenon gamma spectrometers with the shielding grid has been started in the eighties. Even the first samples of such detectors [69] allowed to obtain sufficiently good energy resolution (2.7 % for energy of 662 keV) and high efficiency of gamma radiation detection (about 15 %). Modern gamma detectors on the base of compressed xenon [70] has the much better parameters.

Figure 1.5.1 shows the general arrangement of xenon gamma detector. All internal detector elements, except of anode, are made of stainless steel and metalloceramics. External detector elements are made of Teflon and aluminum alloys. Chamber construction is designed for internal pressure of up to 100 atm.

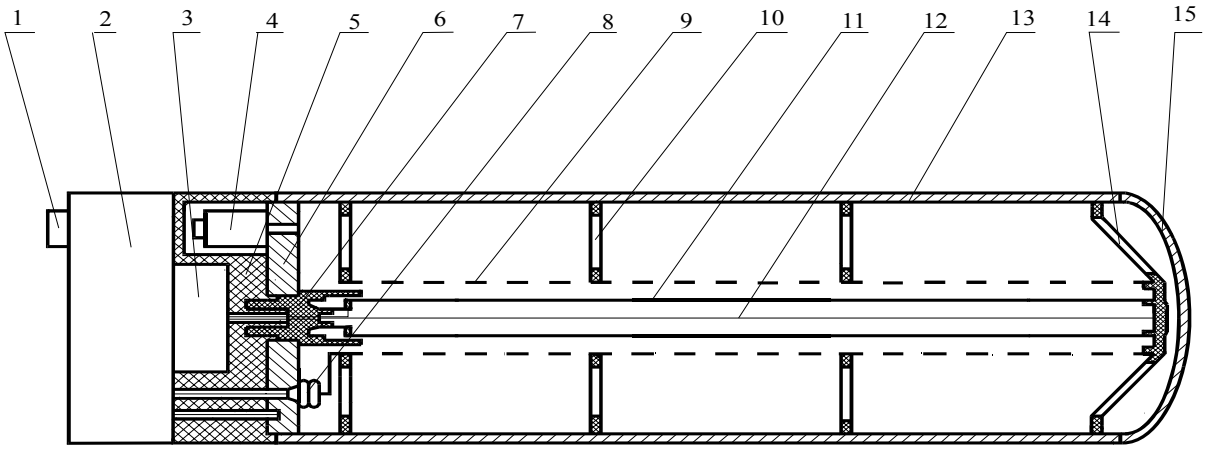

Figure 1.5.1 – General arrangement of cylindrical gamma spectrometer with the shielding grid. 1 - connector, 2 – high voltage power supply, 3 – charge-sensitive amplifier, 4 – valve, 5 – Teflon insulator, 6 - flange, 7 – metalloceramics pressure seal, 8 – high voltage input for the shielding grid, 9 – shielding grid, 10 – vibroprotective ceramic insulators, 11 - anode, 12 – metal filament with zero potential, 13 - body, 14 – figured ceramic insulator, 15 – ellipsoidal lid.

Detector's chamber has intrinsic electronics block. It includes charge-sensitive amplifier, connectors for high voltage to the shielding grid and chamber body, small high voltage filter for voltage stabilization on the grid and small-sized high voltage power supply. High voltage power supply is powered with - 24 V and forms the 12.5 kV and 21.5 kV potentials for the shielding grid and cathode of cylindrical detecting chamber. At this its consumption is no more than 20 Wt.

External insulation coating made of Teflon film isolates the chamber body with high potential from the environment.

Listed below are general technical characteristics of gamma detector with the shielding grid:

- operating gamma energy range is 50 – 5000 keV and depends on detector volume;

- high energy resolution: 2 % - for energy of 662 keV (^{137}Cs) and 1.5 % for energy of 1170 keV (^{60}Co);
- neutron activation degree is 20 times lesser that of scintillation detectors on the base of *NaI*;
- liquid nitrogen or any other additional cooling systems are not required; operating temperature range of xenon gamma detectors is 10-200 ^{o}C;
- possibility of gamma spectrometers of 0.2 to 10 l working volume (0.1–5 kg of xenon) for different applications;
- energy resolution independence on the volume of working substance (xenon);
- operating life time is more than ten years;
- considerable low cost relative to semiconductor spectrometers.

One of that detector advantages is high energy resolution as against the scintillation detectors. In the point of energy resolution view they can be placed between solid-state (semiconductor) and scintillation detectors and provide the resolution of about 13-16 keV.

Figure 1.5.2 demonstrates the typical gamma spectra measured with this detector during 2000 sec, when gamma sources are perpendicular and parallel to the main detector axis at the distance of 100 cm from its sensitive surface.

Figure 1.5.3 shows the energy resolution dependence of xenon and *NaI(Tl)* detectors on gamma rays energy. This dependence has characteristic declining feature: the higher energy corresponds to the lesser energy resolution. For comparison this figure includes the energy resolution values measured for scintillation *NaI(Tl)* crystal of 200 mm diameter and 100 mm height. As shown in the figure, the energy resolution of compressed xenon-based gamma detector within whole region of interest at least 4-5 times better that that of scintillation gamma detector.

Xenon detector has two detection efficiency: for side and front measurements. Efficiency of gamma full energy peak detection was measured with gamma sources placed at the distance of 1 m from detector. The results obtained for the most typical gamma-line energies are listed in Table 1.5 [71].

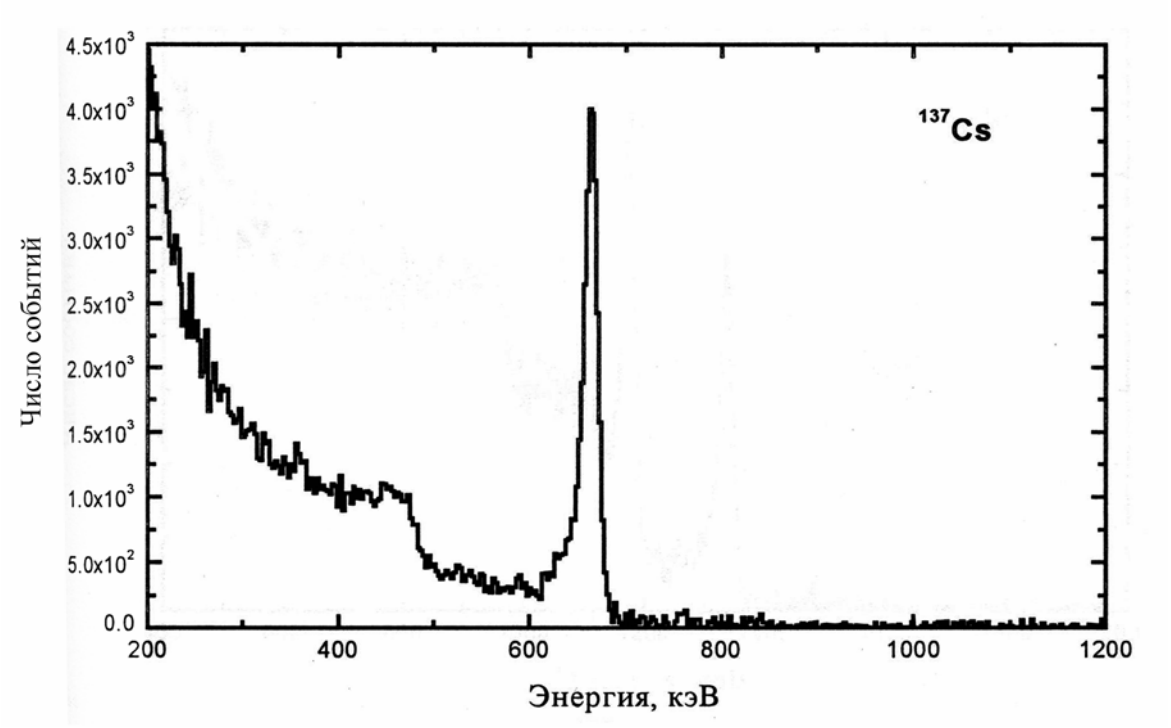

Figure 1.5.2 – Spectrum of ^{137}Cs gamma source measured with *Xe*-detector in perpendicular direction at the distance of 100 cm during 2000 s, FWHM =15.5 keV

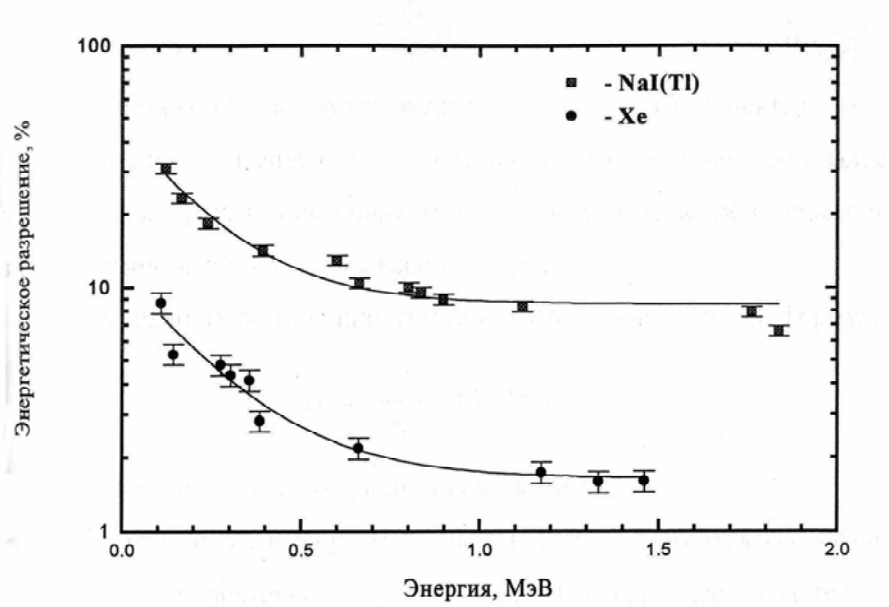

Figure 1.5.3 – Dependence of gamma detector energy resolution on gamma rays energy for xenon and scintillation detectors

Table 1.5 – Detection efficiency of gamma detector for typical gamma radiation energies.

Energy	Detection efficiency (%)	
	In perpendicular	In parralel
662	3.3 ± 0.2	10.8 ±0.4
1173	1.5 ±0.2	4.0 ± 0.2
1332	1.2 + 0.2	3.3 ±0.2

Dependence of full energy peak position on the energy of gamma rays is linear. Disalignment is no more than 1 % within the energy range of up to 1.5 MeV.

1.6 Semiconductor detectors

At present the solid state semiconductor detectors (SCD) occupy the leading position in gamma and X-ray spectrometry. It is mainly caused by their resolution capability providing the precision spectrometric measurements. There are prospects of creating the crystals on their base with enough large sensitive volume to increase the detection efficiency.

Detectors on the base of germanium and silicon are mainly used. In comparison with other semiconductor materials such as, for example, *HgI_2, CdTe, GaAs*, they have much better characteristics that allows manufacturing the solid-state detectors with record energy resolution but high cost.

Table 1.6 demonstrates the basic characteristics of the most often used solid-state detectors.

1.6.1 Germanium SCD

At present, germanium- and silicon-based SCD are made of two types: planar and coaxial. The most widespread detectors are so called drift-lithium ones, in what the acceptor impurity atoms are compensated by lithium ions. Such detectors are designated as *Si(Li)* and *Ge(Li)*. Planar *Si(Li)* and *Ge(Li)* detectors are used for detecting the X-ray and low energy gamma radiation from energy of 10 keV. Coaxial *Ge(Li)* detectors are used for detecting the gamma radiation with energy below 10 MeV.

Table 1.6 – Basic characteristics of some semiconductor materials [72, 73]

Material	Wide of energy gap (eV)	Effective charge	Density (g/cm)	Energy for electron-hole pair (eV)	Operating temperature (K)	Mobility ($cm^2/(V·s)$)		Carrier life time (s)	Resolution (%)
						electron	hole		
Ge	0.67	32	5.33	77	2.96	3600	4200	$2.5·10^{-5}$	0.46
Si	1.1	14	2.33	77 300	3.76 3.61	2100	1100	$2.0·10^{-5}$	-
GaAs	1.35	31.33	5.36	130 300	4.51 4.2	8600	400	10^{-8}	2.60
GaSe	2.03	31.34	4.55	300	6.3	60	215	10^{-9}	-
GaP	2.2	23	4.13	-	-	300	150	10^{-8}	-
CdTe	1.5	48.52	5.86	300	4.43	1050	80	10^{-6}	3.80
CdSe	1.7	41	5.74	-	-	650	-	-	-
HgI_2	2.26	80.53	6.40	300	4.2	100	4	10^{-6}	3.50

At the beginning of eighties the new methods of *Ge* purification were developed [73], that allows growing the large crystals of high pure germanium HPGe with electrically-active impurity atoms concentration of less than $2\text{-}10^{-10}$ 1/atom. HPGe can have the self-conductance of n- or p-type depending

on the purification efficiency. In this connection the high pure germanium detectors are designated as HPGe(p) and HPGe(n).

The main advantage of HPGe-based detectors is the possibility of their storage at the room temperature in contrast to *Ge(Li)* detectors that should be stored under the liquid nitrogen temperature. Besides, the HPGe-based detectors can be of the larger size than *Ge(Li)* detectors. It allows for creating the gamma radiation detectors not only with high energy resolution but with good efficiency in the region of gamma radiation detection. Characteristics of some SCD made of high pure materials are listed in Table 1.7.

Table 1.7 – Characteristics of SCD made of high pure materials [74]

Detector type	Geometry	Operating energy range	Material	Size*	Energy resolution (keV) at 1.33 MeV
GEM	Coaxial	40 keV to 10 MeV	P - type HPGe	10%-100%	1.75-2.30
GMX	Coaxial	3 keV to 10 keV	N –type HPGe	10%-80%	1.80-2.40
GLP	well	10 keV to 10 MeV	P - type HPGe	70%-120%	2.10-2.30

*- is given in % efficiency relatively to *NaI* of 3x3 inches.

There should be noted some peculiarities of HPGe(n) and HPGe(p) detectors [74, 75]. Detectors on the base of n-type germanium are more sensitive to low energy gamma rays in comparison with Si detectors. Detectors have the best energy resolution of 118 eV at 5.89 keV and efficiency of 20 % up to 200 keV.

Another advantage of HPGe(n) detectors is their higher radiation resistance [76] and possibility of operation under intensive neutron flows.

The new possibilities of HPGe-detector applications are caused by development of crystal segmentation technology. HPGe detector segmentation technology was developed at the end of 80-s [77] and is based on dividing the detector into two segments – upper (top) and side. Upper layer (segment) is used for detecting the low energy gamma rays with energies below 150 keV. The main process of gamma ray interactions in this region is the photo effect. Compton photons and background events are rejected by lower (bottom) segment included in anticoincidence circuit. High energy gamma rays are detected by bottom segment that is shielded from low energy gamma rays by upper segment.

Segmentation allows for increasing the sensitivity of HPGe-based spectrometer in a several times.

At present, the maximal volume of HPGe(n) crystals is about 200 cm^3, and that of HPGe(p) crystals is 350 cm^3 [78]. Arrays of HPGe(n) detectors are used for obtaining the high sensitivity.

Radiation resistance of solid-state gamma spectrometric detectors is much lesser than that of scintillation detectors and considerably depends on the radiation type, crystal type and size. During operation the characteristics of those detectors can notably change, since the irreversible radiation damage can accumulate in the crystals under the influence of ionizing radiation. Different types of ionizing radiation interaction with detector material cause the defects in its crystal lattice that, in most

cases, grow proportionally to radiation doze. The larger size of solid-state detector, the earlier its energy resolution degrades under ionizing radiation.

For neutron radiation, the threshold value of total neutrons passed through the solid-state gamma detector unit of square, from what the energy resolution starts to degrade, is 10^7-10^8 cm^{-2} depending on the crystal size [79].

Significant influence of densely ionizing radiation on the basic characteristics of solid-state detectors makes essential difficulties for their long-term operation under proton or neutron flows.

So, in spite of the fast development of germanium-based semiconductor detector technology, the basic problems restraining the wide use of these detectors are extremely difficult production process, high cost, relatively low radiation resistance, and need in cooling to cryogenic temperatures.

1.6.2 Gallium arsenide *GaAs*

Parameters listed in Table 1.6 show that the gallium arsenide (*GaAs*) is one of prospective materials for production of uncooled detectors of ionizing radiations. Using the adequate technology of detector production its can be used uncooled. Very important *GaAs* advantage among all listed materials is the highest electron mobility at the room temperature. Holes also have the good mobility. Components of this compound have high atomic numbers (Z_{Ga} = 31, Z_{As} = 33) that allows obtaining almost the same X-ray and gamma detection efficiency as for germanium detectors of the same volume.

Unfortunately, now the detectors on the base of semi insulating and high-resistance *GaAs* are suite only for particles detection [80], but not for spectrometry. Detectors with spectrometric properties first were obtained on epitaxial layers of *GaAs* grown by liquid phase epitaxy method.

Because of the small (50—100 μm) thickness of epitaxial layers the *GaAs*-detectors on their base are suitable only for X-ray and low energy gamma radiation spectrometry. Such detectors have sufficiently high energy resolution. For example, the resolution of 2.5 keV at 59.54 keV gamma line of ^{241}Am and 2.6 keV at 122 keV line of ^{57}Co was obtained at the room temperature [81]. At this, the resolution was mainly determined by noises of detector-preamplifier system.

The possibility of creating the spectrometric detectors on the base of high pure doped crystals of *GaAs* was studied. Detectors made on the base of iron-doped epitaxial layers had sufficiently good spectrometric characteristics: resolution at T=300 K for α-particles of ^{241}Am (E_a=5.49 MeV) was 17.2 keV, and for gamma line of ^{57}Co (E_γ = 122 keV) was 3.8 keV for detector with epitaxial layer thickness of 100 μm [81]. The result obtained for gamma photons was completely caused by electronics noises.

To increase the gamma radiation detection efficiency the attempt was made to produce the detectors with two surface barriers at the opposite plate sides. Two-barrier structure allowed for 20 % increasing the detection efficiency for ^{235}U gamma radiation with energy of 185 keV.

The results obtained with epitaxial layers grown by gas-transport epitaxy method worth to be noted [82]. Detector of 2 mm^2 square with epitaxial layer thickness of 300 μm has shown the reverse current of $1.2 \cdot 10^{-9}$ A at bias potential of 250 V. At this potential the energy resolution for 122 keV gamma line (^{57}Co) was 1.9 keV, for 59.54 keV line (^{241}Am) – 1.7 keV, and for 22.4 keV (X-rays from ^{237}Np) – 1.5 keV at the room temperature.

Small thickness of epitaxial layers and small working surface of *GaAs*-based detectors prevent from their wide application as the uncooled spectrometers. However, in cases where size is not critical, due to the small currents the detectors made of gallium arsenide has advantage over the silicon detectors.

1.6.3 Cadmium telluride *CdTe*

Recently the solid-state detectors on the base of *CdTe (CdZnTe)* crystals find the more and more wide application for detection of gamma radiation. Thanking to improving the production technology the crystals are made with required and, in some cases, unique physical properties, that allows for creating on their base the ionizing radiation detection units with good spectrometric and operating characteristics.

They have the high radiation detection efficiency, relatively good signal/noise ration, and high energy resolution at the room temperature. Linearity in counting and current operating modes within the wide range of measured dose rate and high radiation resistance of this material [83] allows for its use at production of dosimetric units with large radiation resource.

It favors to prospective using of detectors on the base of *CdTe* and *CdZnTe* both in systems of dosimetric control at nuclear fuel production, use, and reprocessing facilities and in spectrometric systems used for radionuclides assay.

Reference [84] has shown the possibility of spectrometric measurements of X-ray, gamma, and alpha radiations with such crystal. All studies was carried out with crystal thickness of 0.8 and 2 mm.

Figure 1.6.1 shows the ^{241}Am and ^{152}Eu spectra obtained with *CdZnTe* detector with crystal thickness of 0.8 mm. The bias potential of 70 V was applied to detector crystal; the shaping time constant was 2 μsc. Working surface of detector was not collimated during the measurements. Full width at half maximum for 40.11 keV line ($K_{\alpha 1}$ - line of *Sm* arising as a result of ^{152}Eu atoms' β^+ decay) is about 5 keV that corresponds to relative resolution of 12 %.

The presented results show the possibility of *CdTe* (*CdZnTe*)-based detector use for detection of characteristic K-seris X-rays of heavy elements during XRF analysis and spectrometry.

In addition to gamma radiation, the study of spectrometric characteristics of *CdZnTe* was carried out in [84] for charged particles. Detector crystal of 5x5x1 mm was placed in the shielded chamber. Detector bias supply was selected as 100 V, pulse shaping time - 2 μs. Working area in the crystal center was selected by collimator of 3 mm diameter. To study the detector characteristics and select the optimal operating conditions the following alpha sources were used: ^{226}Ra, ^{233}U, ^{239}Pu, ^{238}Pu. The sources were

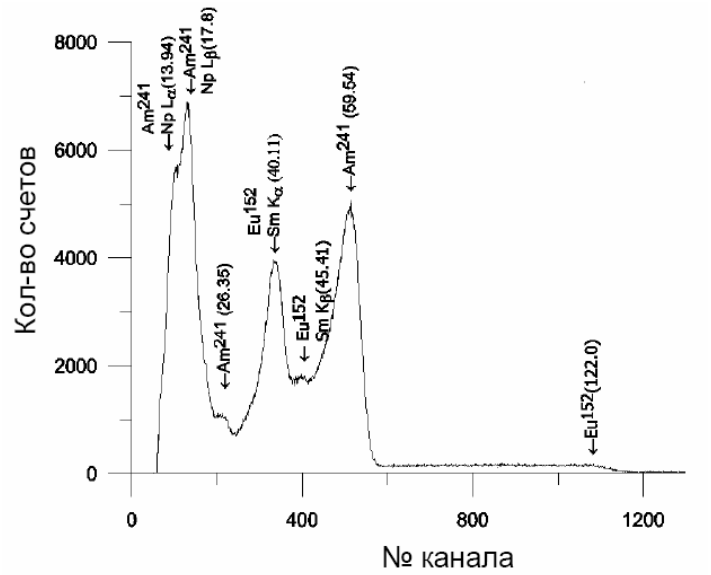

Figure 1.6.1 – Gamma radiation spectra of ^{241}Am and ^{152}Eu

placed by turn at the distance of 15 mm from the crystal surface. Measurements are performed in the air. Figure 1.6.2 demonstrates the alpha spectrum obtained for ^{226}Ra source.

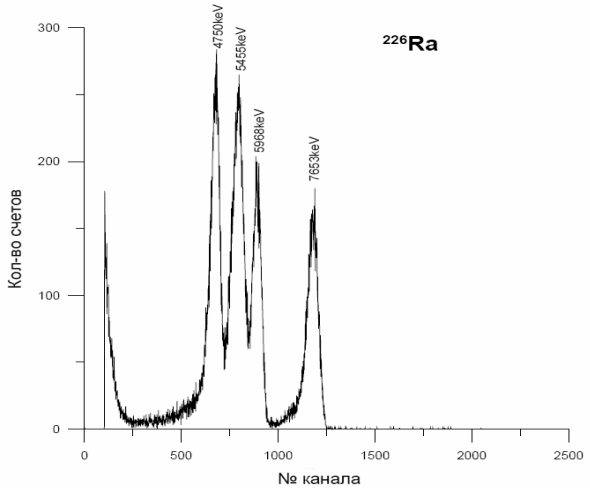

Figure 1.6.2 – Alpha spectrum of ^{226}Ra source.

The studies carried out have shown the possibility of *CdTe* (*CdZnTe*)-based detector use for detecting the characteristic K-series X-rays from heavy elements during XRF analysis and gamma radiation spectrometry.

Detection units with *CdZnTe* detectors have the energy resolution at the room temperature that is satisfactory for some practical applications. Ionizing radiation spectrometer has been developed and manufactured that can be used as the analyzer of radionuclide spectrum within the energy range of 20 keV to 3 MeV with energy resolution up to 10 % (59.6 keV, ^{241}Am).

In whole, the cadmium telluride detectors are inferior to germanium detectors in efficiency and energy resolution, so they used for specific measuring applications, especially when manufacturing the compact detectors.

Further enhancement of spectrometric characteristics of these detectors makes its possible to widen their application. This may be achieved by both increasing the quality of the crystal itself production, and enhancing the parameters of other components of detection unit, for example, by reducing the noise by use of thermoelectric coolers, and using the processor for preliminary pulse shape processing. When pulses are discriminated by the shape, the energy resolution improves from 40 to 9 keV [84].

1.6.4 Mercury two-iodide HgI_2

First message on use of tetragonal mercury two-iodide as uncooled detector of ionizing radiations appeared in 1971 [85]. That study demonstrated the prospects of mercury two-iodide use for X-ray and gamma radiation spectrometry.

The plates of 0.5-1 mm thickness are usually used for manufacturing the spectrometric detectors on the base of HgI_2. At the present-day technology level of detector production the high specific resistance of HgI_2 (10^{13}—10^{14} ohm/cm) provides the low leakage currents (10^{-10}—10^{-12} A) down to the voltages of 2000—2500 V. Sharp increase of dark current and, correspondingly, detector noises is observed at the temperatures starting from 55 °C. Change in counting detector efficiency in the range of (-40)–(+50) °C doesn't exceed 10 % [86].

Study of counting efficiency in the full energy peak of HgI_2-detectors have shown that after bias supply to detector with sensitive area thickness more than 1 mm, the energy spectrum shape is changed with time, that is explained by effect of detector polarization. Polarization effect is also observed in thinner crystals, at this, it so more then more intensive the radiation flow and lesser the bias applied to detector. One more reason of HgI_2-detector spectrometric characteristics degradation is the accumulation of radiation defects in the detector sensitive area [87].

Improvement of HgI_2 growing methods allows for significant enlarging the sensitive volume of detectors and achieving the higher spectrometric results. Thus, for example, for detector of 10x8x0.5 mm there was obtained the resolution of 1.2; 2.0 and 4.5 keV at the energy of 60; 122 and 662 keV, respectively [85].

The greatest progress was achieved in manufacturing the small volume detectors intended for X-ray spectrometry at the room temperature. Good results were obtained for low energy X-ray spectrometry [87].

According to [88], the resolution of X-ray HgI_2-spectrometer can be improved by moderate cooling of detector. It was found, that the temperature near 0° C is optimal. Results show that in low energy region the spectrometric properties of HgI_2-detectors are close to those of silicon detectors. However, at higher energies the resolution and efficiency of HgI_2-detectors are essentially worse that of silicon detectors. Best resolution for 1 mm thickness HgI_2-detectors is 5 keV at 662 keVB (^{137}Cs) [89], but counting efficiency of that detectors is much lesser that efficiency of large germanium detectors.

Most of detectors on the base of HgI_2 with sensitive layers above 1 mm have the poor spectrometric characteristics due to short drift length of carriers that prevents to full charge accumulation. However, in some applications not requiring the spectrometry, thick HgI_2-detectors can have some advantages over other counter types, for example, as against the scintillation detectors that have larger size and require high voltage power supply for photomultiplier operation. These advantages include the small weight and volume of thick HgI_2-detectors, as well as small power consumption. Using the thick crystals of HgI_2 the portable counters for gamma radiation fields control can be created.

On the base of large crystals grown by method of temperature oscillations the portable gamma counters were made with sensitive area thickness up to 1.5 cm and active surface up to 17 cm^2 [88]. When bias supply was 1000 V/cm the leakage current didn't exceed 100 pA that allows to use the high voltage capacitor requiring periodic charging every 8-20 hours for bias supply in portable variant of the counter. Gamma radiation detection efficiency of such detectors was equal to Ø3.8x3.8 cm *NaI* scintillator.

Figure 1.6.3 shows the ^{137}Cs and ^{60}Co spectra demonstrating the spectrometric properties of HgI_2-detectors with thickness of 1 cm. As Figure 1.6.3 indicates, they can obtain the fully separated peaks even for gamma radiation energy more than 1 MeV. Spectra are close to those obtained with *NaI* scintillators of equivalent efficiency.

Unexpected result was obtained in work [90] during the study of radiation resistance of HgI_2-detectors when they were irradiated with fast neutrons (E_n = 8 MeV). HgI_2-detector signal amplitude negligibly changes right up to 10^{15} cm^{-2} fluence, while the signal of *CdTe*-detectors sharply drops as early as at 10^{11} cm^{-2}, and that pf silicon detectors – at 10^{13} cm^{-2}. Energy resolution of HgI_2-detectors for α-particles with energy of 5.5 MeV is almost constant in the fluence range of 10^9 to 10^{15} cm^{-2}. Thus, detectors on the base of HgI_2 can operate as the charged particle spectrometers with moderate resolution under neutron filed of high intensity.

Reference [91] made conclusion on principal possibility to obtaine the same energy resolution with uncooled HgI_2 as with cooled *Si(Li)* and *Ge* SCD. Real values of uncooled HgI_2 energy resolution are essentially worse that calculated data. The main reasons are electronics noises up to photon energy of 30 keV and charge gathering fluctuations due to inhomogeneity of detector sensitive volume properties.

2 Neutron detectors

To detect the neutron radiation, the secondary radiation (alpha or gamma) is most often used that produces following ionization within the working volume of detector. So the gas fillings or scintillation materials are also used for neutron detection, what contain the nuclides with high neutron (mostly thermalized) cross-section. Such nuclides are ^1H, ^3He, ^6Li, ^{10}B, *Cd,* and *Gd* in natural mixture, ^{235}U. So all thermal neutron detectors contain the nucleus of these nuclides in one or another way - either directly in the composition or as an external radiator. For example $CdWO_4$ *(CWO)*, $Gd_2SiO_5(Ce)$ (*GSO*).

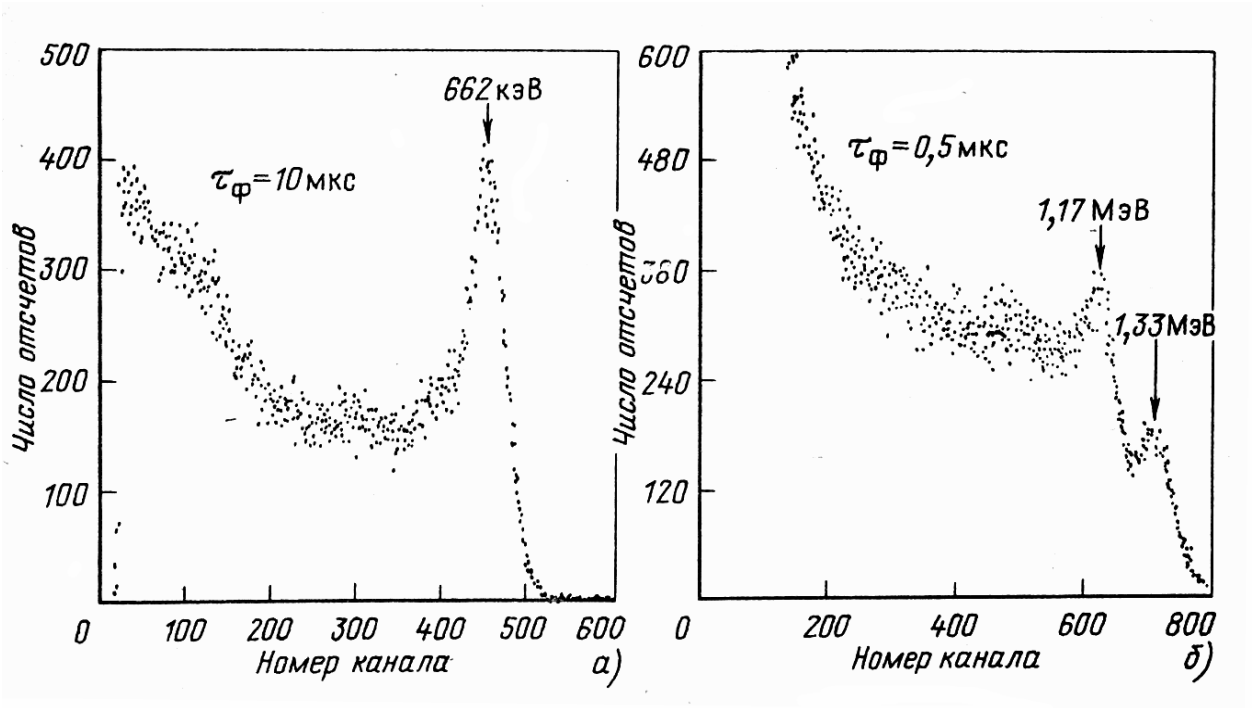

Figure 1.6.3 – Gamma spectra of ^{137}Cs (а) and ^{60}Co (б) measured on 1 cm width HgI_2-detector

The scintillators take the great place among the neutron detectors. As well as for gamma radiation the neutron scintillation detectors are divided into three main groups – solid, liquid, and gaseous. The solid detectors are presented by inorganic and organic poly- and monocrystals. Among liquid detectors there are mostly the organic compounds. Base of gas-filed detectors is ^{3}He and gaseous compounds of *Li* and *B*.

Given review will not consider the fast neutron detectors and fission chambers because of essentially lower (by two and more orders) detection efficiency.

PM-based detectors are very convenient for neutron detection. Hydrogenous body of plastic detector, in what any dopes can easily be added to, is neutron moderator itself. Almost unlimited volume and configuration of plastic detector allows for high efficiency of neutron detection. Recently achievements allows for using another PM advantage – its high fast performance (see below).

Also the important technological achievement is possibility to manufacture **PM fiber-scintillators**– PM tubes [92]. These tubes, having the advantages of PM scintillators, are flexible and can be used as optical fibers (light guides).

LiI scintillator has the high cross section of $^{6}LiI(n,\alpha)T$ reaction on the thermal neutrons. Thermal neutron detection efficiency achieves 80 %. However, at this the gamma quanta can be detected also. To separate the neutron peak the second scintillator with low neutron detection efficiency is used. Gamma spectrum is subtracted from total spectrum, obtaining as a result only the gamma lines caused by neutron interactions.

In Reference [93] *NaI(Tl)* is used as a second scintillator. Result and principle of operation of such detector are clear from Figure 2.1.

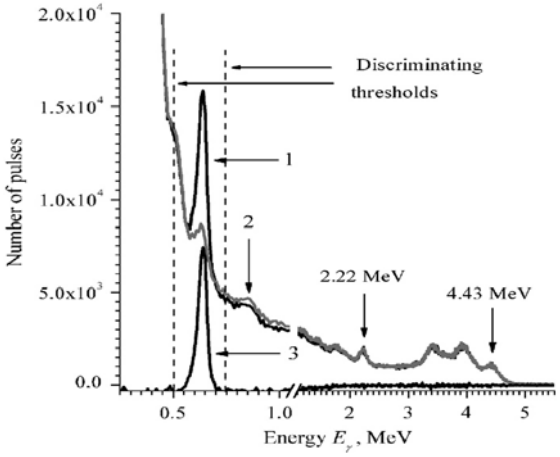

Figure 2.1 – Gamma spectra of *Pu-Be* neutron source obtained by *LiI+ NaI(Tl)* detector (curve 1), *NaI(Tl)* detector (curve 2) and differential resulting spectrum (curve 3)

In Reference [94] there used the monocrystal ***CWO*** for neutron detection, and two filters: *LiI* powder of 10 mm thickness – for neutrons and *Pb* of 50 mm thickness – for gamma quanta.

Gamma radiation specific for neutron interactions with scintillator body and moderator is detected: 145.8 keV and 273.4 keV – peaks of radiation capture on ^{186}W nuclei and 558 keV on ^{113}Cd nucleus, 2.22 MeV – line of thermal neutron absorption by hydrogen nucleus. Figures 2.2, 2.3 present two energy regions of *Pu-Be* neutron source gamma spectrum obtained with *CWO* crystal of Ø40x40 mm [95]. Spectra were obtained by using the gamma and neutron filters (50 mm of *Pb* and 10 mm of *LiF*).

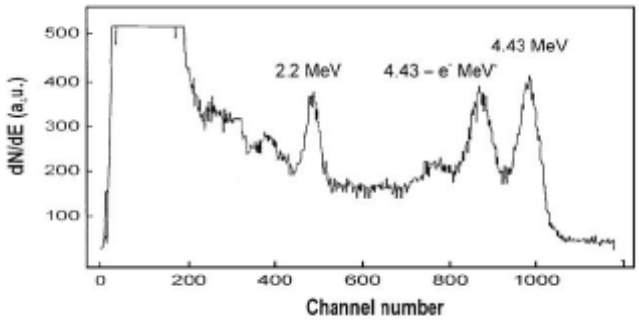

Figure 2.2 – Amplitude spectrum of *Pu-Be* source obtained with *CWO* crystal (high energies)

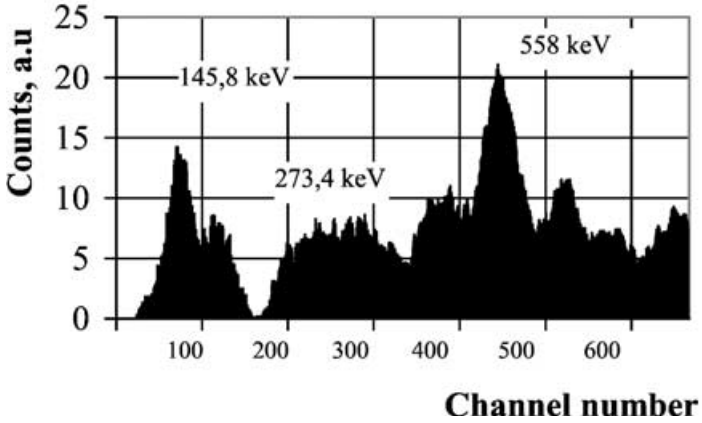

Figure 2.3 – Amplitude spectrum of *Pu-Be* source obtained with *CWO* crystal (low energies)

Table 2.1 demonstrates the comparison of neutron detection efficiencies for $^{6}LiI(Eu)$, *GSO*, *CWO* scintillators.

Table 2.1 – Thermal neutron detection efficiencies

Scintillator	Detector	Detector size	Energy of secondary particles or γ-quanta (keV)	Detection efficiency (%)
$^{6}LiI(Eu)$	Monocrystal	25x2	$^{6}Li(n,\alpha)T$	87
GSO	Crystal	63x3	30-1000	67
CWO	Crystal	80x2	20-100 30-1000	3.4 11.8
CWO	Monocrystal	40x40	30-1000	14.3

Use of ***BGO*** scintillator for neutron detection is described in chapter 1.1.3.

Figure 2.4 demonstrates the neutron spectrum obtained with plastic and *BGO* scintillators and capabilities of the standards on energy calibration [21].

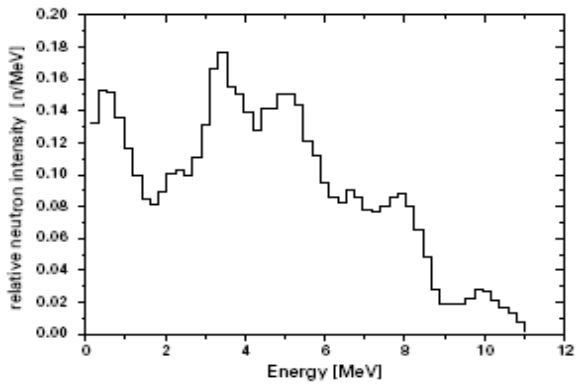

Figure 2.4 – Energy distribution of *Am-Be* source neutrons detected by combined *BGO*-plastic detector

3 Gas counters

3.1 Gas-filled counters

Classic gas-filled counters of X-ray, gamma and neutron radiation are well known and didn't essentially change by now [96,97].

Spectrometric gas-filled detectors of X-ray and gamma radiation are mostly used in equipment for substance content analysis and are between SCD and *NaI(Tl)*. They don't require low operating temperature, have high gas amplification factor, resistant to temperature and vibration influence, and relatively cheap. Disadvantages are low detection efficiency, load limitation (because of destruction and precipitation of quenching dopes on the electrodes and counter wells), spectrum distortion at high load.

Maximal thermal neutron detection efficiency of ^{3}He-counters is high and achieves 80 %. Detection efficiency of boron counters with BF_3 filing is several times lesser.

Neutron and gamma gas counters are often used in the field and industrial conditions, especially in Geiger-Muller mode, due to simplicity of recording electronics and reliability of detectors [98].

The new type of gas-filled detector on the base of Gas Electron Multiplier (GEM) is very interested. This detector was proposed by F. Sauli in 1996 at CERN [99] and is the most successful invention of last decades in the field of ionizing radiation detection, especially as applied to fundamental research in nuclear physics and elementary particle physics field [100].

3.2 Radiation detectors on the base of gas electronic multipliers

Gas electronic multiplier is the thin dielectric polyimid (Kapton) film of 5 μm thickness, both sides of what are covered with copper foil of 5 μm thickness with a number of holes, see Figure 3.1.

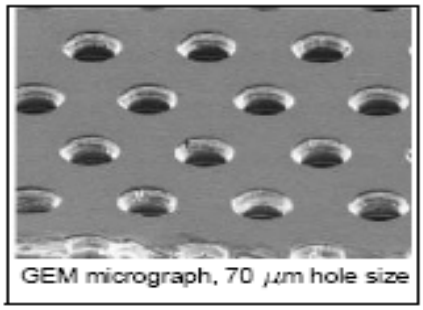

Figure 3.1 – Structure of GEM

Holes are double cone-shaped and arranged in form of hexagonal array with 140 μm spacing and diameter of 60-80 μm on metal and 40-60 μm in the film center. GEM is produced by using the photolithography and chemical etch of the metal and dielectric on the both film sides.

When supplying the voltage of 400-500 V between the metal electrodes the high electric field of ~50 kV/cm strength arises in the holes. When reducing the hole diameter, the electric field in the hole approximates to the field of in-plane interval.

Primary electrons born by radiation in the gas gap in front of GEM drift along the force lines and are focused in the holes, where avalanche is developed under exposure of electric field. Thus, each hole is an independent proportional counter. Appreciable part of avalanche electrons can leak from the holes to the gas gap, that can be used for amplification in subsequent cascades or for detection at anode reading electrode. The GEM capability of operation in cascade configuration is one of its advantages over other gaseous detectors.

Unique property of GEM-based detectors is the possibility of spatial separation of amplification processes and visualization of event with good resolution.

Reference [101] proposed the GEM-based neutron detector structure, see Figure 3.2. Thickness of *Gd* and *CsI* layers is 5 μm. At this, the detection efficiency is 5%.

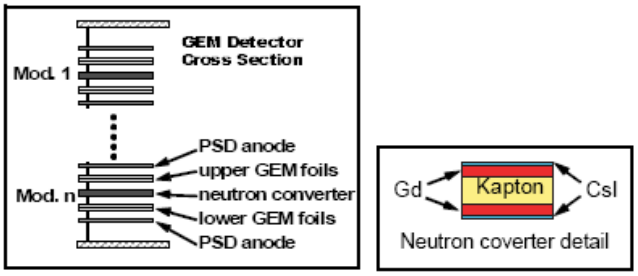

a) b)

Figure 3.2 – GEM-based neutron detector: a) basic structure; b) scheme of neutron converter.

4 Solid-state photoelectric multipliers (photodiodes)

Conventional and wide used scintillator-photodiode system allows for detecting the ionizing radiations within the wide energy and intensity range in 10-100 ns with energy resolution of about 10 %. Photoelectric multipliers (PEMs) have the following disadvantages: in-time instability of characteristics, high voltage supply, insufficient mechanical strength and weight.

Alternative to conventional vacuum PEMs are solid-state photoreceivers presented by photodiodes (PDs) that have some disadvantages until recently, namely, lack of internal amplification and high dark current preventing of weak light signals detection. Now, with developing the electronics the photoreceivers become more actual and have such advantages over the vacuum PEM as lower power supply, lower power consumption, small dimensions and low weight, higher reliability and stability of characteristics, insensitivity to magnetic fields, high linearity of luminescent characteristics within the wide (up to eight orders) range of light flux intensity [102].

At present, there are 3 types of photoreceivers:

- avalanche photodiode;
- silicon photoelectric multiplier
- PIN photodiode;
- metal-dielectric semiconductor photodiode.

4.1 Avalanche photodiode

Avalanche semiconductor devices appeared almost in the same time as the first diodes and transistors. Electronic avalanche itself is rather typical phenomena for all semiconductor devices. Exactly the avalanche breakdown is the frequent reason for failure of transistors, diodes, and other semiconductor units operation.

From the very beginning, a lot of attempts were made not only to protect against the avalanches in semiconductor but to use the avalanche effect (multiplication) in detectors for detection of weak signals from external events. This task was found to be complex, and developed devices were expensive and

short-lived. However, last time, due to the new technology achievements the avalanche detectors start to be used in nuclear physics and physics of elementary particles.

Because of some special properties, the avalanche detectors compete with traditional detectors. Use of silicon devices with avalanche amplification is the most effective for detecting the weak light fluxes, exactly in this field the avalanche detector advantages are most obvious. Namely, they have:

- high signal-to noise ratio due to internal amplification, and therefore can be used for detecting the low light flow intensities; usual silicon photodiode can detect the light flows starting from several thousands of photons, while even the usual avalanche detectors detect the light flow of several hundreds of photons.
- high quantum efficiency of light detection. If the quantum efficiency of the best PEMs is about 25 % (usually, 10-15 %), then efficiency of APD (Avalanche PhotoDiode), as a rule, is more than 50 % and achieves 90 %. Photon detection efficiency of MAPD can be about 30 %;
- high time resolution (better 1 nanosecond) due to small depth of depletion area.

Avalanche photodiodes have all useful properties of usual silicon detectors. However, detector operation in avalanche mode imposes the special requirements to stability of operating point, since the avalanche multiplication factor strongly depends on the voltage and temperature. For example, multiplication factor of EG&G's APD of C30626E type at M=100 decreases by 6.7 % when temperature increases by 1^0C. This, when increasing the temperature by 15 ^{0}C, the multiplication factor M changes from 100 to 1. Temperature factor for Hamamatsu's APD of S5345 type with M=100 is -3.3 %/^{0}C.
These requirements limit the application of avalanche detectors [103].

4.2 Silicon photoelectron multiplier

Avalanche photodiodes with structure of microcells (micropixels), each of those is the counter of unit photons are able to detect the low light intensities (a few tens or even units of photons) having at this the high internal multiplication factor $M \approx 10^6$ like some PEMs [103].

Development of avalanche photodiodes with negative feedback that dampers the avalanche allows creating the avalanche photodiode operating in so called "Geiger" mode (APDg). Such APDg has high multiplication factor ($10^5 \div 10^7$). However, at this the dead time become large (about of microseconds).

As the gas-filled Geiger-Muller counter that can detect only the fact of ionizing particle passing, the APDg can only detect the fact of photoelectron generation under external light influence, but not their number. Thus, given photoreceiver can't be used for detecting the intensity of incident radiation.

In order to resolve the problem of radiation intensity detection, the new photodetector type was developed, namely, silicon micropixels avalanche photodiode MAPD (Micropixels Avalanche PhotoDiode). MAPD – is not widely recognized abbreviation of given photodiode type, it also is named as

- SiPM (Silicon PhotoMultiplier);
- MPGM APD (Multipixel Geiger-mode Avalanche PhotoDiode);
- SSPM (Solid State PhotoMultiplier);
- G-APD (Geiger-mode Avalanche PhotoDiode);
- GMPD (Geiger-Mode PhotoDiode);
- DPPD (Digital Pixel PhotoDiode);
- MCPC (MicroCell Photon Counter);
- MAD (Multicell Avalanche Diode).

Given detector type is the photoreceiver on the base of arranged array of pixels (approximately of 10^3 mm^{-2}) realized on the common carrier. Each pixel is the APDg operating in Geiger mode with multiplication factor of about 10^6, but whole MAPD is the analog detector, because the output MAPD signal is the sum of signals from all pixels triggered at photon absorption.

It should be noted, that when incident radiation intensity is high, i.e. probability of several photoelectrons generation in single pixel is significant, as a rule, all pixels triggers at this and output MAPD signal becomes saturated. Thus, there is the upper limitation of spectrometric detection of light intensity.

MAPD is the new type device for detecting the low intensity light flashes (at the level of unit photons) with duration of few units hundreds of nanoseconds. As the vacuum PEMs, the MAPD can become the wide-used device due to the following properties:

- high intrinsic multiplication of about 10^6, that essentially reduce the requirements to electronics;
- small dispersion of multiplication factor (about 10 %) and, as a result the low noise-factor;
- low sensitivity of multiplication factor to supply voltage and temperature changes;
- detection efficiency for visible light is as that of vacuum PEMs;
- possibility of nanosecond light flash detection without distortion of detected pulse shape;
- possibility of operation both on pulse counting and spectrometric modes;
- good time resolution (tens of picoseconds);
- low supply voltage (25—60 V);
- insensitivity to magnetic field;
- small-size (crystal size is about of 1x1 mm^2 to 5x5 mm^2), see Figure 4.1.

Main disadvantage of SiPM is its small size. At present, the maximal size of some experimental diodes is no more than 5x5 mm that essentially limits their application.

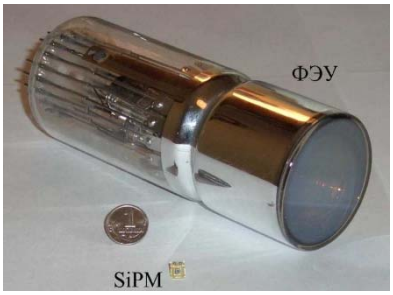

Figure 4.1 – Photo of vacuum PEM and SiPM.

4.3 PIN photodiode

PIN photodiode structure is designed in such a way as to avoid the disadvantages of pn-type photodiode, Figure 4.2. All basic detection principles are the same.

Introduction of intrinsic (i-type) semiconductor between p and n layers of impurity semiconductor allows for significant increasing the spatial charge region size. Within the i-layer there are almost absent the free carriers, and the force lines of electrical field starting from donors in the n-region pass the i-layer without screening and stop on acceptors of p-region.

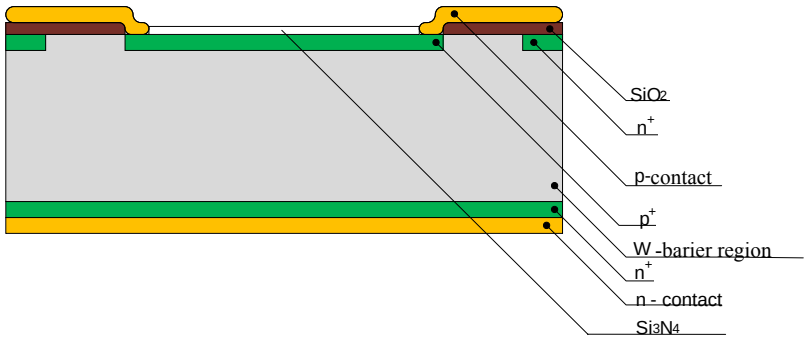

Figure 4.2 - PIN-photodiode construction

Width of i-layer is usually 500-700 μm. In spite of i-region the doped layers are made very thin. That is done to provide that all optical radiation is absorbed within i-layer and the time of charge carry from i–region to doped regions is reduced. So, the main advantage of pin-photodiode is high switching rates, since the radiation is absorbed within i-layer where the charge carriers have the high speeds due to the drift carrying over.

Another advantage is the high quantum efficiency, since the i-layer thickness is usually larger than reverse absorption coefficient and all photons are absorbed within the i-layer.

4.4 Metal-dielectric semiconductor photodiode

In reference [104] issued in 1975 the silicon-based metal-dielectric semiconductor (MDS) structure was proposed to be used as the avalanche photodiode. This type of photodiodes features the

multiplication factors unachievable for convenient photodiodes and cardinally improvement of noise characteristics. Main disadvantage of those structures is the low reproducibility of wide-gap layer doping process.

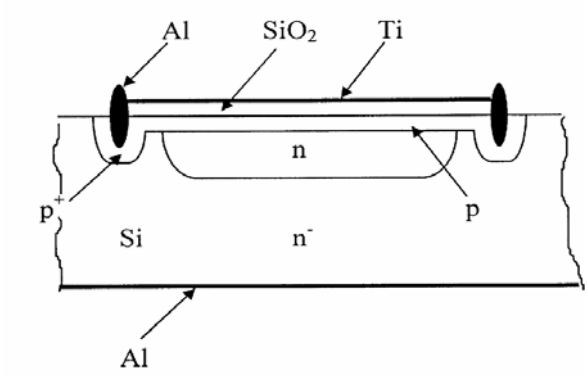

Figure 4.3 – Construction of MD-p-n-photodiode

The given type of diodes is an intermediate between conventional avalanche photodiodes and photosensitive MDS structures intended for operating in avalanche mode. According to its construction, it is the planar photodiode with thin low-doped collector, what receiving site is covered with dielectric layer and semitransparent metal coating connected to collector electrode, see Figure 4.3.

According to the principle of operation this diod is the MDS device in what diode structure provides carrier sink from the semiconductor-dielectric boundary to external electrode connected with metal coating of dielectric. This allows for MDS structure operates in avalanche mode under continuous shifting mode. In operating mode the thin collector layer is fully depleted and is used for reducing the energy of carriers entering to dielectric-semiconductor boundary.

4.5 Comparison of secondary radiation detectors

Table 4.1 presents the comparative characteristics of solid-state PEMs and other photoreceivers used for photon detection.

Table 4.1 – Comparison of secondary radiation detector characteristics

Parameter	Avalanche photodiode	PIN-diode	Vacuum PEM	MDS structure	SiPM
Light detection efficiency (%)					
470 nm	50	50	20		15
590 nm	60-70	60-70	7-15		25
670 nm	80	80	< 1		15
Multiplication	100-200	1	10^6-10^7	10^3	10^6
Noise factor (F)	≥ 2	1	1.3 - 4.0	5	1.1 - 1.3
Threshold sensitivity (S/N=1), (photons)	~10	~200	1	10	1
Bias supply (V)	100-1000	20-200	1000-2000	100-1000	50
Operation in magnetic field	Yes	Yes	No	Yes	Yes

4.6 Scintillators used in combination with photodiode

In implementation any device the important part is right selection of scintillator and photomultiplier. Scintillator is selected according to following requirements: well transparency to intrinsic radiation, high light yield, high gamma detection efficiency, hygroscopic property of scintillating material, and short luminescence time.

The radiation spectrum of classic *NaI(Tl)* scintillator is significantly shifted against the photodiode sensitivity area. So, the parameters of scintillator-PD system on the base of this scintillator are inferior to characteristics of the system on the base of vacuum PEM. At the same reason there are no any results with plastic scintillators.

Good match with PD was obtained for *CsI(Tl)* what luminescence spectrum maximum is at 560-590 nm.

In the systems using the photodiode the *BGO* scintillators with radiation maximum at 480 nm, *LiI(Sn)* – at 530 nm, *CWO* – at 540 nm, *CsI(Sm)* – at 700-900 nm, and *ZnS(Ag)* – at 450-470 nm can be also used.

CdS(Te) scintillators have the luminescence spectrum maximum at 730 nm, high energy yield, fast time performance. Conditions of spectral matching with silicon PDs are close to optimal.

Zinc selenide-based scintillators also have the high energy yield. However, their performance is worse than that of *CdS(Te).* Scintillators on the base of cadmium sulfide with spectrum maximum at 1020 nm, what spectrally match the silicon photodiodes are also obtained.

LSO and *LYSO* scintillators also have the radiation emission well matching with the photosensitivity of SiPM.

5 Spectrum shifting light guides

Large size scintillation detectors can be used in practice of radiation monitoring. At this there is a problem of gathering and detecting the scintillation radiation. Using the spectrum shifting light guides allows for increasing the light concentration and reducing the photo detector dimensions [105]. It allows increasing the photosensitive surface area without complication of electronic equipment.

Principle of spectrum shifting light guide operation is based on conversion of detector scintillation light. For this purpose, the special luminescent compositions are loaded in the light guide what shift the scintillation spectrum to region of maximal PEM sensitivity and increase the light intensity.

Estimations have shown that for very large detectors used, for example, in physics of elementary particles, the 1 m^2 polymethyl methacrylate light guide can 17 times amplify the light signal in the water. Use of polystyrene increases this effect approximately by 1.5 times.

6 Conclusion on detectors

Summary of solid inorganic scintillator characteristics is listed in Table 6.1.

Analysis of modern detectors' capabilities has shown that it is impossible to recommend the certainly best detector for NM accounting and control purposes, since the task have many parameter. However, in absence of apparent achievements in this direction some progress is evident.

Table 6.1 – Characteristics of solid inorganic scintillators

Material	Density (g/cm^3)	Hygroscopicity	Refraction factor	Radiation length	Luminescence time, slow component (ns)	Luminescence time, fast component (ns)	Relative light yield, % (photoel./keV)	dE/dx MeV/sm	Energy resolution (%)	Wavelength of max. emission (nm)
NaI(Tl)	3.67	Yes	1.85	2.59	230	5	100 (8.8)	-	6-8	415
CsI(Tl)		Weak	1.79	2.45	700	20	30 (4.8)	-	10	550
BGO	7.13	No	2.19	1.11	300-600	No	12-13 (0.8)	9.2	10.1	480
BaF_2	4.88	Weak	1.56	2.06	600	<0.9	3-5 (0.14)	6.5	18	195-220
CaF_2-Eu	3.19	No	1.44	-	-	-	8.4 (29)	-	9-10.5	430
$YAlO_3$:Ce	5.35	No	1.94	2.36	250	17-35	30-40 (2)	-	-	350-390
$Y_3Al_5O_{12}$:Ce	4.56	-	-	3.56	-	-	30 (1.4)	-	-	550
BeO	-	-	-	-	320	10	4.1-6.7	-	-	-
$LaBr_3$(Ce)	5.3	No	-	-	-	30	45-60	-	3-5	390
$LaCl_3$(Ce)	-	-	-	2.8	-	30	50	-	-	-
ZnO	-	-	-	-	3.8	0.4	(10)	-	-	295
LSO:Ce	7.4	-	-	1.14	-	40	75 (2.5)	-	10	420
$CdWO_4$	-	-	-	-	-	-	(19.5)	-	7.5	500-600
GSO:Ce	6.71	No	1.9	1.39	600	30-60	40	-	9.5	435-450
CdI_2	5.76	-	-	1.50	-	3	10	-	-	540

Significant enhancement of neutron coincidence counters' time characteristics was achieved with use of sandwich from polystyrene and *BGO* instead of ^{3}*He*-counters.

Lanthanum bromide is prospective one in the view of its use on radiation monitors with spectrometric mode for selecting the unauthorized radioactive material movement events under condition that its cost will reduce in time, and possible crystal size will be increased.

Undoubtedly, detectors on the base of micro and nano technologies: gas electronic multipliers, thin-fiber plastic scintillators, nanoscintillators are promising. Nanoscintillators are the result of the youngest and badly researched direction of scientific way on what the hopes are pined.

By our opinion, the capabilities of spectrum shifting light guides what can give the positive effect during detection of low neutron and gamma fluxes are not used at all.

However there is a hope of success in developing the production technologies for photodiodes in order to use them instead of vacuum PEMs. The hopes in this direction are related to increasing the multiplication factor and decreasing the photodiode cost.

7 Russian gamma spectrometers

At present in Russia there are several companies manufacturing the gamma spectrometers and software for them. All companies are easily arranged by geography of initial work places of companies' employees or administration:

- from Joint Institute of Nuclear Research, Dubna, Moscow region: STC "Aspect", "Parsek", ltd..
- from FSUE SRC "CNIIP", Moscow: Business group "Green Star".
- from FSUE "VNIIFTRI", Mendeleevo, Moscow region: SPE "Doza". STC "Amplituda". "LSRM", Ltd..
- from FSUE "VNIIM", St.-Petersburg: STC "Radec".
- from Ioffe PTI of RAS, St.-Petersburg: JSC "Technoexan".

We will try to perform independent analysis of the most used and known spectrometric systems that can be used for nondestructive isotopic assay of nuclear materials with germanium and scintillation detectors. Information has been received from promotional sheets and www-sites of this manufacturers http://: www.aspect.dubna.ru, www.greenstar.ru, www.amplituda.ru, www.rtc.ru/industry/industry.shtml, www.technoexan.ru, www.parsek.ru, www.doza.ru.

Our apologies to those Russian instrumentation manufacturers whose devices weren't reviewed in this report since by the time of preparing this report we, unfortunately, don't have all necessary information.

7.1 SPE "Doza", Zelenograd

7.1.1 Scintillation gamma spectrometer «Прогресс-гамма» ("Progress-gamma")

Basic hardware:

- scintillation detection unit (DU) on the base of Ø63×63 mm *NaI(Tl)* crystal with built-in power supply, amplification and ADC units;
- lead shield of 50 mm;
- «Прогресс-гамма» software ("Progress-gamma") of 2000 edition;
- PC with printer.

Technical specifications:

- relative energy resolution at 661 keV line is no more than 8.5 %
- energy detection range is 0.2-3 MeV;

- minimal activity detected for
  - Cs-137 3 Bq;
  - Th-232 7 Bq;
  - Ra-226 8 Bq;
  - K-40 40 Bq;
- basic measurement error is no more than 30 %;
- weight (with shield, without PC) is 170 kg;
- power consumption is no more than 400 Wt;
- operating temperature range is +10 to +40 °C.

Figure 7.1.1 presents the appearance of scintillation gamma spectrometer “Прогресс-гамма”.

Figure 7.1.1 – Scintillation spectrometer “Прогресс-гамма”

7.1.2 Semiconductor gamma spectrometer “Прогресс-ППД” (“Progress-SCD”)

Basic delivery set:

- detection unit of the base of high pure germanium detector with efficiency of 10% to 60% and more (made by EG&G «ORTEC» or «Canberra») with preamplifier and Dewar;
- power supply and pulse amplification units (different variants);
- lead shield (5 mm thick or low-background composite one of 8 cm);
- ADC card (8K or 16K) or separate analyzer unit;
- «Прогресс-ППД» software (“Progress-SSD”) of 2000 edition;
- PC with printer.

Technical specifications:

- relative energy resolution at line of 1332 keV is no more than 1.8 – 2.0 %;
- energy detected range is 0.05 to 3 MeV;
- integral non-linearity is no more than 0.1 %;
- minimal detected activity is determined by detector sensitivity;
- basic measurement error is no more than 10 %;
- weight (with shield, without PC) is 300-700 kg;
- power consumption is no more than 400 Wt;

– operating temperature range is +10 to +40 °C.

7.1.3 Software suite "Прогресс-2000" (“Progress-2000”)

«Прогресс-2000» is the software suite for resolving the wide range of radiation control tasks from measurements in the field of certifying the food, drink water, construction materials, forestry products and others to monitoring and radiation control at nuclear fuel cycle facilities as well as for resolving a lot of research tasks related to radioactivity measurements.

The «Прогресс-2000» suite structure includes the software modules allowing resolving one or another radiation control tasks. All modules are integrated in operating system Windows that allows their easy using in other programs, and combining with standard text processors and data base control systems.

Peculiarities:

– possibility to resolve all basic spectrometric tasks of radiation control in accordance with requirements of existing regulatory documents;
– possibility to measure the different radiation types’ characteristics using the same suite;
– possibility of integration study of the same object with the same software;
– use of Windows operating system (Win-98, Millenium, XP versions);
– easy of use and low requirements to personnel training for most of tasks;
– complete methodological and metrological support;
– automated calculation of measurement error;
– possibility of network;
– built-in data base;
– multifactor control of measurement circuit operability and stability of its metrological characteristics;
– a large set of standard protocols and possibility of their fast edition.

7.1.4 Spectrometric system "МУЛЬТИРАД" (“MULTIRAD”) with "ПРОГРЕСС" (“PROGRESS”) software. STC «Amplituda», Zelenograd

System components (see Figure 7.1.2):

• set of digital spectrometric and radiometric measuring circuits;
• personal computer with installed programs "Прогресс" (“Progress”) and "Таблицы ядерных данных" (“Nuclear data tables”).

Detection units that are part of measuring circuits are connected to computer via USB port. Number of detection units connected to the single computer is unlimited. Content of each system (number

Figure 7.1.2 – Spectrometric system "MULTIRAD"

and type of measuring circuits) is determined by measuring tasks it is intended for.

List of gamma measuring circuits used in " MULTIRAD" system:

- scintillation gamma spectrometric;
- semiconductor gamma spectrometric.

Technical specification of scintillation gamma spectrometer:

−detector type is *NaI(Tl)*[1];

−detector size is 63x63 mm;

−energy resolution (FWHM) at ^{137}Cs line (662 keV) is no more than 8.5 %;

−energy range is 0.05 to 3 MeVB;

−minimal detected activity (per counted sample) for:

- ^{137}Cs is 3 Bq;
- ^{232}Th is 7 Bq;
- ^{226}Ra is 8 Bq;
- ^{40}K is 40 Bq;

−basic measurement error is no more than 10 %;

−weight with lead shield (without PC) is 120 kg;

−power consumption is o more than 200 Wt;

−operating temperature range is +10 to +40 °C.

Technical specification of semiconductor gamma spectrometer:

−detector type is high pure *Ge*;

−energy resolution at 1332 keV line is no more than 2 keV;

[1] Depending on the measurement task the gamma spectrometric circuit may include the other types of scintillation detectors (*CsI(Tl)*, $CsF_2(Eu)$ and others) of different size. The gas-filled spectrometric detectors can also be used.

−energy resolution at 122 keV line is no more than 1 keV;

−energy range detected is 0.05 to 3 MeV;

−integral nonlinearity is no more than 0.1 %;

−minimal detected activity is determined by detector sensitivity and measurement geometry;

−basic measurement error is no more than 10 %;

−weight (with shield, without PC) is 300-700 kg;

−power consumption is no more than 400 Wt;

−operating temperature range is +10 to +40 °C.

Components:

−detection unit of the base of high pure germanium with efficiency of 10 % to 50 % and more of EG&G «ORTEC» or «Canberra» production (different models);

−Dewar vessel;

−set of connection cables;

−lead shield (thickness of 5 cm or 8 cm, low-background composition);

−power supply and pulse amplification units (different types);

−ADC card (8K or 16K) or autonomous analyzer unit;

−"Прогресс-ППД" (“Progress-PPD”) software;

−PC with printer.

7.2 JSC STC “Aspect”, Dubna

7.2.1 Gamma radiation scintillation spectrometer ГАММА-1С (GAMMA-1S)

Device is put in the State Register of measuring means, № 15294 – 96.

Components:

- scintillation detection unit БДС-Г on the base of 63x63 mm NaI(Tl) monocrystal with built-in amplifier, high voltage transducer, stabilization system on the base of reference light guide peak, and thermocompensation of conversion characteristic (set of ADC “АЦП - 1К - В1” and DU “БДС – Г” can be replaced with DU “УДС - Г63х63 – USB” with built-in ADC and USB interface);
- spectrometric analog-to-digital converter АЦП - 1К - В1 with buffer memory and “live”/real time timer in IBM PC constructive with PCI interface bus;
- lead screen-shield “Экран - 1СГ” (on floor);
- personal computer with printer;
- applied software "LSRM" in Windows media implementing the measurement procedure and developed by “VNIIFTRI”, certificate №746/04.

Basic technical data and characteristics:

- energy range detected is 0.05 to 3 MeV.
- number of channels is 1024.
- energy resolution at 661 keV line of ^{137}Cs- is no more than 8 %.
- integral nonlinearity is no more than ±1%.
- operating temperature range is 10 to 35 ^{o}C.
- all-mains power consumption is 250 VA (220 V, 50 Hz).
- time instability is no more than 1 %.
- maximal input statistical load is 50000 s^{-1}.
- minimal detected activity is agreed to measurement procedure.

Figure 7.2.1 demonstrates the ГАММА-1С scintillation spectrometer appearance.

Figure 7.2.1 – Scintillation spectrometer ГАММА-1С

7.2.2 Semiconductor gamma radiation spectrometer ГАММА-1П (GAMMA-1P)

Technical specifications of semiconductor spectrometer ГАММА-1П are listed in Table 7.2.1.

Table 7.2.1 Basic technical characteristic of ГАММА-1П spectrometer

Energy range detected, MeV	0.05 - 10
Number of channels	8192
Integral nonlinearity, %, no more than	0.05
Maximal input load, s^{-1}	5 10^{4}
Energy resolution (depending on resolution of detector used) at gamma radiation line of 1332 keV (^{60}Co), keV	1.8 – 3.5
Operating temperature range, ^{o}C	from 10 to 35

ГАММА-1П spectrometer components:

- Germanium semiconductor detector, HPGe or Ge(Li);
- External spectrometric charge-sensitive preamplifier ПУГ-01;
- Spectrometric device including the spectrometric amplifier, high- and low voltage power supply selected from those proposed in table 7.2.2;

Table 7.2.2 – Spectrometric devices

Spectrometric device, constructive	**components**	**Output detector supply rating**	**Output preamplifier supply rating**	**Input signal parameters**	**Output signal parameters**
СУ-03П, monoblock		Polarity (+/–) 50 – 4000 V, 100 μA Automated rise and fall no more than 15 V/s	± 24 V ± 12 V	Polarity: (+/-) Rise time <200 ns Fall time constant >50 μs	Polarity: (+) Maximal amplitude 10 V Shaping time constants 0.5; 1. 2; 4; 6; 10 μs
СУ-04П, NIM-module	Units: БНН-01 УИС-02 БНВ-05 (or БНВ-08)	Polarity (+/–) 50 – 4000 V, 100 μA; {or 25 – 1000, 100 μA} Automated rise and fall no more than 15 V/s	± 24 V ± 12 V	Polarity: (+/-) Rise time <200 ns Fall time constant >50 μs	Polarity: (+) Maximal amplitude 10 V Shaping time constants 0.5; 1. 2; 4; 6; 10 μs
СУ-05П, Euromechanics module	БНН-03 УИС-04 БНВ-07 (or БНВ-09)	Polarity (+/–) 50 – 4000 V, 100 μA {or 5 – 100 V, 100 μA, or 50 – 1000 V, 100 μA} Automated rise and fall no more than 15 V/s	± 24 V ± 12 V	Polarity: (+/-) Rise time <200 ns Fall time constant >50 μs	Polarity: (+) Maximal amplitude 8.2 V; Shaping time constants 2; 6 μs

- Spectrometric analog-to-digital converter (ADC) is chosen by interface type and required characteristics (table 7.2.3);

Table 7.2.3 – Spectrometric ADC

ADC type	Constructive	Interface	Conversion method	Conversion frequency, MHz (time, μs)	Number of inputs	Number of conversions
АЦП-8К-2М	PC-card	ISA (16 бит)	Wilkinson	100	2	1
АЦП-8К-В1	PC-card	PCI	Wilkinson	100	1	1
АЦП-8К-В2					2	2
АЦП-8К-П1	PC-card	PCI	Convergence (step-by-step)	(3.5)	1	1
АЦП-8К-П2					2	2
БПА-02	Euromechanics	RS-232	Wilkinson	100	1	1
БПА-02N	NIM					
АЦП-USB-8К-В	Device	USB	Wilkinson	100	1	1
АЦП-USB-8К-П	Device	USB	Convergence (step-by-step)	(3.5)	1	1
АЦП-RS-8К-В	Device	RS232/485	Wilkinson	100	1	1
АЦП-RS-8К-П			Convergence (step-by-step)	(3.5)		

- IBM PC with printer;
- Low-background combination lead screen-shield;
- Applied "LSRM" software for Windows OS.

7.2.3 PC-based analyzers of АИ (AI) series

Basic components:

– Spectrometric analog-to digital converter (Figure 7.2.2) selected by interface type and characteristics required (see Table 7.2.4);

Table 7.2.4 – Spectrometric ADCs

ADC type	Constructive	Interface	Conversion method	Conversion frequency, MHz (time, μs)	Number of inputs	Number of transform.	Resolution	Max. input signal amplitude, V
АЦП-1К-2М	PC-card	ISA (16 bit)	Wilkinson	100	2	1	1K	10
АЦП-8К-2М							1K – 8K	
АЦП-4К-LT	PC-card	ISA (8 bit)	Wilkinson	50	1	1	1K – 4K	10
АЦП-4К-mPC	Industr. computer							
АЦП-1К-В1	PC-card	PCI	Wilkinson	100	1	1	1K – 4K	10
АЦП-1К-В2					2	2	1K – 4K	
АЦП-8К-В1					1	1	2K – 8K	
АЦП-8К-В2					2	2	2K – 8K	
АЦП-1К-В8					8	1	1K	
АЦП-8К-П1	PC-card	PCI	Convergence (step-by-step)	(3.5)	1	1	1K, 2K, 4K, 8K	5
АЦП-8К-П2					2	2		
БПА-03-8К-В	Euromechanic	CompactPCI	Wilkinson	100	1	1	2K – 8K	10
БПА-03-8К-П			Convergence (step-by-step)	(3.5)			1K, 2K, 4K, 8K	5
АЦП-USB-8К-В	Device	USB	Wilkinson	100	1	1	2K – 8K	10
АЦП-USB-8К-П	Device	USB	Convergence (step-by-step)	(3.5)	1	1	1K, 2K, 4K, 8K	5
АЦП-RS-8К-В	Device	RS232/485	Wilkinson	100	1	1	1K – 8K	10
АЦП-RS-8К-П			Convergence (step-by-step)	(3.5)			1K, 2K, 4K, 8K	5

– Personal computer with printer;

– LsrmLite, SpectraLine analyzer software for Windows operating system;

– AnGamma, An analyzer software in MSDOS OS.

Summary of technical specifications of single-plate ADC are listed in Table 7.2.5.

Table 7.2.5 – Summary of technical data and characteristics

Operating amplitude range, V	0.05 – 10
Number of channels	1024, 2048, 4096, 8192
Number of inputs	1; 2; 8
Differential nonlinearity, %	0.3 – 1
Integral nonlinearity, %, no more than	0,03
Code series generator frequency (conversion time)	100 MHz (3.5 μs)

7.2.4 Software

Software for spectrometric systems developed jointly with “LSRM”, Ltd. Provides the operation with all analyzers of SPC “Aspect”.

Basic Software:

– Alpha-beta-gamma spectrometric analysis - Lsrm2000;

– Analyzer control - LsrmLite;

– Analyzer control and spectra processing - LrsmAnalyser.

Software performs the general spectrometric analysis for all spectrometer types (scintillation and semiconductor) and any radiation type (alpha, beta, gamma).

Set of programs resolves the specific actual tasks with using the specialized spectrometric systems:

- Control of radioactive material movements - LsrmCustoms;
- Passportization of radioactive waste - Diogen;

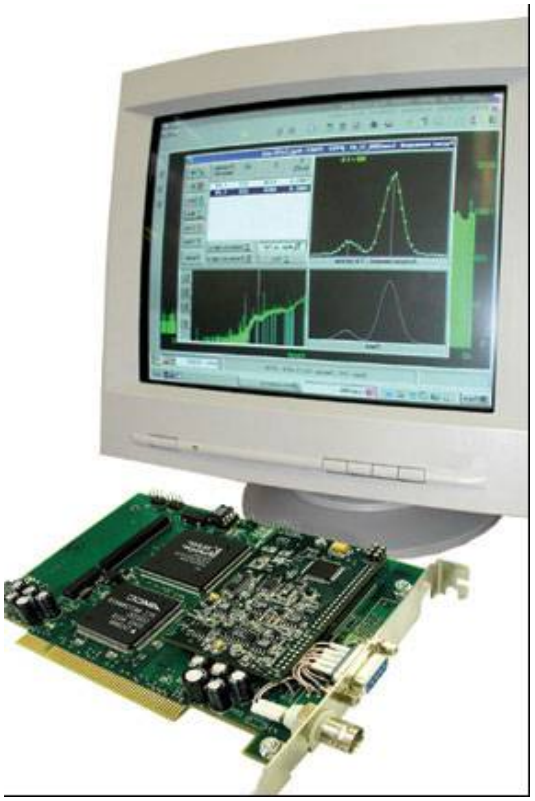

Figure 7.2.2 – Spectrometric single-plate ADC

- Liquid media monitoring - LsrmWater;
- Gamma monitoring with geographical gridding - LsrmCar;
- Radon activity measurements by method of sorption in activated charcoal - LrsmRadon.

7.3 "Parsek", Ltd., Dubna

7.3.1 Spectrometric analog-to-digital converters

7.3.1.1 4K-USB scintillation pulse-height analyzer 4K-CAA

4K-USB pulse-height analyzer (Figure 7.3.1) is intended for detecting and accumulating the spectra of γ–quanta with energy from 20 keV to 6 MeV and intensity up to 10^6 s^{-1}. Analyzer is made in form of constructive integrated with scintillation block connected to USB port without any external power supply. Technical specifications are listed in Table 7.3.1.

Analyzer components:

1. Detection unit of БДЭГ4-43-04А type.
2. computer keyboard controlled PEM power supply.
3. PEM pulse amplifier.
4. high-speed accumulating spectrometric ADC.

Table 7.3.1 – Technical characteristics

γ – quanta enegy range	20 keV to 6.0 MeV
Resolution for ^{60}Co energy	7.0 %
Constant dead time	1 μs
Memory size	$2^{32}\times4096$
Integral nonlinearity	0.04 %
Differential nonlinearity	± 1.0 %
Detection window determined from keyboard	Along all range
Power consumption	1.8 Wt

7.3.1.2 В4К-САЦП-USB High-speed 4k-USB spectrometric ADC

High-speed 4k-USB spectrometric leveling convergence ADC accumulating the spectrometric information with intensity up to 10^6 s^{-1}. Table 7.3.2 shows the technical specifications.

Table 7.3.2 – Technical specifications

Conversion type	Convergence with leveling
Number of measuring inputs	1
Input pulse duration no less than no more than	 0.5 μs 5.0 μs
Memory channel size	$2^{32}\cdot$ 4096
Number of conversion bytes	12 (4096)
Constant dead time	1 μs
Integral nonlinearity	0.04 %
Differential nonlinearity	±1.0 %
Time instability, not worse than	0.04 % in 8 hours of operation
Acquisition time (memorization time)	1.5 μs (or by order)
Consumption for +5 V power supply	370 mA (1.8 Wt)
Constructive:	Plastic case 150x80x30 mm
Bus type	USB

7.3.1.3 4К-САЦП-USB Spectrometric 4K ADC with USB interface and power supply from USB bus

Wilkinson spectrometric analog-to-digital converter with increment memory of large capacity (size) made in form of external device connected to USB port is intended for transforming the microsecond pulses to digital pulse code and accumulating the spectrometric information using the only USB port supply. Technical characteristics are listed in Table 7.3.3.

Table 7.3.3 – Technical characteristics

Conversion type	Wilkinson
Number of measuring inputs	1
Measured pulse-height	from 40 mV to 4.0 V
Input pulse duration not less than not more than	 0.5 μs 20.0 μs
Memory size	2^{32}*4096
Number of conversion bytes	12 (4096)
Conversion frequency	100 МГц
Integral nonlinearity	0.04 %
Differential nonlinearity	± 1.0 % at level of $5•10^4$ per channel
Time instability, not worse than	0.1 % in 8 hours of operation
Acquisition time (memorization time)	5.0 μs (or by order)
Consumption for +5 V power supply	470 mA (2.35 Wr)
Bus type	USB
Constructive	Plastic case, 150*80*30 mm

7.3.1.4 4К-САЦПППП - 3-input leveling convergence 4K ADC

Three-input spectrometric ADC used for measuring the high intensive flows (up to $4·10^5$ s^{-1}). It makes possible to store the spectra acquired in one card memory space and simultaneously read from another memory space. Number of conversion bytes - 12 or 10 can be programmatically selected. Technical characteristics are listed in Table 7.3.4.

Table 7.3.4 – Technical characteristics

Conversion type	Convergence with leveling
Number of simultaneously connected sensors	3
Positive pulse height measured	from 40 mV to 4.0 V
Duration of input pulse rise-up portion Not less than Not more than	 0.4 μs 10.0 μs
Memory channel capacity for each input	232
Number of conversion bytes for each input	12 (4096) or 10 (1024)
Integral nonlinearity	0.1 %
Differential nonlinearity	1.5 %
Maximal integral load for three inputs (per one of them)	400000 s^{-1}
Time instability (in 8 hours of operation)	1.0 channel
Bus type	PCI

7.3.1.5 САЦП-НМВ-16К – accumulating spectrometric 16K ADC of “zero dead time” (PCMCIA variant)

Table 7.3.5 summarizes the technical characteristics.

Table 7.3.5 – Technical characteristics of САЦП-НМВ-16К

Polarity of pulses analyzed Pulse height Input pulse shape Pulse duration	positive from noise level to 4 V "Gaussian" from 1.0 to 40 μs
Amplitude-code conversion accuracy	214 (16 к)
Integral nonlinearity Differential nonlinearity	0.03 % +0.5 %
Dead time	absent
Software	Full-scale mode of multichannel pulse-height analyzer
Bus type	PCMCIA / ISA

7.3.1.6 Stand-alone multichannel ADC

Technical characteristics are listed in table 7.3.6.

Table 7.3.6 – Technical characteristics

Conversion type	Wilkinson
Number of simultaneously connected sensors	3
Measured pulse height	from 50 mV to 5 V
Duration of input pulse rise-up portion, not less than not more than	 0.4 μs 10.0 μs
Memory channel size for each input	2^{32}
Number of conversion bytes for each input	10 (1024)
Output time (aperture time)	5.0 μs
Conversion frequency	50 MHz
Integral nonlinearity	0.1 %
Differential nonlinearity	1.5 %
Maximal integral load for three inputs (per one of them)	48000 s^{-1}
Time instability (in 8 hours of operation)	1.0 channel
Bus type	PCI/ISA

7.3.1.7 16 K “zero dead time” accumulating ADC

Technical characteristics are listed in Table 7.3.7.

Table 7.3.7 – Technical characteristics

Polarity of analyzed pulses	Positive
Pulse height	From noise level to 4 V
Input pulse shape	"Gaussian"
Pulse duration	from 1.0 to 40 μs
“Amplitude-code” conversion accuracy "	214 (16 к)
Integral nonlinearity	0.03 %
Differential nonlinearity	+0.5 %
Dead time	Absent
Software	Full-scale mode of multichannel pulse-height analyzer
Bus type	PCMCIA / ISA

7.4 JSC “Technoexan”, St-Petersburg

7.4.1 Multichannel pulse-height analyzer MCA 2048

Destination and basic parameters

MCA2048 is intended for multichannel analysis of pulse-height distribution of pulses from different detectors. MCA2048 construction is the card inserted in ISA slot of personal computer backbone. It is delivered with software package for detecting and analyzing the pulse-height spectra.

Main destination of MCA2048 (Figure 7.4.1) is operation as-multichannel pulse-height analyzer when detecting the signals from different detectors: scintillation, solid-state, ionizing chambers and proportional counters. Technical characteristics are listed in Table 7.4.1.

Generator FWHM is no more than one channel. Logic signals– TTL, active state– high level.

External signals – analog and (if required) logic are connected through the LEMO connectors installed at the back of card.

There is a constructive in form of small-sized external module connected to serial port of computer.

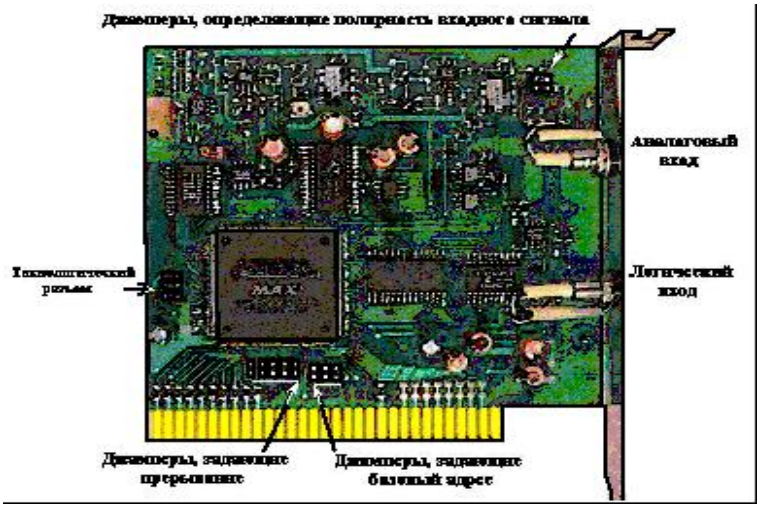

Figure 7.4.1 - MCA2048 constructive

Table 7.4.1 – Technical characteristics

Maximal analog pulse height	5 V
Duration of analog pulse rise up portion during operation in mode of internal strobing	Not less than 0.5 μs
Installation of detection threshold in internal strobing mode maximal threshold value threshold installation accuracy	By program 1.25 V 8 bit
Input impedance of analog input	10 kOhm
Number of conversion bytes (channels)	11 (2048)
Conversion time (including writing to memory cycle)	1.2 μs
Buffer memory channel size	2^{32} -1
Integral nonlinearity (along all conversion range) in external strobing mode, not more than in internal strobing mode, not more than	 0.01 % 0.1 %
Differential nonlinearity, not more than	1 %
Time destination of working regime, no more than	10 min

7.4.2 Software

Software allows for installing the module parameters, on-line displaying the accumulation of time spectra, writing and storing the data on hard drive.

7.5 STC “Radec”, St.-Petersbutg

7.5.1 Gamma radiation spectrometer РКГ-1К (RKG-1K)

Spectrometer is made on the base of high pure germanium detector.

Technical characteristics are listed in Table 7.5.1.

Table 7.5.1 – Technical characterstics

Energy range of detected gamma quanta, MeV	0.05 – 2.8
Energy resolution, keV	
- for 0.122 MeV energy	0.85
- for 1.332 MeV energy	1.9
Relative detection efficiency of HPGe detector in comparison with 76x76 mm NaI(Tl) detector determined by full energy peak with energy of 1.33 MeV, %	Not less than 30

components:

- detection units on the base of HPGe with Dewar;
- detection unit preamplifier;
- spectrometric device Multispektrum (BSI);
- shielding block against external radiation background;
- set of connection cables;
- software.

7.5.2 Spectrometer-radiometer МКГБ-01

The device has the certificate of measuring mean type approval RU.C.38.001.A N 10702.

Components:

- detection units БДЕГ-80, БДЕГ-60, БДЕГ-К;
- analog-to-digital converter MD-198;
- personal computer IBM-PC of any configuration;
- controlled unit of high voltage (HV) power supply, low voltage (LV) power supply unit;
- power supply and amplification units for БДЕГ-К;
- programs for acquiring and processing the radionuclide spectra by PC;
- low-background shielded boxes for БДЕГ, БДЕГ-К units.

7.5.3 AScinti-W software

AScinti-W software implements the processing of spectra obtained from scintillation detectors by the algorithm based on matrix method (of windows). The errors are calculated according to GOST and include the system and random components. The measurement is performed according to approved measurement procedure, which provisions are implemented in program.

Analysis results are calculated by AScinti-W program using the efficiency calibrations calculated by reference spectra of radionuclide activities.

The sensitivity matrixes contained in calibration file are required for calculation by method of windows.

Standard version of AScinti-W allows determining the specific activities of gamma radiating radionuclides ^{226}Ra, ^{232}Th, ^{40}K, ^{137}Cs; ^{222}Rn in environment samples and carbon sorbent.

At present STC “Radec” has developed the similar software with identical (similar) interface for spectrometers with solid state detectors.

7.6 Central Research Institute of Robotics and Engineering Cybernetics, St.-Petersburg

7.6.1 Field gamma spectrometer

Field gamma spectrometer ПГС (PGS), Figure 7.6.1, is intended for on-line estimation of samples’ radionuclide content in order to identify the radionuclides for their activity measurement, as well as for determination of nuclear explosion products age and exposure rate of gamma radiation. Technical specifications are listed in Table 7.6.1.

Figure 7.6.1 – Field gamma spectrometer PGS

Components of PGS gamma spectrometer:

1 – spectrometric gamma radiation detection unit;

2 – data processing unit;

3 – unified charge-feeding unit;

4 – Notebook.

Table 7.6.1 - Technical specifications of ПГС spectrometer

Basic technical specifications:	
Energy range of detected gamma radiation, MeV	0.03...3.0
Energy resolution for gamma radiation energies of 661 keV (^{137}Cs), no more than, %	8.5
Number of spectrometer channels	1024
Maximal statistical load not less than, s^{-1}	$5 \cdot 10^4$
Basic error of radionuclide specific activity measurement in samples at single-component event, no more than, %	±30
Instability of calibration characteristic in 8 hours of continuous operation, not more than %	2
Basic error of radiation exposure rate measurement, not more than %	15
Time destination of working regime, not more than, min	30

7.6.1 Survey gamma spectrometer ГСП-01 (GSP-01)

It is intended for manual survey of radioactive anomaly sources by accompanying gamma radiation under conditions of variable background, detection of gamma radiation energy spectra within the range of 20 to 3000 keV. It is made on the base of *NaI(Tl)* detector of D50x50mm. According to the detection characteristics the spectrometer corresponds to category 1H of GOST R516 35- 2000. Technical characteristics are listed in Table 7.6.2.

Table 7.6.2 – Technical characteristics

Basic technical characteristics:	
Energy range of radiation detected, keV	20-3000
Energy resolution at 662 keV, %	Not more than 9
Number of conversion channels	1024
Effective detection area (E = 662 keV), cm^2	Not less than 14
Continuous operation under power supply from 3 batteries (1.2V, capacity of 1Ah), hours	Not less than 10

7.7 “Green Star” Business Group, Moscow

Spectrometric complexes СКС manufactured by “Green Star” Business Group are used at all nuclear fuel cycle stages: exploration, mining, enrichment, production of fuel rods and assemblies, process control at chemical combines and nuclear power plants, spent fuel reprocessing, radiation monitoring of industrial enterprises and environment, nuclear waste storage and disposal.

СКС complexes are based on impulsive signal processors of SBS series.

Spectrometric complex СКС-07П_(Г*) (Г – gamma detecting detector, *- number of detection unit according to technical terms). For example, according to technical terms, Г35 corresponds to semiconductor detection unit GEM 15P4, Г39 corresponds to scintillation detection unit БДЭГ-50(50)Н, Р27 corresponds to X-ray detection unit AXR100CRF.

7.7.1 Spectrometric complexes СКС-07П_Г1…36 (SKS-07P_G…-36)

Spectrometric complexes from СКС-07П_Г1 to СКС-07П_Г36 (SKS-07P_G1 - SKS-07P_G36), Figure 7.7.1, are intended for measuring the gamma radiation activity of counted samples, determining the uranium enrichment and plutonium isotopic composition, automated processing the measurement results, data output and storing in form convenient for user.

Figure 7.7.1 – Spectrometric complexes from SKS-07P_G1 - SKS-07P_G36

Spectrometric complex is the measuring system that includes:

- measuring circuit with detection unit on the base of high pure germanium;
- impulsive signal processor SBS-75 built-in personal computer (for operation under high loads the pulse shaper DL-1 or DL-2 is used);
- specialized software: «Gamma Basic», «Gamma Pro», «FusMat»;
- manual documentation;
- complex is equipped with nitrogen or electromechanical system of detector cooling;
- delivery set can include the lead shield of 50 mm or 100 mm thickness, device for filling up with liquid nitrogen, etc.

Basic technical specifications:

- energy range of detected radiation is from 50 keV to 3000 keV;
- energy resolution at 1332,5 keV is from 1.7 to 2.4 keV;
- integral nonlinearity of conversion characteristic in not more than ±0.05 %;
- maximal input statistical load is not more than 10^5 s^{-1} (up to $2 \cdot 10^5$ s^{-1} when using the pulse shaper DL-1);
- instability of complex conversion characteristic for 24 hours of continuous operation is not more than ±0.02 %;
- complex provides up to 16384 channels of 2^{24}-1 pulse/channel capacity;
- limit of allowing basic error of conversion characteristic in counted sample measurement geometry is not more than ±25 %.

7.7.2 Spectrometric complex СКС-07П_Г37…48 (SKS-07P_G37…48)

Spectrometric complexes from СКС-07П_Г37 to СКС-07П_Г48 (SKS-07P_G37 - SKS07_G48), Figure 7.7.2, are measuring system that includes:

- measuring circuit with scintillation gamma radiation detection unit;
- impulsive signal processor SBS-79 built in personal computer (for operation under high loads the processor can be equipped with DL-pulse shaper);
- specialized software «Scint Basic»;
- lead shield;
- manual documentation.

Basic technical specifications

- energy range of radiation detected is from 50 keV to 3000 keV;
- energy resolution at 661.5 keV is from 6 to 10.5 %;
- maximal input statistical load is not more than $2 \cdot 10^6$ s^{-1} (up to $5 \cdot 10^6$ s^{-1} when using DL-pusle shaper);

- instability of complex conversion characteristic for 24 hours of continuous operation is not more than ±2%;
- complex supports 2048 channels of 2^{24}-1 pulse/channel capacity;
- integral nonlinearity of conversion characteristic is not more than ±1 %;
- limit of allowable basic relative error of activity measurement in counted sample geometry is not more than ±25 %.

Figure 7.7.2 – Spectrometric complex with SKS-07P_G37 - SKS07_G48

7.7.3 Specialized spectrometric complexes СКС-07П-Г (SKS-07P-G)

Use of mobile and stationary spectrometric complexes СКС-07П-Г (SKS-07P-G) is implemented for radioactive waste control task at Rosatom facilities.

Mobile spectrometric passportizer (passport detector) of extensive gamma radiation sources (Figure 7.7.3) allows for measuring the activity and nuclide content of gamma radiating sources of any geometries and dimensions (cube, cylinder, sphere, plane) taking into account the correction for inhomogeneous radionuclide distribution, as well as allows for determining the activity distribution directly by measured sample geometry using the mathematical simulation by Monte Carlo method.

«Паспортизатор РАО» (“Passportizer of radioactive waste”) is spectrometric complex (Figure 7.7.4) intended for activity measuring the counted samples by gamma radiation in geometry of 200-l drum or container with liquid or solid radioactive waste.

“Passportizer” is the measuring device that includes:

- measuring circuit with corresponding detection unit (scintillation detector or detector on the base of HPGe crystal);

- impulsive signal processor SBS-75 built-in personal computer;
- «Гамма Про» software;
- electromechanical rotator;
- lead shield;
- operating documentation.

Figure 7.7.3 – Mobile spectrometric passportizer

Figure 7.7.4 - «Паспортизатор РАО» passportizator of radioactive waste

The series of spectrometric complexes «Нырок» (“Nyrok”) is produces for control of bottom sediments of Rosatom facilities.

Spectrometric complex “Nyrok-2” is developed on the base of solid-state detector with portable Dewar placed in stainless steel case and having the hermetic hose with internal diameter sufficient for arrangement the set of cables within hose what are used for acquiring the signal from detector and inputting the power supply to detector. Among the mobile spectrometric complex “Nyrok-2” components there is the impulsive signal processor SBS-75 installed into the expansion slot PCI of portable, environment-proof according to IP54 notebook powered from stand alone voltage batteries (Figure 7.7.5). Specialized «Гамма Про» (“Gamma Pro”) software included in the complex allows determine the counted sample activity in extensive source geometry.

Results of “Nyrok-2” spectrometric complex field operation have shown the effectiveness and perspectives of given development use for radiation monitoring the bottom sediments.

Spectrometric complex “Nyrok-1” is developed on the base of two alternating detection units with *CdZnTe* crystal or *NaI(Tl)* scintillation crystal. Spectrometric complex “Nyrok-1” (Figure 7.7.6) includes:

- impulsive signal processor «Колибри» (“Colibry”) КС-003 «Т» model with built-in program;
- detection unit on the base of 0.5 cm^3 *CdZnTe* crystal with signal cable of 1.5 m length;
- БДЭГ-50(50)Н detection unit with signal cable of 1.5 m length;
- Remote rod of 3 m length;
- hermetic water-proof case for installation of any detection units and impulsive signal processor «Колибри» with connection to Notebook;

Figure 7.7.5 – Mobile spectrometric complex “Nyrok-2”

Figure 7.7.6 – Spectrometric complex “Nyrok-1”

– notebook PC;

– set of specialized software for spectra acquisition –analyzer emulator «Esbs», and for spectra processing - «ScintBasic».

7.7.4 Impulse signal processor SBS-75

SBS-75 processor (Figure 7.7.7) provides operation with any detection unit types, scintillation detectors, phoswich detectors, proportional counters, ionization chambers, detectors on the base of crystals of high pure germanium, silicon, cadmium telluride, etc.. Technical characteristics are listed in Table 7.7.1.

Figure 7.7.7 - SBS-75 processor

Table 7.7.1 - SBS-75 technical characteristics

Interface type	PCI
Conversion time	1.8 μs, double buffering
Integral nonlinearity	0.025 % (0.01)
Differential nonlinearity	1 % (0.5)
Additional temperature error of conversion characteristic	0.005 %/°C (0.002)
Additional temperature error of high voltage source	0.01 %/°C (0.005)
Input signal polarity	«+» and «-»
Time constant of whitening filter	2 μs (others can be ordered)
Gain	10-2500
Number of conversion channels	8192, 4096, 2048, 1024, 512, 256
Maximal input statistical load	Up to 10^5 s^{-1}
Time resolution of pile-up rejector	400 ns
Polarity of high voltage	«+» and «-»
High voltage range	1.25 kV / 1 μA, Rout=30 kOhm ; 5 kV / 100 μA, Rout=6 MOhm
Maximal power consumption from control unti power source	4 Wt
Card length	188 mm
Card weight	200 g
Preamplifier power supply	+24V/50 mA and +12V /100 mA

7.7.5 Impulsive signal processor SBS-70

SBS-70 impulsive signal processor (Figure 7.7.8) is specially designed for measuring the nuclear radiation spectra under high loads. SBS-70 impulsive signal processor differs from SBS-75 processor by substantially higher throughput. When installing the SBS-70 processor in IBM-compatible PC of Desktop or Notebook type the user receives at his disposal the modern spectrometer of nuclear radiations with the best metrological characteristics.

SBS-70 can be used for measuring the radiations from samples and objects at all nuclear fuel cycle stages including radioactive and nuclear material identification, control and accounting, for ensuring the IAEA safeguards for technological and process control, for environment control. Depending on peculiarities of measuring task the impulsive signal processor SBS-70 provides joint operation with scintillation (*NaI(Tl)*, *CsI(Tl)*, phoswich detectors), gas-filled (proportional counters, ionization chambers) and solid-state (germanium, silicon, cadmium telluride) detectors.

SBS-70 device is the standard PCI-card of half size that contains all circuit engineering required for precise spectrometric measurements:

- zero pole compensation circuit;
- spectrometric amplifier with signal shaping circuits depending on the time;

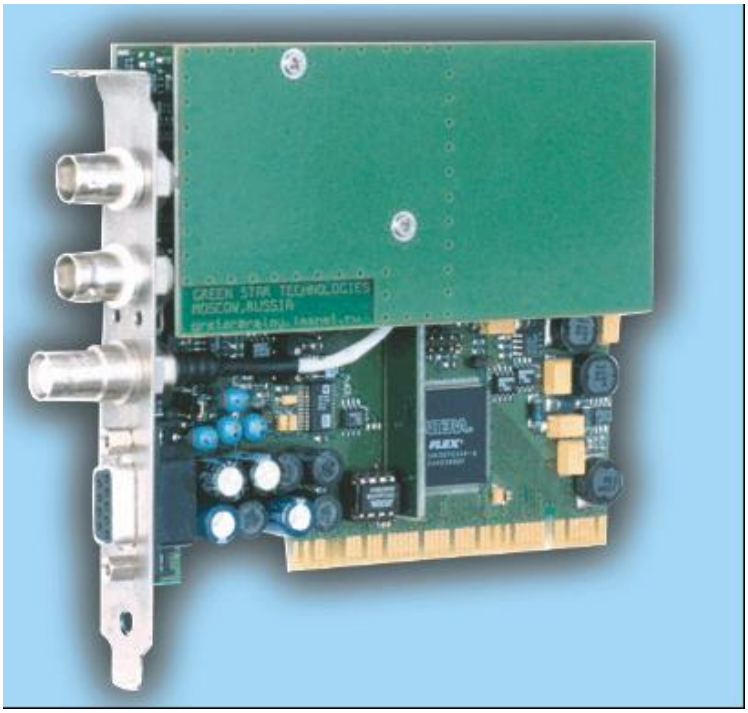

Figure 7.7.8 - SBS-70 impulsive signal processor

- key base line restorer, pile-up rejecter;
- ADC with fixed conversion time;
- buffer memory;
- double-range high voltage power supply of detector;
- preamplifier power supply;
- interface schemes for parameter control;
- terminal of access to PC backbone.

Processor is widely used in multichannel systems. It is possible to combine up to 32 spectrometers in single system.

7.7.6 Impulsive signal processors SBS-77, SBS-78, and SBS-79

The processors (Figure 7.7.9) are intended for operation with low resolution detectors: scintillation, gas-filled, and solid-state *Si(Li), Si p-i-n, CdTe, CdZnTe, HgI_2* etc.

Simplified SBS-79 processor is designed for low cost technological applications and does not include the fast counting circuit with pile-up rejecter, the input signal and high voltage polarity is determining at order and can't to be changed by user.

SBS-78 processor is developed for operation under high and super high loads (counting rates). When operating with scintillators on the base of *NaI(Tl)* the spectrometric circuit survives at load up to $2 \cdot 10^6$ s^{-1} with throughput of $2 \cdot 10^5$ s^{-1}, and when using an additional DL-shaper the system operates up to $5 \cdot 10^6$ s^{-1} with throughput of $5 \cdot 10^5$ s^{-1}. In addition the Peltie cooler power supply unit can be installed in

SBS-78 processors for operation with *Si p-i-n* and *CdTe* X-ray detectors. Polarity of input signal and high voltage is also determined at order.

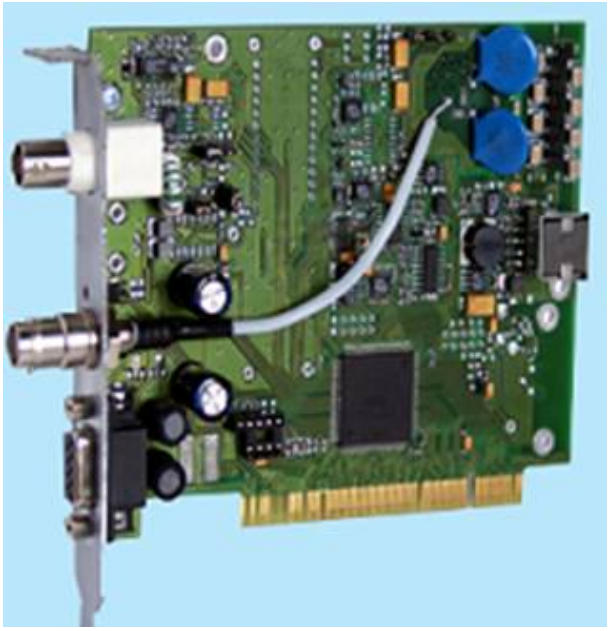

Figure 7.7.9 - SBS-77, -78, -79 processors of impulsive signals

SBS-77 processor is the universal one, the input signal and high voltage polarity as well as the integration time constants (adapting the measuring circuit to different scintillator types) can be changed by user.

Processors are widely used in multichannel systems and also have great possibilities for system-defined soft and hard ware integration in complex spectrometric systems.

Technical characteristics (typical):

Conversion time	0.8 μs, double analog buffering
Integral nonlinearity	0.025 (0.01) %
Differential nonlinearity	1 (0.3) %
Additional temperature error of conversion characteristic	0.005 (0.002) %/C
Additional temperature error of high voltage supply	0.01(0.005) %/C
Gain change range	2-512 or 20-5120 by order
Number of conversion channels	4096, 2048, 1024, 512, 256
Maximal input statistical load (when operating with NaJ(Tl) detectors)	$2 \cdot 10^6$ s^{-1} $5 \cdot 10^6$ s^{-1} when using DL-shaper
Time resolution of pile-up rejector (for SBS-77 and SBS-78)	150 ns
High voltage supply	.0-1.5 kV/1 mA, R_{out} = 30 kOhm
Preamplifier power supply	$\pm$ 12V/100 mA
Bus interface	PCI

7.7.8 Impulsive signal processor «Колибри» (“Colibry”)

Impulsive signal processor “Colibry” (Figure 7.7.10) is a complete spectrometric device that includes: spectrometric circuit (amplifier, analog-to-digital converter), calculator, graphical data display unit, keyboard, preamplifier power supply, high voltage supply. Spectrometer is intended for problem-oriented measurements such as determination of uranium enrichment, territory containment, equipment holdups, radiation exposure, etc. The spectra acquired, if necessary, can be processed with usual IBM-compatible computer after their transition through the standard serial interface RS-232.

Figure 7.7.10 – Impulsive signal processor “Colibry”

Device provides the operation of scintillation, gas-filled detection units, as well as solid-state detectors (for example, *CdTe, CdZnTe, HgI2, Si, HPGe,* etc.). There are two basic spectrometer modifications:

- N (simplified) – for operation with scintillation detectors connected by single- or bi-wiring scheme;
- T (universal) – for operation with any detector types.

Spectrometer can include the software suite consisting of applied program library for different problem-oriented tasks. Thus, the “Colibry” users are able to determine and order the structure and functions of internal programs as well as the hardware configuration. Depending on the task the operator can load the required program to spectrometer and replace it with other as required.

Technical characteristics of “Colibry” gamma spectrometer are listed in Table 7.7.2.

7.7.9 Specialized software

Specialized spectrometric assay software developed by “Green Star” Business Group (Figure 7.7.11) is untended for complex mathematical and software support of automated work station of spectrometric analysis on the base of SBS impulsive signal processor both in single-card and multi-card versions.

Table 7.7.2 – Technical characteristics of “Colibry” gamma spectrometer

Characteristic	Value
Amplifier gain	Programmable from 2 to 512, Roughly - 8 steps by 6 dB, Smoothly– 1024 values within 6 dB range
Shaping time constant	1 μs (for T modification) or other by order
Input impulse polarity	Negative for N modification. Positive or negative (programmatically set up) for T modification
Time constant of zero pole compensation circuit (for T modification)	> 40 μs
Base line restorer	Active controlled
Number of channels	2048, 1024, 512, 256, 4096 and 8192 additionally determined at order
Integral nonlinearity	< 0.05 %
Differential nonlinearity	< 0.5 %
Additional temperature error of conversion characteristic	< 0.1 %/C for N modification < 0.01 %/C for T modification
Output potential of high voltage supply	1536 V/500 μA (programmable– 1024 values) or another by order
Output impedance of high voltage supply	30 kOhm
Preamplifier power supply	±12 V, 100 mA and ±24 V, 50 mA additionally indicated at order
Processor memory	128 kB, 512 kB by additional order
Computer interface	RS232
Operating temperature range	from -20 °C to 40 °C

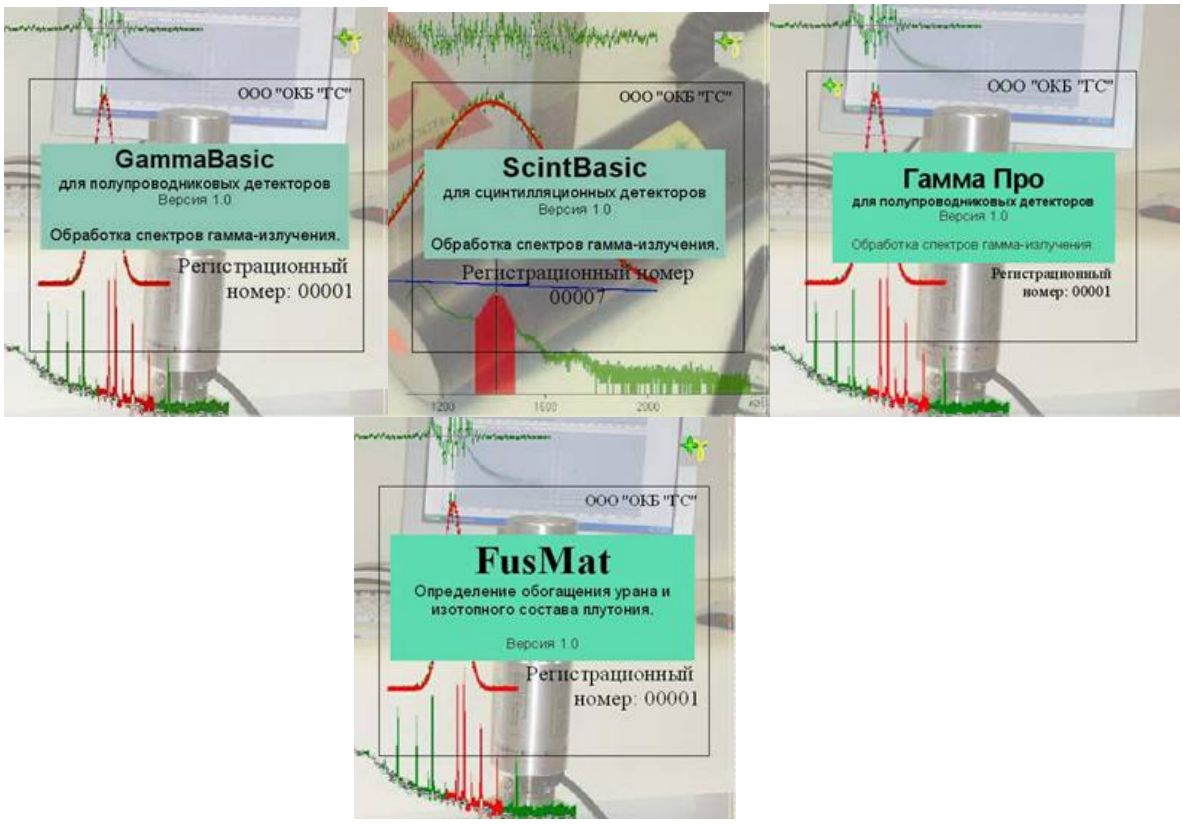

Figure 7.7.11 – Spectrometric analysis software

Software suite includes:

- analyzer emulator program «Esbs» providing the complete set up of spectrometric complex and acquisition of spectrometric data;
- X-ray and gamma radiation processing programs «GammaBasic», «ScintBasic», «Гамма Про», «FusMat» allowing for preparing all spectrometer calibrations, data on nuclides and elements, their lines, and for processing the spectra including qualitative and quantitative analysis.

All spectra processing programs are registered in Branch Fund of Algorithms and Programs of RF State Coordination Center of Information Technologies and are certified in RF Rostechnadzor system.

The main result of software application is determination of radionuclide activity values in the object studied and estimation of each measurement uncertainty (P=0.95 or P=0.99).

The method of experimental spectrum expansion on lines of radionuclides included in working identification library is used as the analysis method in the programs.

Programs perform the analysis of gamma radiation spectra stored in files of definite format.

Programs implement the support of up to 16384 channel spectra inclusive.

To work with programs there are required:

- IBM – compatible personal computer;
- Processor not worse than Intel Pentium II 300 MHz;
- RAM of not less than 32 MB;
- Spare footprint is not less than 10 MB;
- Hand manipulator of “mouse” type.

Software operates under Microsoft Windows 95/98/Me/NT/2000/XP environment.

7.8 Comparative analysis of gamma spectrometers

All information used for comparative analysis of Russian gamma spectrometers was taken from open press (information from official sites of manufacturers, dodgers, posters, articles and reports).

We propose to perform the comparative analysis of gamma spectrometers using the following criteria:

- by technical characteristics (energy resolution, integral nonlinearity, long-term instability of conversion characteristic for 24 hours of continuous operation, maximal statistical load - counting rate);
- by use of native components in spectrometer (detection units, analyzers, software).

7.8.1 Comparative analysis of Russian gamma spectrometers by technical characteristics

Basic technical data and characteristics of **scintillation** gamma spectrometers are listed in Table 7.8.1.

Basic technical data and characteristics of **semiconductor** gamma spectrometers are listed in Table 7.8.2.

Table 7.8.1 - Characteristics of scintillation gamma spectrometers

Spectrometer name (manufacturer)	Energy resolution at ^{137}Cs peak (%)	Integral nonlinearity, not more (%)	Long-term instability, (%)	Maximal statistical load (s^{-1})
Scintillation gamma spectrometer “Прогресс-гамма” (“Progress-gamma”) Manufacturer - SPE “Doza”	< 8.5	-	-	-
Spectrometric system "МУЛЬТИРАД" (“MULTIRAD”), Manufacturer - STC “Amplituda”	< 8.5	-	-	-
Scintillation gamma spectrometer ГАММА-1С(“GAMMA-1S”) (KSC STC “Aspect”)	< 8.0	±1	Not more 1	$5 \cdot 10^4$
Field gamma spectrometer Manufacturer - Central Research Institute of Robotics and Engineering Cybernetics	< 8.5	-	± 2.0 for 8 hours of continuous operation	$5 \cdot 10^4$
Spectrometric complex СКС-07П_Г37…48 Manufacturer - BG “Green Star”	from 6 to 10.5 for detection units of different size	±1	± 2.0 for 24 hours of continuous operation	$2 \cdot 10^6$ ($5 \cdot 10^6$ when using the DL-shaper)

Table 7.8.2 – Characteristics of semiconductor gamma spectrometers

Spectrometer name (manufacturer)	Energy resolution at 1332keV peak from ^{60}Co (keV)	Integral nonlinearity, not more (%)	Long-term instability (%)	Maximal statistical load (s^{-1})
Semiconductor gamma spectrometer “Прогресс-ППД” (“Progress -SCD) Manufacturer - SPE “Doza”	1.8 to2	0.1	-	-
Spectrometric system "МУЛЬТИРАД" (“MULTIRAD”) Manufacturer - STC “Amplituda”	< 2	0.1	-	-
Semiconductor gamma spectrometer ГАММА-1П (“GAMMA-1P”) Manufacturer - JSC STC “Aspect”	1.8 to 3.5	±0.05	-	$5 \cdot 10^4$

Gamma radiation spectrometer РКГ-1К Manufacturer - STC “Radec”	1.9	-	-	-
Spectrometric complex СКС-07П_Г1…36 (SKS-07P_G1…36) Manufacturer - BG “Green Star”	1.7 to 2.4 (Ge – detector)	±0.05	± 0.02 for 24 hours of continuous operation	10^5 ($2 \cdot 10^5$ when using DL-shaper)

7.8.2 Comparative analysis of Russian gamma spectrometers

Basic technical data and characteristics of **scintillation** gamma spectrometers are listed in Table 7.8.3.

Table 7.8.3 – Characteristics of scintillation gamma spectrometers

Spectrometer name (manufacturer)	Detection units	Analyzer	Software
Scintillation gamma spectrometer “Прогресс-гамма” (“Progress-gamma”) Manufacturer - SPE “Doza”	Scintillation DU on the base of *NaI(Tl)* with Ø 63×63 mm crystal and built-in units of power supply, amplification and ADC		«Прогресс-гамма» (“Progress-gamma”)
Spectrometric system "МУЛЬТИРАД" (“MULTIRAD”) Manufacturer - STC “Amplituda”	63x63 mm *NaI(Tl)* Scintillation detectors of other types (*CsI(Tl)*, $CsF_2(Eu)$ and others) and sizes can be used		«Прогресс-гамма» (“Progress-gamma”)
Scintillation gamma radiation spectrometer ГАММА-1С (GAMMA-1S) Manufacturer - JSC STC “Aspect”	БДС-Г (BDS-G) on the base of 63x63 mm *NaI(Tl)* monocrystal with built-in amplifier, high voltage transducer, stabilization by light guide reference peak, and temperature compensation of conversion characteristic	Spectrometric analog-to-digital converter АЦП - 1К - В1	Applied software "LSRM" («LSRM», Ltd.)
Multichannel pulse height analyzer MCA 2048 Manufacturer - JSC “Technoexan”	БДЭГ (BDEG)		
Spectrometer-radiometer МКГБ-01 (MKGB-01) Manufacturer - STC “Radec”	БДЕГ-80, БДЕГ-60, БДЕГ-К (BDEG-80, BDEG-60, BDEG-K)	Analog-to-digital converter MD-198 (BSI, Riga)	AScinti-W program
Field gamma spectrometer (Central Research Institute of Robotics and Engineering Cybernetics)	СБДГ	БОИ	
Spectrometric complex СКС-07П_Г1…36 (SKS-07P_G1…36) Manufacturer - BG “Green Star”	БДЭГ *NaI(Tl)*, *CsI(Tl)*, *CsI(Na)*, *CsI*, $CdWO_4$, $YAlO_3(Ce)$, *BGO*, *LYSO*, BaF_2, etc. of different size	Impulsive signal; processors SBS-77, SBS-78, SBS-79 or «Colibry»	Specialized software «ScintBasic»

Basic technical data and characteristics of semiconductor gamma spectrometers are listed in Table 7.8.4.

Table 7.8.4 - Characteristics of semiconductor gamma spectrometers

Spectrometer name (manufacturer)	Detection units	Analyzer	Software
Scintillation gamma spectrometer “Прогресс-гамма” (“Progress-gamma”) Manufacturer - SPE “Doza”	Detection unit on the base of high pure germanium detector with efficiency of 10% to 60% and more (of EG&G «ORTEC» or «Canberra» produciton)	ADC-card (8K or 16K) or independent analyzer unit	«Прогресс-ППД» (Progress-SCD)
Spectrometric system "МУЛЬТИРАД" (“MULTIRAD”) Manufacturer - STC “Amplituda”	Detection unit on the base of high pure germanium detector with efficiency of 10% to 50% and more of EG&G «ORTEC» or «Canberra» production (different variants and modifications)	ADC-card (8K or 16K) or independent analyzer unit	«Прогресс-ППД» (Progress-SCD)
Scintillation gamma radiation spectrometer ГАММА-1С (GAMMA-1S) Manufacturer - JSC STC “Aspect”	Germanium semiconductor detector (HPGe of EG&G «ORTEC» or «Canberra» production or Ge(Li))	Spectrometric device that includes: spectrometric amplifier, high voltage power supply, low voltage power supply of the types: СУ-03П, СУ-04П, СУ-05П and АЦП-8к, usb-8к, Rs-8к	Applied software "LSRM" («ЛСРМ», Ltd.)
Multichannel pulse height analyzer MCA 2048 Manufacturer - JSC “Technoexan”	SSD of EG&G «ORTEC» or «Canberra» production		
Spectrometer-radiometer МКГБ-01 (MKGB-01) Manufacturer - STC “Radec”	SSD of EG&G «ORTEC» or «Canberra» production	Spectrometric device Multispektrum (BSI, Riga)	Processing program
Spectrometric complex СКС-07П_Г1…36 (SKS-07P_G1…36) Manufacturer - BG “Green Star”	Germanium and silicon detectors of Canberra, ORTEC, BSI, IFTP production. Cadmium telluride, mercury diiodide detectors. Xenon detectors (MEPhI). Different variants and modifications.	Impulsive signal processor SBS-75	Specialized software «GammaBasic», «Гамма Про» (“Gamma Pro”), «FusMat»

Proceeding from content of Tables 7.8.1-7.8.4 the following conclusions can be made:

1. the technical characteristics (energy resolution, integral nonlinearity, long-term instability of conversion characteristic) of both scintillation and semiconductor gamma spectrometers are approximately the same.

2. the gamma spectrometers of BG “Green Star” have the maximal statistical load advantage over the others.
3. scintillation detection units are assembled by almost all Russian manufacturers of gamma spectrometers.
4. only part of manufacturers produce the analyzers (processors) (JSC STC “Aspect”, BG “Green Star”, “Parsek”, Ltd. And some other companies).
5. SPE “Doza” and STC “Amplituda” have the common specialized software «Прогресс» (“Progress”).
6. JSC STC “Aspect” uses the applied software "LSRM".
7. BG “Green Star” has developed and certified the own specialized software intended for determining NM isotopic composition.

8 Modern Russian radiation monitors

At present the number of Russian radiation monitor manufacturers has greatly reduced as compared with period of 5-10-years' prescription. Some of enterprises stopped productizing of these devices others went out of business, for example, RIIT (Research Institute of Impulse Technologies, Moscow). Now there are two basic available manufacturers including the Internet, , namely SCP “Aspect” and FSUE VNIIA. Information has been received from promotional sheets and www-sites this manufacturers.

8.1 Scientific and production center “Aspect”, Dubna

One of the first that copes with manufacturing the radiation monitors in Russian Federation was SPC “Aspect”, Dubna. At present the "Янтарь" (“Jantar”) radiation monitors of SPC “Aspect” production are used at custom points of Russian Federation mainly.

Components

There are three monitor modifications: pedestrian, vehicle, and rail.

Basic system components include:

• pillars with detectors and electronic unit;

• control console, PC can also be used as the control console.

In addition, the systems can include the videodetection system, modem, additional signaling devices, light signals, and turnpikes.

Characteristics

- Operation mode – continuous, automated.
- Continuous operation when 220 V power is switched off – not less than 10 hours.
- Life time - 12 years.
- Trunck channel with RS-485 interface.

- Protocol– MODBUS

Pedestrian version - Янтарь-2П (Jantar-2P)	**Vehicle version - ЯНТАРЬ-1А (Jantar-1A)**	**Railway version - ЯНТАРЬ-1Ж (Jantar-1G)**
Detection threshold for control zone of 0.7 m, not more than:	Detection threshold, not more than:	Detection threshold, not more than:
Cs - 137 11 kBq	Cs - 137 300 kBq	Cs - 137 900 kBq
Co - 60 7 kBq	Co - 60 150 kBq	Co - 60 450 kBq
Ba - 133 11 kBq	Ba - 133 340 kBq	Ba - 133 900 kBq
For control zone of 1.5 m:	Pu 3,5 g	Pu 11 g
Pu 0.3 g	U 374 g	U 1747 g
U 5.7 g	Shielded Pu 80 g	Shielded Pu 348 g
Shielded Pu 22 g	•	•

Radioactive and nuclear material detection threshold are given for detection probability of 0.5, confidence probability 95 %, background intensity not more than 20 μR/h, false alarms not more than 10^{-3}. Uranium and plutonium have weapon graded isotopic composition.

Peculiarities

- Light and sound alarm signaling.
- Automated adaptation to natural background changes.
- Writing the event information to archive: date, time, detector counting rate, channel type (gamma or neutron). When monitor is equipped with video detection system the video reel of alarm object is additionally written.
- Gamma detector is based on organic plastic scintillators.
- Neutron detector is based on ^{3}He-proportional counters.
- Operating temperature range – from -50 °C to +50 °C.
- Lightning guard of force and signal lines.
- Software access to detector parameters.
- Remote access possibility.
- Self-diagnostic system.

8.2 ОСРК (OSRK), RSC “Kurchatov Institute”, Moscow

Radiation monitoring the human groups is implemented by pedestrian radiation monitors ППМ-01 (PPM-01), ППМ-02 (PPM-02), and ППМ-02-01 (PPM-02-01), as well as radiation monitoring installations УРК-02 (URK-02) used both independently and as the components of automated systems of radiation control, Figure 8.2.1.

Figure 8.2.1 – Radiation monitors of OSRK production

ППМ-01 (PPM-01)	Construction is made on form of arch consisting of two 2100 mm height pillars and top brace rod, in which there are infrared presence detector and alarm sound and optical signaling device. Each pillar contain two detection units made on the base of organic plastic scintillator and two amplifier-discriminator units. One of pillars has the microprocessor device for information processing and the power supply unit. Detection threshold is 0.3 g of *Pu* and 10 g of ^{235}U
ППМ-02 ППМ-02-01 (PPM-02, PPM-02-01)	Monitors are made as monoblocks, consist of detection devices УДГ-02 and control device УПХ-05 (UPH-05). Detection devices include the detection unit and amplifier-discriminator unit. Control device has the microprocessor device for information processing, alarm signaling device and power supply unit. Monoblocks are installed on structural components of buildings. PPM-02 monitor consists of four detection devices, and PPM-02-01 monitor consists of two detection devices.
УРК-02 (URK-02)	Consist of gamma radiation detection devices UDG-02I, infrared detector, and alarm signaling device BSR-03I.

8.3 JSC “SNIIP-KONVEL”, Moscow

Radiation control systems РИГ-08М (RIG-08M), Figure 8.3.1, are intended for continuous monitoring the radiation background of photon ionizing radiation and signaling on increase of radiation background relative value above the established threshold. Photon ionizing radiation background is controlled by value of measured effective doze rate.

Figure 8.3.1 – Radiation control system RIG-08M

The systems have two versions: RIG-08M-1 with single pillar and RIG-08M-2 with two pillars.

Possible system use:

- RIG-08M-1 with operating distance of 1.5 m and maximal speed of controlled material movement of (4.0±0.4) km/h;
- RIG-08M-2 with distance between pillars of 0.8 m and maximal speed of controlled material movement by pedestrians of (4.0±0.4) km/h;
- RIG-08M-2 with distance between pillars of 4 m and maximal speed of controlled material movement.

Table 8.3.1 – RIG-08M characteristics

Measurement range of photon radiation effective doze rate, μZv/h	
Limits of allowable basic relative error of effective doze rate measurement, %	±30
Energy range of photon radiation detected, MeV	0.01 – 1.25
Sensitivity to ^{137}Cs radiation, $(s^{-1})/(\mu Zv/h)$, not less than: for РИГ-08М-1 for РИГ-08М-2	 5000 10000
Intrinsic background level, not more than, μZv/h	0.04

8.4 FSUE RFNC VNIIEF, Sarov, Nizhegorodsky region

Pedestrian radiation monitor КПРМ-П1 (KPRM-P1)

Monitor is all-metal structure consisting of basic and detection pillars, within which the main monitor components are placed.

Operation modes:

-monitor self-diagnostic;

-background control;

-control of radioactive material “carry through”;

- control of radioactive object “carry through” monitor control zone;

- control of unauthorized access to monitor components.

There is indication of monitor operation modes and equipment diagnostic results.

Monitor includes (Figure 8.4.1):

- passage pillars;
- detection units - 4 pcs (2 per each pillar), total area of detecting elements is 5500 cm^2;
- sound and light signaling devices;
- infrared controlled zone occupation device;
- RS-232 or RS-485 interface.

Figure 8.4.1 - KPRM-P1 radiation monitor

Technical characteristics

Detection threshold of monitor for gamma radiation background of 25 μR/h and control source movement with speed of 1.0 to 1.2 m/s through the passage zone is:

- 0.3 g of plutonium in minimally radiating configuration (sphere);
- 10 g of high enriched uranium (^{235}U content is not less than 89 %) in minimally radiating configuration.

Hand-held radiation monitor БИРК-3 (BIRK-3)

Monitor’s detection limit under conditions of 25 μR/h background and control source movement relative working surface of monitor at the distance of (10.0±0.5) cm with speed of (0.50±0.05) m/s is:

– 0.1 g of plutonium in minimally radiating configuration;

– 3.0 g of high enrichment uranium (^{235}U content is not less than 89 %) in minimally radiating configuration.

False alarm frequency of the monitor is not more than 1 false alarm per 1 min of continuous monitor operation.

Monitor weight is mot more than 1 kg.

Figure 8.4.2 – Radiation monitor BIRK-3

8.5 FSUE VNIIA, Moscow

Radiation monitors of TCPM61, TCPM82, TCPM85 (TSRM) series (Figure 8.5.1)

Monitors include the power supply and control units, , 1 to 8 detection units (DU) and set of connecting cables. Depending on the number of detection units there are implemented the pedestrian and vehicle versions of radiation monitors.

TSRM61, TSRM82 monitors detect the gamma radiation. TSRM85 series monitor detects the neutron radiation.

CsI(Tl) scintillator is used as a detector in TSRM61, TSRM82 monitors, and ^{3}He-neutron counter is used in TSRM85.

Figure 8.5.1 – Radiation monitors of TSRM61, TSRM82 series

The monitor characteristics are listed in Table 8.5.1.

Table 8.5.1 –TSRM-61 technical characteristics

Detection limit with single DU during 3 s control period:			
	TSRM61	**TSRM82**	**TSRM85**
For nuclear materials at the distance of 50 cm (g)	10 (^{235}U); 0.3 (^{239}Pu)	1.8 (^{235}U); 0.15 (^{239}Pu)	100 (^{239}Pu)
For radioactive substances at the distance of 50 cm (kBq)	-	87 (^{60}Co); 102 (^{137}Cs); 70 (^{241}Am); 107 (^{226}Ra)	-
For gamma radiation exposure rate excess over background (μR/h)	-	12 (^{60}Co); 3.4 (^{137}Cs); 0.47 (^{241}Am); 10.8 (^{226}Ra)	-

Hand-held radiation monitor ГНОМ (GNOM)

Monitor consists of small-sized remote detection unit, control unit, and coupling bar of up to 3 m length, see Figure 8.5.2.

Weight of monitor without bar is 0.43 kg.

Detection limit for scanning rate not more than 0.5 m/s at the distance of 10 cm is 2 g of ^{235}U; 0.15 g of ^{239}Pu.

Figure 8.5.2 – Radiation monitors of ГНОМ series

9 Processing algorithms of radiation monitor data

Conditions of monitor operation have a wide range of basic parameters:

- absolute background value can differ by several orders;
- time background instability can vary from constantly low and stable background at the check point distant from locations of nuclear and radioactive materials to high instable background at the entrances of main production facility;
- measurement times can change from a fraction of a second for hand-held RM to 5-7 seconds for vehicle RMs;
- required false alarm probabilities are from 10^{-2} and less for hand-held RMs and from 10^{-3} to 10^{-6} for pedestrian and vehicle RMs.

There are two monitor operation modes possible – with stoppage of objects to be controlled and without it. At this, the different processing methods and algorithms that satisfy the specific requirements and conditions of RM operation are used.

Given report presents the algorithms of some basic criteria and methods of statistical processing used for continuous radiation monitoring:

1) Neumann-Pearson criterion;
2) Moving average method;
3) Plausibility relation criterion;
4) Digital recursive filter method;
5) A priori probability method;
6) Half-sum method;
7) Relative variance method.

First four methods are the most known and a long time used in RM technology. A priori probability method was also proposed and described in details more than 15 years ago. Last two methods are newer proposals issued as the patents.

Neumann-Pearson criterion and relative variance method perform the result analysis of sequential measurements. Other methods imply the fragmentation of measurement time interval by subintervals (probability ratio test), analysis of superimposed measurements performed with some delay in time (moving average method) or take into account the results of neighbor measurements (methods of digital recursive filter, a priory probability, and half-sum).

9.1 Neumann-Pearson test

Neumann-Pearson test is most powerful and simple in case the conclusion should be select from two hypothesizes [106, 107]. Neumann-Pearson test was most frequently used as the method of statistical processing of continuous on-line information from ionizing radiation detectors of RM at the beginning of RM technology development [108-111]. We can assert that the different incarnations of this test are used now in all algorithms presented in given report.

When null hypothesis is fully defined and alternative hypothesis is undefined the Neumann-Pearson test is as follows.

The critical domain Ω_α is determined by selected test significance α (probability of false detection) from the expression:

$$\int_{\Omega_\alpha} p_k(K_\phi, \sigma^2_{K_\phi})dk = \int_{L}^{\infty} p_k(K_\phi, \sigma^2_{K_\phi})dk = \alpha\,, \tag{9.1}$$

Where *k*- random value distributed with probability density function $p_k(K_\phi, \sigma^2_{K_\phi})$, K_ϕ – mean background value, $\sigma^2_{K_\phi}$ - corresponding variance; *L* – threshold value determining the critical domain, in other words, the *threshold* or *detection level*, fig 9.1. If p_k is Poisson distribution, the integration is replaced with summing:

$$\sum_{i=L}^{\infty} \frac{K_{\phi}^{i} \cdot e^{-K_{\phi}}}{i!} = \alpha \qquad (9.2)$$

Further, if k falls into range of $k \geq L$, the hypothesis of source presence is accepted without indication of its detection probability. Otherwise, the hypothesis of only background presence is accepted.

In case of normal distribution the threshold L is in fact determined simply as a sum of average background K_{ϕ} and some addition consisting of its standard deviation $\sigma_{K_{\phi}} = \sqrt{K_{\phi}}$ multiplied by fractile z of corresponding distribution of k

$$L = K_{\phi} + z\sqrt{K_{\phi}} \, . \qquad (9.3)$$

Fractile z value is determined by test significance parameter α and doesn't depend on the mean distribution value.

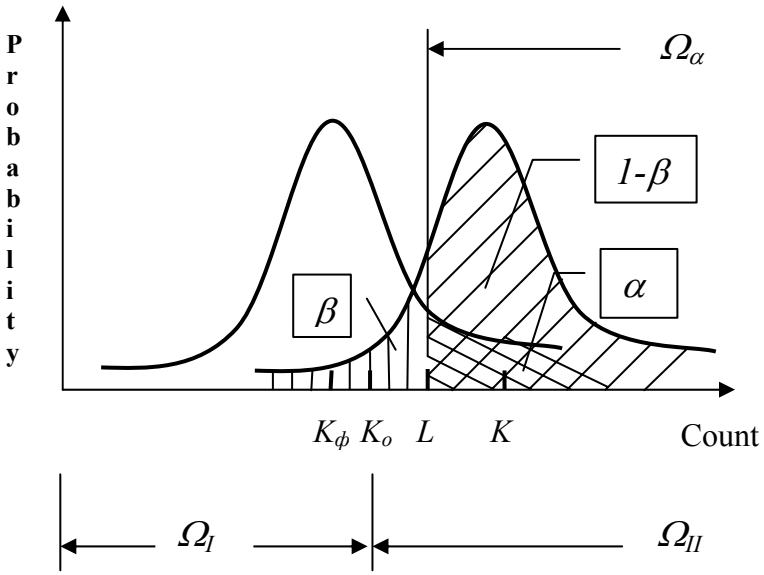

K_{ϕ} – mean background; K_0 – a priori threshold; L – threshold;

K – mean background plus addition radiation; β – probability of undetectable radiation.

Fig. 9.1 – Parameters of null and alternative hypotheses

In case of Poisson distribution the threshold determination is not simple and the expression (9.2) is needed to be used in an explicit form, in which the parameter α depends on the mean background distribution value.

9.2 Moving average method

The most frequently used processing method of radiation monitor detector measurement results is the method of sliding exposition time interval or moving average [112,113]. The method concept is the signal from detector is measured during exposition time T congruented with duration of signal excess

over the background not sequentially, but in parallel with some delay τ, as presented on Figure 9.2. The count obtained is then processed by Neumann-Pearson test.

Exposition time interval as though discretely moves with some shift τ. There is the optimal ratio n of time interval T to subinterval τ, $T= n\tau$. Value of n depends on the object movement speed. According to [114] the best result for pedestrian monitor is obtained at $n=4$.

If none of n measurements has shown significant signal excess over the background, the decision is made about absence of radiation source. On case of any of n measurements has shown the signal excess over the background the conclusion is made on radiation source presence.

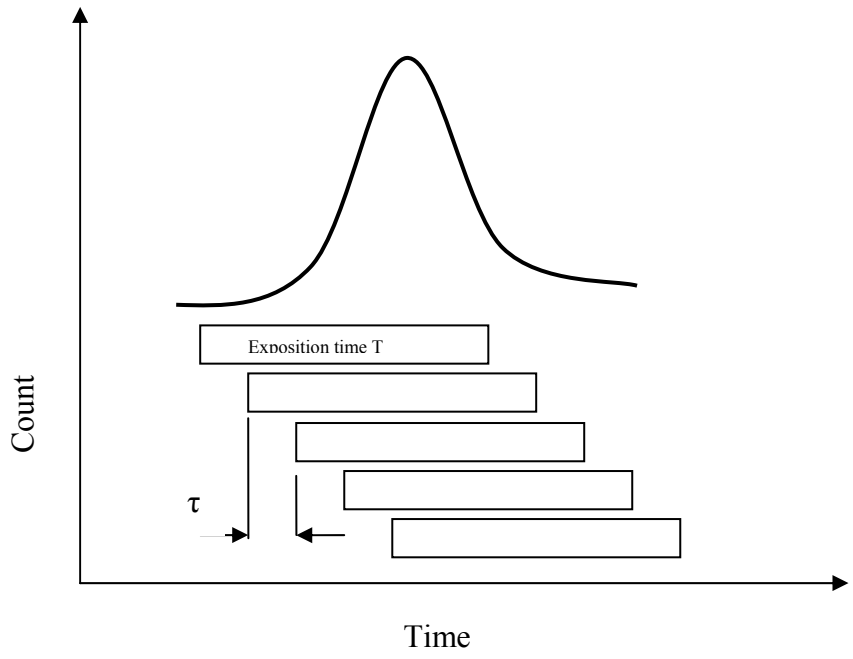

Figure 9.2 – Moving interval principle

Sometimes the measurement results can then be summed up [114]. n measured count values are summed up and the total count ${}^{\Sigma}K$ is processed. At this, the Neumann-Pearson test is also used with threshold ${}^{\Sigma}L$ that is determined as

$$ {}^{\Sigma}L={}^{\Sigma}K_{\phi} + z\sqrt{{}^{\Sigma}K_{\phi}} \, . \qquad (9.4) $$

The moving interval method was widely used not only at the early stages of radiation monitor development and creation, but at present [115] due to its easy implementation within the framework of analog electronics. In particular, the radiation monitors developed and manufactured at VNIIA use namely this processing test.

9.3 Probability ratio test

Alternative to Neumann-Pearson test in moving interval algorithm is probability ratio test [113,116,117]. This test is based on method of *maximal probability* [106]. Essence of method is the *probability Π(X, θ)* is determined for *n* independent observations with probability function $p(x_i,\theta)$ depending on parameter θ as follows

$$\Pi(X,\theta)=\prod_{i=1}^{n} p(x_i,\theta). \tag{9.5}$$

In this case the distribution parameter is its mathematical *expectation value*, i.e. mean value x_i.

Expression

$$\frac{\partial}{\partial\theta}\ln\Pi(X,\theta)=0 \tag{9.6}$$

is called *probability equation*. It reflects the condition of maximum *Π(X, θ)* existence.

Assuming the mean $K_ф$ for hypothesis H_o, and the mean equal to detection threshold L for hypothesis H_1, we will take the relation of two plausibilities *Π(X, $K_ф$)* and *Π(X,L)*. Taking into account the exponential kind of Gauss probability density distribution the logarithm of this relation will simplify the expression form

$$Z=ln(\Pi(X,\ K_ф)/\Pi(X,L)) \ . \tag{9.7}$$

In practice the method means that the exposition time interval is divided into sequential *n* subintervals or the sum of *n* neighbor count values is taken. When background $K_ф$ is known and detection threshold L is selected (as for Neumann-Pearson test) the value z_i is calculated for each count value x_i [118]. Value z_i is equal to probabilities ratio (probability if observed count x_i is the random value distributed with mean value of $x_{cp}= L$ and probability if $x_{cp}= K_ф$) logarithm.

For normal Gauss distribution z_i is determined as, for example, in reference [113] from expression[2]

$$z_i=\ln(K_ф/L)+(x_i-K_ф)^2/2\sigma^2_{K_ф}-(x_i-L)^2/2\sigma^2_L \quad . \tag{9.8}$$

For Poisson distribution z_i is determined as, for example, in reference [116] from the expression

$$z_i = x_i\cdot\ln(L/K_ф)-(L-K_ф) \ . \tag{9.9}$$

Parameter Z is determined by summing the counts under number of measurement subintervals n,

$$Z=\sum_{i=1}^{n} z_i \ . \tag{9.10}$$

Z value is compared with parameters *A* and *B*.

A and *B* parameters are determined as

[2] Reference gives an approximate expression of z_i parameter, to obtain its exact value the first member is required.

$$A = \ln[(1-\beta)/\alpha], \tag{9.11}$$

$$B = \ln[\beta/(1-\alpha)], \tag{9.12}$$

where α and β – probabilities of the I and II types errors.

If $Z \le B$, the conclusion is made on source absence, if $Z \ge A$ the source is considered as present. Sometimes the practical criterion of source absence is $Z \le 0$, otherwise the decision is taken on its presence [118].

According to [116] the best results are obtained for n is in the range of 6 to 12.

Probability ratio test is frequently used when detecting the neutron radiation [119,120] remarkable for low counting rates.

According to [121] data the probability ratio test has advantages in cases of insignificant signal excess over background. When there is a large signal additional to background, it is not advisable to use relatively complex test requiring calculations, since it doesn't have any power advantage, but may cause delay in time for making decision. It is especially significant in case of hand-held and pedestrian monitors operating without stopping the objects controlled.

9.4 Digital recursive filter

Method of digital recursive filter as applied to portal technologies was proposed in [122].

The method essence is the parameter N'_i value is determined for each pair of events N_{i-1}, N_i

$$N_i' = 0{,}75\, N'_{i-1} + 0{,}25\, N_i. \tag{9.13}$$

Detection threshold N'_{nop} is calculated as in Neumann-Pearson test

$$N'_{nop} = \mu_0 + z\cdot\sqrt{\mu_0} \tag{9.14}$$

Parameter N_i' is compared with N'_{nop}. If $N_i' \ge N'_{nop}$, the hypothesis of additional radiation presence is taken, otherwise the hypothesis of only background presence is taken.

9.5 A priori probability test

Use of a priori probability concept in Neumann-Pearson test in case of random short-time radiation excess over background detection was proposed in [123].

Parameters K and σ_K^2 of statistics corresponding to hypothesis H_1 are undefined. Definiteness can be achieved by using the concept of a priori probability [124].

Let's the mean background value K_ϕ is known in advance. If for any reasons a priory to know about source presence or assume it and, at this, k pulses count during exposition time, the estimations of mean value K and variance σ_K^2 will be determined as:

$$K = \frac{1 + K_\phi + \frac{K_\phi^2}{2!} \ldots + \frac{K_\phi^k}{k!} \ldots + \frac{K_\phi^{k+1}}{(k+1)!}}{1 + K_0 + \frac{K_\phi^2}{2!} \ldots + \frac{K_\phi^k}{k!}} (k+1) \quad , \tag{9.15}$$

$$\sigma_K^2 = \frac{1 + K_\phi + \frac{K_\phi^2}{2!} \ldots + \frac{K_\phi^k}{k!} \ldots + \frac{K_\phi^{k+2}}{(k+2)!}}{1 + K_0 + \frac{K_\phi^2}{2!} \ldots + \frac{K_\phi^k}{k!}} (k+1)(k+2) - K^2 \quad . \tag{9.16}$$

Expressions for K and σ_K^2 completely define the alternative hypothesis. One can believed that there are two known distributions – of background $p_k(K_\phi, \sigma_K^2)$ with mean K_ϕ and $p_k(K, \sigma_K^2)$ distribution corresponding to source presence with mean K.

K_0 value, starting from which the condition

$$p_k(K_\phi, \sigma_K^2) \geq p_k(K, \sigma_K^2) \tag{9.17}$$

is met will divide the Ω domain into two parts Ω_I and Ω_{II} presented in Figure 9.1. It is more probable that event k was caused by background fluctuations within Ω_I domain, and by source presence within Ω_{II} domain. Thus, the $k \geq K_0$ condition defines the critical domain, the more complete than it was defined by detection level L. Expansion of critical domain increases the test power, i.e. the probability of source detection. However, at this the condition of test significance α should be met.

So, the alternative hypothesis of source presence will be taken is the selected detection level is exceed or two following conditions are simultaneously met for considered event group: all group members are not less than K_0 and total probability of taking the false hypothesis is not more than the selected level of test significance.

The following conditions are required and sufficient for taking the alternative hypothesis:

$$k_i \geq L' \tag{9.19}$$

or

$$K_0 \leq k_i \leq L' , \tag{9.20}$$

$$\alpha_{ep} \leq \alpha . \tag{9.21}$$

There is an optimal value of level L' providing the maximal test power at the same false alarm frequency.

As to radiation monitors, the number of random events in the group considered is determined by number of measurements performed during employee stay duration within the sensitive monitor area. As a rule, this number equal to two, three and doesn't exceed five.

9.6 Half-sum method

One of Neumann-Pearson test adaptations to radiation monitoring task was proposed in [125].

Processing algorithm practically almost repeats the algorithms of a priori probability method. There is proposed to divide the count definitional domain into three parts by two detection threshold: upper L and lower L'. Upper detection threshold is the threshold of Neumann-Pearson test. Lower detection threshold L' is defined as

$$L' = K_\phi + (z-1)\sqrt{K_\phi}\ , \tag{9.22}$$

where z – fractile corresponding to accepted significance level of Neumann-Pearson test.

Decision on only background presence is taken when the measurement result k_i is less than L'

$$H_0: k_i < L'\ . \tag{9.23}$$

Decision on source presence is taken when k_i is not less than L

$$H_1: k_i \geq L\ . \tag{9.24}$$

If k_i falls into the interval between two detection thresholds L' and L, another measurement k_{i+1} is made, for which the procedure of comparing with L' is carried out, and in case of $k_i < L'$ the mean value k_i^{cp} of two neighbor measurements k_i and k_{i+1} is calculated

$$k_i^{cp} = (k_i + k_{i+1})/2.$$

k_i^{cp} value is compared with L'

$$H_0: k_i^{cp} < L'\ , \tag{9.25}$$

$$H_1: k_i^{cp} \geq L'\ . \tag{9.26}$$

9.7 Relative variance method

Method proposed in [126] is based on analysis of η parameter equal to counter value of relative standard deviation of detected radiation net counting rate minus background b:

$$\eta = \frac{n-b}{\sqrt{n/t_n + b/t_b}}\ , \tag{9.27}$$

where n – total counting rate of background and additional radiation; t_n – total counting rate measurement time; t_b – background measurement time.

Parameter η is compared with its threshold value η_{nop} defined as

$$\eta_{nop} = \frac{n_{nop}-b}{\sqrt{n_{nop}/t_n + b/t_b}}, \tag{9.28}$$

where n_{nop} – detection threshold of Neumann-Pearson test.

If $\eta \geq \eta_{nop}$, than hypothesis of additional radiation presence is taken;

If $\eta < \eta_{nop}$, than hypothesis of only background presence is taken.

The problem of presented processing methods and tests' advantages and disadvantages can be solved by testing these algorithms in equal real or simulated conditions.

References

1. Birks J.B. The Theory and Practice of Scintillation Counting. London : Pergamon Press, 1964.
2. Medvedv M.N. Scintillation detectors. M., Atomizdat, 1977.
3. Cirlin Y.A., Daich A.R., Radyvaniuk A.M. Scintillation detection blocks. M., Atomizdat, 1978.
4. Cirlin Y.A., Globus M.E., Sysoeva E.P. Optimization of gamma-ray detection by scintillation crystals. M., Energoatomizdat, 1991.
5. Persyk D.E., Moi T.E. IEEE Trans. Nucl. Sci., т. NS-29, 1978, p. 615.
6. Grassman H., Lorenz E., Moser H.G. Nucl. Instr. Meth., 1985 r., T. 228, p. 323.
7. Shamovsky L.M. Cristalphosphors and scintillators in geology. M., Nedra, 1985.
8. Sakai E. IEEE Trans. Nucl. Sci. 1987, T. NS-34, p. 418.
9. Weber M.I., Monchamp R.R. J. Appl. Phys. 1983, T. 44, p. 5496.
10. Nestor O.H., Huang C.Y. IEEE Trans. Nucl. Sci. 1975, T. NS-22, p. 68.
11. Murashita M.H., Saitoh H., Tobimatsu K. Nucl. Instr. Meth. 1986, vol.A243.
12. Collaboration, L3. Nucl. Instr. Meth. 1990, т. A289.
13. Jaaskelainen M., Sarantites D.G., Woodward R. et al. Nucl. Instr. Meth., 1983, т. 204, p. 385.
14. M.R., Farukhi. Nucl. Radiation Detector Materials. Massachusetts, 1982.
15. Melcher R.D., Manenta R.A., Schweitzer J.S. IEEE Trans. Nucl. Sci. 1989, т. NS-36.
16. Angert N.B., et al. Gamma ray scintillation detector on base BGO monocristals. VANT: Common and Nuclear Phisics., 1988, № 2 (42), p. 69.
17. Kamanin V.V. et al. Comparative analyses of NaI(Tl) and $Bi_4Ge_3O_{12}$ crystals under a neutron and gamma ray registration. Instruments and experimental techniques, 1988, № 6, p. 61-64.
18. Shirakawa Y. Development of a direction finding gamma-ray detector. Nucl. Instr. Meth. 2007, т. B263, p. 58.
19. Geist W.H. et al. Evaluation of a fast neutron coincidence counter for the measurements of uranium samples. Nucl. Instr. Meth. 2001, т. A470, p. 590.
20. Hausser O., et al., Nucl. Instr. and Meth. 1983, т. A213, p. 301.
21. Vincke H. et al. Response of BGO detector to photon and neutron sources: simulations and measurements. Nucl. Instr. Meth. 2002, т. A484, p. 102.
22. Laval L., Moszynski M., Allemand R. Nucl. Instr. Meth. 1983, т. 206.
23. Farukhi M.R., Swinehart C.F. IEEE Trans. Nucl. Sci. 1971, т. NS18.
24. Crahan G., Yamamoto H. Nucl. Instr. Meth. 1991, т. A307.
25. Murashita M.H., Saitoh., Tobimatsu K. Nucl. Instr. Meth. 1986 r., vol. A243.
26. Hoffman E.J., Dahebom M., Ricci A.R. IEEE Trans. Nucl. Sci. 1986 r., vol.NS-33.
27. D.F.Anderson. Nucl. Instr. Meth. 1986 r., vol.A287.
28. Laval L., Moszynski M., Allemand R. Nucl. Instr. Meth. 1983, т. 206.
29. Sper. P. Nucl. Instr. Meth. 1987 r., vol.A254.

30. Afanasiady L.Sh. et al. Time and energy resolution of BaF_2 scintillator with radiation converter. Instruments and experimental techniques, 1989, № 5, p. 85-86.
31. Shulgin B.V. et al. Scintillation detectors on base CaF_2-Eu monocristals. Russian Atomic Energy, т. 75, iss. 1, july 1993, p. 28.
32. Pastor C. The phostron: a phoswich counter for neutron and charged particle detection. Nucl. Instrum. and Meth. in Phys. Res., 1984, т. A 227, p. 87.
33. Pelletier-Allard N., Pelletier R. High-resolution spectroscopic study of Er:YAlO3. Nucl. Instr. Meth. 1998, т. 275-277, p. 374.
34. Autrata R., Schaner P. Scanning. 1983 r., vol.5.
35. Baryshevsky V.G. et al. $YA1O_3$:Ce fast scintillators for radiation detectors. Instruments and experimental techniques, 1992, № 3, p. 86.
36. Levenetc V.V. et al. Using CdTe and CdZnTe detectors made in HPhTI for measurement of gamma and alpha radiation. http://www.lsrm.ru/PPSR/2005/tz20.htm.
37. Zorenco Y.V. et al. Journal of applied spectroscopy. 1988, т. 49, № 3, p. 514.
38. Baryshevsky V.G. et al. Instruments and experimental techniques, 1993, № 3, p. 51.
39. Beliaev R.A. Beryllium Oxide. M., 1980.
40. Shulgin B.V. et al. Scintillation properties of BeO monocrystals. Journal of applied spectroscopy. 1988, т. 47, № 2, p. 286-291.
41. Milbrath B. Will lanthanium halide scintillators make NaI(Tl) obsolete? NWS06 Meeting of American Physical Society. Tacoma, Washington, 18 Apr. 2006.
42. Autrata R., Schaner P. Scanning. 1983, т. 5.
43. R. Pania, R. Pellegrinia, M.N. Cintia, P. Bennatia, M. Betti. LaBr3:Ce crystal: The latest advance for scintillation cameras. б.м. : Nuclear Instruments and Methods in Physics Research, 2007.
44. Van Loef E.V.D., Dorenbos P., van Eijk C.W.E., Kramer K.W., Gudel H.U. Scintiilation properties of $LaBr_3$:Ce3+ crystals: fast, efficient and high-energy-resolution scintillators. Nucl. Instrum. and Meth. in Phys. Res., 2002, т. A 486, p. 254.
45. Van Loef E.V.D., Dorenbos P. et. al. : Appl. Phes. Lett., 2000, т. 77.
46. Canberra Catalog. Scintillation detectors. 2007.
47. Nicolini R. at al. Investigation of properties of a 1x1 $LaBr_3$:Ce scintillator. Nucl. Instrum. and Meth. in Phys. Res., 2007, т. A 582, p. 554.
48. Barzilov A. at al. Experimental Study of $LaBr_3$(Ce) Gamma-Ray Detector Performance in Mixed Radiation Field. 2006 Division of Nuclear Phisics Annual Meeting. Nashvill, Tennessee.
49. Shah K. S., Glodo J., Klugerman M., Moses W. W., Derenzo S. E., and Weber M. J. LaBr3:Ce Scintillators for Gamma Ray Spectroscopy. 2002, University of California.
50. Shah K.S., Glodo J., Kligerman M., et al. s.l. : Nucl. Instr. Meth. A., 2003, Vol. 505, p. 76.
51. Balcerzyr M., MoszynskiM., Kapusta M. s.l. : Nucl.Inst. Meth. A., 2005, Vol. 537, p.
52. D., Luckey. Nucl. Instr. Meth. 1968 r., T. 62, p.

53. Simpson P.J. et al. Superfast timing performance from ZnO scintillators. Nucl. Instr. Meth. 2003, т. A505, c. 82.
54. Wilkinson J., Ucer K.B.,Williams R.T. Nucl. Instr. Meth. 2005 r., T. 537, p. 66.
55. Demidenko V.A. et al. Scintillation properties of ceramics based on zinc oxide. Radiation Measurement, 2007, т. 42, p. 549.
56. Katagiri, M. et al. 2004. Scintillation materials for neutron imaging detectors. Nucl. Instrum. Methods Phys. Res. 2004, т. A 529, c. 274.
57. Zo Thet. Beliaev V.N. X-ray and annigilation radiation detectors on base LSO cristals. M., MPhEI, 2007.
58. Basharuly N.V. et al. “Scintillators 2000” conference. In “Abstracts of International conference under inorganic scintillators and its using. Moscow, 2000.
59. Higher M. Resolution PET by means of a new scintillator LSO. Aachen : RWTH, 1999.
60. Rogers J.G., Batty C.J. Afterglow in LSO and its possible effect on energy resolution. IEEE Trans. Nucl. Sci., 2000, 43(6):438-445.
61. Burahas S. et al. Neorg. Mater., 1996, т. 32, p. 1525.
62. Nagornaya L. et al. ProNucl. Instr. Meth. 2005, т. A537, p. 163.
63. Ryzhikov V.D. et al. Nucl. Instr. Meth. 2005, т. A537, p. 424.,
64. Sung-Woo Kwak et al. Nucl. Instr. Meth. 2005, A537, p. 449.
65. Gen N.S. et al. Operational characteristics of plastic melt scintillators. Instruments and experimental techniques, 1988, № 4, p. 35.
66. Pomerancev V.V et al. Gamma spectrometric and own radiation background of plastic scintillators. Russian Atomic Energy, т. 63, iss. 2, august 1987, p. 118.
67. Afanasiady L.Sh. Liquid scintillators with high *n-γ* separating ability. Instruments and experimental techniques, 1988, № 6, p. 58-60.
68. Klassen N.V., Osipian N.V. Features of properties and prospective of nano crystal scintillators using. Report of IFTT RAN.
69. Ulin S.E., Dmitrenko V.V., et al. Cilindrical ionization high pressure Xe chamber. Instruments and experimental techniques, 1995, № 4, p. 46.
70. Dmitrenko V.V., Chernysheva I.V., Gratchev V.M. The progress in developing of large volume high pressure xenone gamma ray spectrometers. Nara : ICDL 99, 1999. 99CH36213.
71. Ulin S.E. Gamma-spectrometer based on compressed xenon (development, research of characteristics and using. M., MPhEI, 1999.
72. Hall R.N. Hp Ge: purification, crystal grown, and annealing properties. *IEEE Trans. on Nucl. Sci.* 1984 r., NS-31, n-1, p. 320.
73. Detectors and instruments for Nuclear Spektroscopy. ORTEC 91/92, p. 2-32.
74. Akimov Y.K. et al. Semiconductor detectors in experimental phisics. M., Energoatomizdat, 1989.

75. Raudorf T.W., Trammel R.C., Darken L.S. N-tipe high purity germanium coaxial detectors . IEEE Trans. on Nucl. Sci., 1979, Ns-26.
76. Pehl R.H., Madden N.W., Elliott J.H. Radiation damape resestence of revers electrode Ge coaxial detectors . IEEE Tans. on Nucl. Sci., 1979. NS-26.
77. Luke, P.N. Gold - mask technique for fabricating segmented electrode germanium detectors. IEEE Trans. on Nucl. Sci., 1984 r. Ns-31.
78. Bellia G., Zoppo A.D. Peformances of large volume p-type HPGe detectors. Nucl. instr. and meth., 1989, A284, p. 122.
79. Raudorf, R.C. Trammel T.W. Performance of reverse electrode HPGe coaxial detector after light damage by fast neutrons. IEEE Trans. on Nucl. Sci., 1984, NS-31.
80. Azimov S.A., et al. Russian Atomic Energy. 1976, т. 40, iss. 4, p. 346-347.
81. E., Sakkai E. Nucl. Instr. and Meth. 1982, т. 196, 1, p. 121-130.
82. Zaletin V.M., et al. Russian Atomic Energy. 1978, т. 44, iss. 4, p. 360-363.
83. Rybka A.V., Davydov L. N., Shlyakhov I. N. et al. Gamma-radiation dosimetry with semiconductor CdTe and CdZnTe detectors. No.1-2, 1994 r., Nucl. Instr. and Meth., T. 53, p. 147 - 156.
84. Levenets V.V., et al. Gamma and alpha spectrometric by semiconductor detectors based CdTe (CdZnTe) made in NSC HPhTI. Kharkov, Ukrain,http://www.kinr.kiev.ua/NPAE_Kyiv2006/proc/Levenets.pdf.
85. Akimov Y.K. et al. Semiconductor detectors in experimental phisics. M., Energoatomizdat, 1989.
86. Gaisler V.A., et al. Diiodid mercourus: manufacturing, properties, using. Novosibirsk, Nauka, 1984.
87. Zaletin V.M., et al. Russian Atomic Energy. 1982 r., T. 52, iss. 3, p. 193-195.
88. Warren J.L. Nucl. Instrum. and Methods. 1983 r., T. 213, 1, p. 103.
89. Van den Berg L., Whiter R.C. IEEE Trans. on Nucl. Sci. 1978 r., T. NS-25, 1, p. 395-397.
90. Sakai E. IEEE Trans. IEEE Trans. Nucl. Sci. 1987, T. NS-34, c. 418.
91. Zaletin V.M., et al. Energy resolution of HgI_2 detectors for x- and gamma-ray. Russian Atomic Energy, т. 63, iss. 2, august 1987, p. 140-142.
92. Yoshiyuki K. et al. Application of a fiber optic grating sensor for the measurement of strain ender irradiation environment. Nucl. Eng. and Design, 2002, v. 217, p. 283-288.
93. Baker J.H. et al. A combined NaI(Tl)+LiI(Eu) detector for environmental, geological and security applications. Radiation Measurement. 2007, 42, p. 937.
94. Reder P.L. et al. Nucl. Instr. Meth. 1994, A340, p. 371
95. Ryzhikov V. et al. Thermal neutron detectors based on complex oxid crystals. Nucl. Instr. Meth. 2002, p. 156-159
96. Reilly D, Ensslin N., and Hastigs S. Jr. Passive Non destructive Assay of Nuclear Materials. LA-UR-90-732 1991, p. 386.
97. Bovin V.P., et al. State and prospective of x-ray gas proportional detectors for development radiometric assay of materials. VANT: Radiation Techniques. 1992, iss. 1, p. 39.

98. Goleva V.I., Shumakov A.V. VANT: Radiation Techniques. 1987, iss. 2 (35), p. 55.

99. Sauli F. GEM: a new concept for electron amplification in gas detectors. Nucl. Inst. and Meth. A386, 1997, p. 531-534.

100. Buzulutskov A.F. Radiation detectors based on gaseous electron multiplicity. Instruments and experimental techniques, 2007, № 3, p. 5-30.

101. Gebauer B., et al. Novel large-area thermal neutron imagine detectors comprising ^{157}Gd/CsI-converter. Nucl. Inst. and Meth. A392, 1997, p. 68-72.

102. Rygikov V.D., Stadnik P.E., Yakovlev Y.A. Scintillator-photodiode system prospective of evolution. Instruments and experimental techniques, 1984, № 2, p. 6-16.

103. Investigation of avalanch photodiod basic characteristics. http://hep.msu.dubna.ru/main/mod/resource/view.php?id=464.

104. Golbrihe N.I., Plotnikov A.F., Gubin V.E. Quantum electronics. M., Nauka, 1975.

105. Beresnev V.I., at al. Spectra-shifter light-pipe for scintillation and Cherenkov' detectors. Russian Atomic Energy, т. 64, iss. 3, March 1988, p. 215-219.

106. Eadie W.T., et al. Statistical methods in experimental physics. North-Holland Publ. Comp. 1971.

107. Pitman E. Basic of statistical conclusion theory. Translated from English, M., Mir, 1986, p. 9.

108. Chambers W. e. a. Portal Monitor for Diversion Safeguards. Rept. LA-5681, Jul. 1974.

109. Arnal T. e. a. Application des controles neutroniques dans les instalation de fabrication et de retraitment des combustibles. Bulletin d'Information Scintifiques et Techniques, N223, May/Juin 1977.

110. Kruse L., Dominguez B. Development of an improved monitor for portal detection of the unauthorized removal of special nuclear material. – Nucl. Mater. Manag., 1982, v. 11, N 4, p. 42-47.

111. Fehlau P. An Application Guide to Pedestrian SNM Monitors. Rept. LA-10633-MS, Feb. 1986.

112. Tomas E. Sampson e. a. Portal Monitor for Diversion Safeguards. Nucl. Techn. Vol. 23, Aug. 1974.

113. Fehlau P., Coop K., Markin J. Application of Wald's Sequential Probability Ratio Test to Nuclear Material Control. Rept. LA-UR-84-2782, 1984.

114. Kositsyn V.F., Shumakov A.V. Atomic technique abroad, № 10, 1988.

115. Fehlau P., Close D.A., Coop K.L., York R. Estimated and observed performance of a neutron SNM portal monitor for vehicles. LA-UR--96-3409, 1996.

116. Coop K. Monte Carlo Simulation of the sequential Probability Retio Test for Radiation Monitoring. - IEEE Transactions on Nuclear Science, v. NS-32, Feb. 1985.

117. Fehlau P., Coop K., Nixon K.V. Sequential Probability Ratio Controllers for Safeguards Radiation Monitors. Proc. 6 Annaul ESARDA Symp. on Safeguards and NMM, Venice, Italy, May, 1984.

118. Shipley J. Sequential likelihood-ratio test applied to series of materials balances.- In: Mathematical and statistical methods in Nuclear Safeguards. New York: Harwood Academic Publishers, 1982.

119. Markin J.T., Stewart J.E., and Goldman A.S. Data Analysis for Neutron Monitoring in an Enrichment Facility. Proc. 4 Annaul ESARDA Symp. Specialist Meeting on Haronization and Standardizatin for Nuclear Safeguards, Petten, Netherlands, April, 1982.

120. Leitner E., Nagib M., Podewils P., Avenhaus R. Evaluation of the Sensitivity of a Neutron Detection System in a Portal Monitor. Proc. 16 Annaul ESARDA Symp., France, Versailles, 1983.

121. Dumesnil P., Greco J.L. Optimization of the processing of the counts from a doorway monitor for radioactive substances. Proc.7 Ann. ESARDA Symp. on Safeguards and NMM, Liege, Belgium, May, 1985.

122. Fehlau P. Comparing a recursive digital filter with the moving-average and sequential probability-ratio detection methods for SNM portal monitor. IEEE Trans. on Nucl. Science, vol. 40, No. 2, April 1993.

123. Kositsyn V.F., Shumakov A.V. A priori probability using for detection of casual short time events. Instruments and experimental techniques, № 4, 1991, p. 99-102.

124. Goldansky V.I., Kutsenko A.V., Podgoretsky M.I. Statistic of nuclear particles counts. M., GIF-ML, 1959. 81 p.

125. Veselova G.P., et al. Radiation monitor method, radiation monitor. Patent RF № 2105323, 1998.

126. Victorov L.V., et al. Detection method of weak radiation flow. Patent RF № 2140660, 1998.